Archaeological and Anthropological Sciences (2022) 14: 4
https://doi.org/10.1007/s12520-021-01431-z

REVIEW

Pigments—Arsenic-based yellows and reds

Elisabetta Gliozzo[1] · **Lucia Burgio**[2,3]

Received: 20 January 2021 / Accepted: 30 June 2021 / Published online: 9 December 2021
© The Author(s) 2021

Abstract
This review offers an update on arsenic-bearing minerals and pigments with the aim of serving as a guide for the study of Cultural Heritage materials in which these materials can be found.
The different As-bearing mineral phases (realgar, pararealgar, orpiment, anorpiment, alacranite, dimorphite, bonazziite, uzonite, wakabayashilite, duranusite, arsenolite and claudetite) and some of their light-induced products are examined. The occurrence of As-sulfides and their trade, use, alteration and degradation are also reviewed. Finally, the analytical techniques commonly used for the identification of arsenic-containing pigments are discussed. The manuscript concludes with a good-practice guide and a summary of key concepts for use by those working in the field of cultural heritage.

Keywords Realgar and pararealgar · Orpiment and anorpiment · Light-induced transformations · Raman and X-ray diffraction · As-containing minerals and pigments · [Alacranite-dimorphite-bonazziite-uzonite-wakabayashilite-duranusite-arsenolite-claudetite] · Pigments

Premise

This Topical Collection (TC) covers several topics in the field of study, in which ancient architecture, art history, archaeology and material analyses intersect. The chosen perspective is that of a multidisciplinary scenario, capable of combining, integrating and solving the research issues raised by the study of mortars, plasters and pigments (Gliozzo et al. 2021).

The first group of contributions explains how mortars have been made and used through the ages (Arizzi and Cultrone 2021; Ergenç et al. 2021; Lancaster 2021; Vitti 2021). An insight into their production, transport and on-site organization is further provided by DeLaine (2021). Furthermore, several issues concerning the degradation and conservation of mortars and plasters are addressed from practical and technical standpoints (La Russa and Ruffolo 2021; Caroselli et al. 2021).

The second group of contributions is focused on pigments, starting from a philological essay on terminology (Becker 2021). Three archaeological reviews on prehistoric (Domingo Sanz and Chieli 2021), Roman (Salvadori and Sbrolli 2021) and Medieval (Murat 2021) wall paintings clarify the archaeological and historical/cultural framework. A series of archaeometric reviews illustrate the state of the art of the studies carried out on Fe-based red, yellow and brown ochres (Mastrotheodoros et al. 2021), Cu-based greens and blues (Švarcová et al. 2021), As-based yellows and reds (this paper), Pb-based whites, reds, yellows and oranges (Gliozzo and Ionescu 2021), Hg-based red and white (Gliozzo 2021) and organic pigments (Aceto 2021). An overview of the use of inks, pigments and dyes in manuscripts, their scientific examination and analysis protocol (Burgio 2021) as well as an overview of glass-based pigments (Cavallo and Riccardi 2021) are also presented. Furthermore, two papers on cosmetic (Pérez-Arantegui 2021) and bioactive (antibacterial) pigments (Knapp et al. 2021) provide insights into the variety and different uses of these materials.

This article is part of the Topical Collection on *Mortars, plasters and pigments: Research questions and answers*

✉ Elisabetta Gliozzo
elisabetta.gliozzo@uniba.it; elisabetta.gliozzo@gmail.com

Lucia Burgio
l.burgio@vam.ac.uk

[1] Dipartimento di Studi Umanistici, Università Di Bari, Bari, Italy

[2] Conservation Department, Victoria and Albert Museum, London, UK

[3] Department of Chemistry, University College London, London, UK

Introduction

The uses of arsenic and related mineral species are numerous and go far beyond the use that has been made of them as pigments. Arsenic has in fact been used as a poison but also as a medicinal remedy: proof of this are the numerous scientific works currently being carried out on arsenic in cancer treatments, using "old" compounds—well known to Chinese and Iranian medicine—and new pharmacological remedies (Bin et al. 2000; Miller et al. 2002; Nriagu 2002; Liu et al. 2008; Bujňáková et al. 2015; Darbandi and Taheri 2018).

Furthermore, arsenic has been and still is a fundamental component of several metal alloys (Mödlinger et al. 2018; 2019; Sabatini et al. 2020 on ancient arsenical copper and bronze) and it is therefore a valuable geo-resource for the countries that extract it (chiefly China and Chile nowadays; Dill 2010). For example, the use of arsenic chalcogenides in optics and optoelectronics represents an ever-expanding field (Bonazzi and Bindi 2008; Jovanovski and Makreski 2020).

Much of the recent literature has focused on the geochemistry of arsenic in polluted contexts and the critical role of biochemical processes for the As cycling in nature (*i.e.*, acid mine drainage and acid rock drainage; see, *e.g.*, Lee et al. 2006, Dogan and Dogan 2007, Saunders et al. 2008, Henke 2009, Catelani et al. 2018), as well as on its use as a component in technologically advanced materials (especially glass and metal). In this review, instead, we focus on arsenic as a constituent of red and yellow pigments, used from ancient times to the modern era. In the first part, we will deal with the mineralogical description, occurrence, properties, alterations and uses of these minerals while in the second part, we will describe the analytical techniques used for the characterization of these pigments and propose a guide for best practice in archaeometry.

Arsenic-based minerals and pigments

Arsenic and As-bearing types of minerals

The average abundance of arsenic in the Earth's crust is of 1.5–2 ppm (Plant et al. 2014). Arsenic is a constituent of several types of mineral deposits and is typically associated with those containing sulfides and sulfosalts. Arsenic-bearing minerals include arsenates, sulfides, oxides and, to a lesser extent, arsenites, arsenides and metal alloys (see O'Day 2006 for a detailed overview on the chemistry and mineralogy of arsenic). Overall, they show all basic colors and bear variable amounts of As, frequently combined with Fe, Co, Ni, Cd, Cu, Ag, Au and Pb.

Minerals containing As can provide pigments with different colours when associated with other chromophores. For example, the green pigment ($CaCu(AsO_4)(OH)$; see Brecoulaki 2014, Buzgar et al. 2014), the blue pigment obtained from processing cobaltite (CoAsS; see Matin and Pollard 2017), in addition to the red and yellow pigments (realgar, As_4S_4, and orpiment, As_2S_3, respectively) which represent the main topic of this review.

Before delving into this matter, however, it is necessary to introduce an important concept regarding the primary, secondary and synthetic nature of the mineralogical phases which will be covered below. Primary minerals are those occurring naturally and include sulfides such as arsenopyrite (FeAsS), realgar (AsS), orpiment and anorpiment (As_2S_3), duranusite (As_4S), dimorphite (As_4S_3), bonazziite (As_4S_4), uzonite (As_4S_5), alacranite (As_8S_9) and wakabayashilite ($(As,Sb)_6As_4S_{14}$).

Synthetic minerals are entirely man-made and are of primary importance in the investigation of pigments since their use is attested from the beginning of the history of painting (*e.g.*, the production of cuprorivaite for Egyptian blue). As for As-bearing pigments, their preparation has been studied in detail and their use has been attested from the fifteenth century (see also Rötter et al. 2007).

Secondary phases are those formed by the alteration of either primary or artificial minerals (see Drahota and Filippi 2009 for a comprehensive review with an environmental focus). Consequently, they can occur both in the natural environment and in altered art works, depending on several factors including temperature, pressure, reactivity with other pigments and especially light exposure. Important secondary phases include the polymorphs arsenolite and claudetite (As_2O_3), pararealgar (As_4S_4) and the so-called χ-phase (see below).

Finally, it should be emphasized that in the pictorial context, all three types of minerals and related pigments may have been used in a more or less conscious way, regardless of their nature. For example, the use of yellow pigments based on orpiment (primary) rather than pararealgar (secondary) and *vice versa* may not always have been the result of a deliberate choice. Moreover, orpiment and arsenolite were long considered the only possible realgar alteration products (before discovering that As_2S_3 cannot form in ambient air and that pararealgar is another possible form of As_4S_4) and therefore the historical literature may not be completely reliable on this matter (see Corbeil and Helwig 1995; Trentelman et al. 1996).

Mineralogical arsenic-bearing phases found (or not yet found) in yellow and red pigments

This section provides information on the composition and structure of the numerous As-bearing sulfides and oxides that have been found in several types of pictorial works. Consequently, it is focused on As-sulfides while As-oxides discussions are limited to arsenolite and claudetite. As for

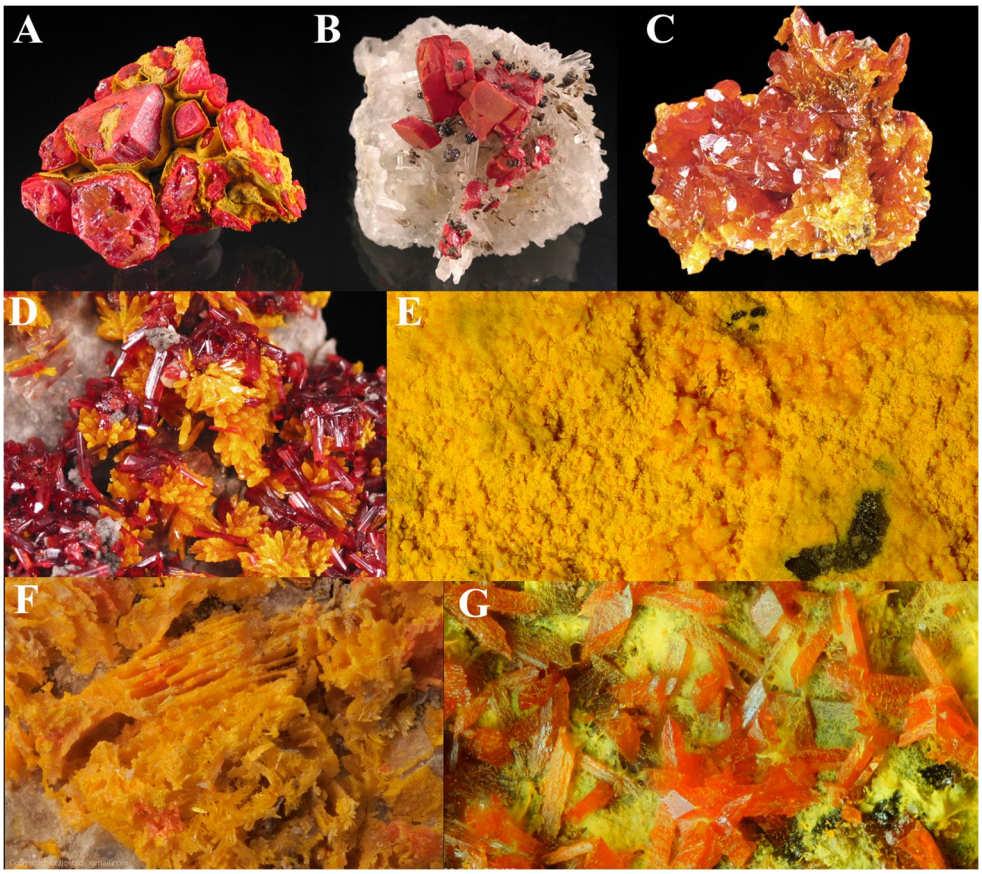

Fig. 1 Realgar and orpiment (**A**) and realgar on quartz (**B**), from Palomo Mine (Castrovirreina, Huancavelica, Peru — Specimen and photo khyberminerals.com). Orpiment (**C**) and orpiment and realgar (**D**) from Quiruvilca District (Santiago de Chuco, La Libertad, Peru — Specimen and photo khyberminerals.com). Pararealgar (**E**) from the Uzon Caldera (Kamchatka, Russia — Photo credits: OT. Ljøstad Mindat.org photo ID #858417). Alacranite (**F**, yellowish) with orange realgar from Lăzăreşti (Harghita, Romania — Photo credits: OT.Ljøstad Mindat.org photo ID # 792647). Reddish realgar and yellow, fibrous uzonite (**G**) from the Uzon Caldera (Kamchatka, Russia — Photo credits: OT. Ljøstad Mindat.org photo ID #859034). [All images are subject to copyright . Permission has been obtained for reproduction in this article. The CCBY licence does not supersede previously copyrighted material; therefore, these images remain under owner's copyright]

sulfides, some phases such as duranusite, χ-phase and wakabayashilite have been added, even if they are either not widely attested or not yet recognized in works of art, because little known or recently discovered. Conversely, As_4S_4(II) (Kutoglu 1976) and jeromite (Lausen 1928) have been omitted since the former has never been found in nature and the latter has been discredited by the IMA Commission.

Among As-sulfides (Fig. 1), the crystal structure of dimorphite, realgar, pararealgar, bonazziite, alacranite, uzonite and wakabayashilite consists of "a packing of cage-like, covalently bonded As_4S_n($n=3$, 4 and 5) molecules held together by van der Waals forces" (Bonazzi et al. 2006); conversely, orpiment and duranusite show layered structures. In the former group, the As:S ratio ranges from As_4S_3 in α- and β-dimorphites, to As_4S_4 in the three polymorphs realgar, pararealgar and bonazziite, to As_4S_4 and As_4S_5 in alacranite and to As_4S_5 in uzonite. Each phase is described below and the main features are reported in Table 1, while cage-like molecules and unit-cells are shown in Fig. 2.

Dimorphite (As_4S_3)

First found by Angelo Scacchi at the Solfatara of Pozzuoli (Naples, Italy; Scacchi 1850, p. 103 "dimorfina"), it was later investigated by Krenner (1907), Whitfield (1970, 1973a), Frankel and Zoltai (1973), Bonazzi and Bindi (2008), Gibbs et al. (2011) and Gavezzotti et al. (2013). Two types are currently known: α-dimorphite and β-dimorphite, although previous nomenclature used I and II instead of α and β. These two orange phases consist of As_4S_3 molecules and have the same space group symmetry (*Pnma*); however, the α-dimorphite is the low temperature phase, stable at room temperature, while β-dimorphite is the high-temperature phase, stable at above 130 °C (Whitfield 1970, 1973a). Both

phases can be obtained by vacuum sublimation, using As and S in stoichiometric proportion. Whether α or β dimorphite is obtained depends on temperature. Gavezzotti et al. (2013) demonstrated that, in this case (*i.e.*, artificial minerals), β-dimorphite is the stable phase. In the surroundings of the type locality (*i.e.*, Solfatara), Gavezzotti et al. (2013) found α-dimorphite associated with mascagnite, salammoniac, alacranite and likely lucabindiite at the Bocca Grande fumarole and β-dimorphite on a pyroclastic breccia at Vesuvius, associated with realgar, lafossaite and anhydrite.

Realgar (As_4S_4)

Also referred to as α-As_4S_4, it is a soft (1/2 on the Mohs scale) red, monoclinic, low-temperature (LT) phase. Although recognized since the eighteenth century (1747 in the IMA list), we must wait until the 1950s to witness the beginning of accurate crystallographic studies (Table 1; Ito et al. 1952; Hall 1966; Clark 1970; Mullen and Nowacki 1972; Roland 1972; Bryndzya and Kleppa 1988, Bonazzi et al. 1996 and 2003a; Kyono 2009). The occurrence of realgar will be examined in the section on the occurrence of As-sulfides further down, while the light-induced modifications are commented below, along with the description of the χ-phase.

Pararealgar (As_4S_4)

Formed by the alteration of realgar, this phase was first described by Roberts et al. 1980 as "powdery to granular fine-grained aggregates that replace realgar (…) yellow to orange-yellow with a resinous lustre, a bright yellow streak, Mohs hardness 1–1½, uneven fracture and no apparent cleavage". The two occurrences investigated by the authors (Gray Rock and Mount Washington copper deposit in British Columbia) were mainly associated with stibnite, although other Fe-, As-, Cu- and Sb-bearing phases were found (*e.g.*, lepidocrocite, pyrite, arsenopyrite, arsenolite, stibnite, tetrahedrite). The crystal structure was determined by Roberts et al. 1980 and Bonazzi et al. 1995. The first authors also fixed reaction rates and temperatures required to transform pararealgar into the HT β-phase (*e.g.*, 5 min at 220 and 420 °C, 10 min at 300 °C) or the "original" LT α-phase (*e.g.*, 1 day at 220 °C).

Alacranite (As_8S_9) and bonazziite

Alacranite is a rare red mineral whose identification has had a troubled history for the variable use that has been made of α and β descriptors (as similarly happened to dimorphite). First, Hall (1966, pp. 16–24) defined three polymorphs of AsS:

a) the high temperature (Bx +) orange form α-realgar (As_4S_4), annealed at 276 °C;
b) the intermediate temperature red (Bx-) form β-realgar and
c) the low temperature orange-yellow (Bx-) form γ-realgar (As_4S_4).

In the later literature, this initial nomenclature was frequently changed or differently used: (a) the α-phase has been sometimes used to indicate "normal" or "true" realgar; (b) the β-phase began to indicate the high temperature phase after Porter and Sheldrick (1972) but this denomination was not accepted by all authors (as pointed out by Douglass et al. 1992); and (c) the γ-phase was likely associated with para-realgar by Douglass et al. (1992). In the text that follows, the nomenclature used is the one reported by the individual authors. This choice can surely create some confusion but it was considered appropriate to shed light on terminological issues which, if not explained, could mislead the reader. For the same reason, it was deemed necessary to present the various information in the chronological order in which they were published.

In 1966, Roland (1966) fixed at 306(± 2 °C) the melting temperature of α-AsS. A few years later, Clark (1970) found the high temperature α-AsS ("high realgar") identified by Hall (1966) in a natural assemblage, namely the Alacrán Ag-As-Sb vein deposit in Chile. The same deposit also provided evidence of another type of "realgar" ("low realgar"), that the author defined "similar, but not identical to "normal" realgar, or β-AsS.

In 1972, Porter and Sheldrick (1972) purified tetra-arsenic tetrasulfide by sublimation and obtained both the mineral realgar, named α-As_4S_4, and a "previously unreported" high-temperature phase, named β-As_4S_4 (Table 1). Later studies by Bonazzi et al. (1995) showed that the As_4S_4 molecules of the latter phase are different from those of pararealgar.

Still in 1972, Roland (1972) explored the issue concerning the temperature of the reaction α-AsS ↔ realgar and provided new structural data on the high-temperature α-AsS phase (Table 1). The inversion T°C was fixed between 239 and 263 °C, depending on composition and boundary conditions (*e.g.*, preparation of the mix and presence of vapour).

In 1986, Popova et al. (1986) reported on the discovery of the high-temperature α-As_8S_9 phase (Альфа-сульфид мышьякю; Table 1) identified by Clark (1970), in the hydrothermal mercury-antimony-arsenic mineralization at the Uzon caldera in Kamchatka (Russia). This natural high-temperature mineral was then named alacranite (Аланранит) and was approved by the IMA committee in that same year (Hawthorne et al. 1988).

The later study performed by Migdisov and Bychkov (1998) clarified the temperature intervals corresponding to

Table 1 Space groups and structural parameters of As sulphides mentioned in the text

Compound	Authors nomenclature and other info	*N/S*	*Crystal system*	*Space group*	a (Å)	b (Å)	c (Å)	β (°)	Vol. (Å^3)	Z	Reference
α-Dimorphite	α-Dimorphite	*N*	*Orthorhombic*	*Pnma*	9.12(2)	7.99(2)	10.10(2)	=α=γ=90	736(3)	4	Whitfield 1970
		N	*Orthorhombic*	*Pnma*	9.1577(7)	8.0332(6)	10.2005(8)	=α=γ=90	750.4(10)	4	Gavezzotti et al. 2013
β-Dimorphite	β-Dimorphite	*N*	*Orthorhombic*	*Pnma*	11.21(2)	9.90(2)	6.58(1)	=α=γ=90	730(2)	4	Whitfield 1973a, b
	β-Dimorphite	*N*	–	–	11.2175(15)	9.9224(13)	6.6075(9)	=α=γ=90	735.44(17)	–	Gavezzotti et al. 2013
Realgar (α-phase)	Realgar, AsS		*Monoclinic*	*P2$_1$/n*	9.27	13.50	6.56	106.62	786.654	–	Ito et al. 1952
	β-As_4S_4 "low r.", "normal r."	*N*	*Monoclinic*	–	9.39(2)	13.54(3)	6.627(5)	106.0(2)	810(3)	–	Clark 1970[a]
	Realgar, AsS		*Monoclinic*	*P2$_1$/n*	9.325(3)	13.571(5)	6.587(3)	106.38(5)	799.7(6)	4	Mullen and Nowacki 1972
	Realgar, α-As_4S_4–s# A1	*N*	*Monoclinic*	*P2$_1$/c*	9.323(2)	13.555(2)	6.588(1)	106.48(2)	798.3(2)	–	Bonazzi et al. 1996
	Realgar, α-As_4S_4–s# A2	*N*	*Monoclinic*	*P2$_1$/c*	9.326(2)	13.560(2)	6.582(1)	106.53(1)	798.0(2)	–	Bonazzi et al. 1996
Pararealgar	$As_{0.997}S$	*N*	*Monoclinic*	*Pc or P2/c*	9.929(4)	9.691(6)	8.503(3)	97.06(2)	812.03	16	Roberts et al. 1980
	As_4S_4	*N*	*Monoclinic*	*P2$_1$/c*	9.909(2)	9.655(1)	8.502(1)	97.29(1)	806.8(2)	4	Bonazzi et al. 1995
	Synthetic β-As_4S_4[b] from s# B2	*S*	*Monoclinic*	*P2$_1$/c*	9.91(2)	9.655(9)	8.526(9)	96.8(1)	–	–	Bonazzi et al. 2006
Alacranite	α-As_8S_9, alacranite	*N*	*Monoclinic*	*P2/c*	9.89(2)	9.73(2)	9.13(1)	101.84(5)	859.9(3)	2	Popova et al. 1986
	Alacranite	*N*	*Monoclinic*	–	9.87(1)	9.73(3)	9.16(2)	101.52(4)	858(4)	–	Žáček and Ondruš 1997
	Alacranite *s.s.* (s# ALA-TL)	*N*	*Monoclinic*	*P2/c*	9.942(4)	9.601(2)	9.178(3)	101.94(3)	857.1(5)	4	Bonazzi et al. 2003b, 2006
β-As_4S_4-As_8S_9 series	Nonst. As_8S_{9-x} s# ALA 15	*N*	*Monoclinic*	*C2/c-P2/c*	9.940(2)	9.398(2)	9.033(2)	102.12(2)	825.0(3)[c]	–	Bonazzi et al. 2003a
	Nonst. As_8S_{9-x} s#ALA 2	*N*	*Monoclinic*	*microdo-mains*	9.936(2)	9.458(2)	9.106(2)	101.90(2)	837.3(3)[d]	–	Bonazzi et al. 2003a
	Nonst. As_8S_{9-x} s#ALA15	*N*	*Monoclinic*	*C2/c*	9.885(7)	9.446(2)	9.118(6)	101.32(3)	834.8(8)	4	Bonazzi et al. 2006
	Nonst. As_8S_{9-x} s#ALA16	*N*	*Monoclinic*	*C2/c*	9.963(3)	9.323(3)	8.962(4)	102.41(3)	813.0(1)	4	Bonazzi et al. 2006
Bonazziite (prev. β-As_4S_4)	α-As_4S_4 "HT poly." or "high r."	*N*	–	–	9.97(1)	9.29(1)	8.88(1)	102.6(1)	803(2)	–	Clark 1970[e]
	(HT) β-As_4S_4	*S*	*Monoclinic*	*C2/c*	9.957(3)	9.335(4)	8.889(5)	102.48(4)	806.7(6)	4	Porter and Sheldrick 1972
	(HT 263 °C) α–AsS	*S*	*Monoclinic*	*C*/c*	9.92(2)	9.48(2)	8.91(4)	101.50(15)	–	–	Roland 1972
	Alacranite As_4S_4[f] = synth. α–As_4S_4	*N=S*	*Monoclinic*	*C2/c*	9.943(1)	9.366(1)	8.908(1)	102.007(2)	811.4(1)	4	Burns and Percival 2001
	Monoclinic As_4S_4	*N*	*Monoclinic*	*C2/c*	9.961(3)	9.347(3)	8.891(3)	102.531(5)	808.1(5)	–	Žáček and Ondruš 1997
	s# B1	*S*	*Monoclinic*	*C2/c*	9.962(2)	9.313(1)	8.871(2)	102.54(1)	803.4(2)	–	Bonazzi et al. 1996
	s# B2	*S*	*Monoclinic*	*C2/c*	9.958(2)	9.311(2)	8.867(2)	102.57(1)	802.4(3)	–	Bonazzi et al. 1996
	Bonazziite	*N*	*Monoclinic*	*C2/c*	9.956(1)	9.308(1)	8.869(1)	102.55(2)	802.3(2)	4	Bindi et al. 2015a, b, c
χ-phase	χ-phase	*S*	–	–	9.707(6)	9.49(2)	9.04(1)	101.05(8)	817.7(20)	–	Douglass et al. 1992[g]
	From light-exp. realgar[h]	*S*	*Monoclinic*	*C2/c*	9.758(5)	9.522(5)	9.074(5)	100.84(5)	828.1(8)	–	Bonazzi et al. 1996
	From light-exp. HT βAs_4S_4[i]	*S*	*Monoclinic*	–	9.757(4)	9.512(7)	9.089(4)	100.97(3)	828.1(8)	–	Bonazzi et al. 1996
Uzonite	Tetra-arsenic pentasulfide	*S*	*Monoclinic*	*P2$_1$/m*	7.98	8.10	7.14	101.0	453.036	–	Whitfield 1973a, b
	Uzonite	*N*	*Monoclinic*	*P2$_1$/m*	7.94	8.08	7.10	100.1	448.44[j]	–	Popova and Polyakov 1985
	Uzonite	*N*	*Monoclinic*	*P2$_1$/m*	7.973(2)	8.096(2)	7.148(2)	101.01(2)	452.9(2)	2	Bindi et al. 2003

Table 1 (continued)

Compound	Authors nomenclature and other info	*N/S*	*Crystal system*	*Space group*	a (Å)	b (Å)	c (Å)	β (°)	Vol. (Å^3)	Z	Reference
As_4S_4(II)	As_4S_4[k]	*S*	*Monoclinic*	$P2_1/n$	11.193(6)	9.994(6)	7.153(4)	92.8(5)	799.2(8)	4	Kutoglu 1976
Orpiment	Orpiment, As_2S_3	–	–	$C_{2h}^5 - P^{2l}/n$	11.46	9.56	4.21	90	–	–	Morimoto 1949
	Orpiment, As_2S_3	*N*	–	$C_{2h}^5 - P^{2l}/n$	11.46(4)	9.57(2)	4.22(5)	90.5(5)	–	–	Morimoto 1954
	Orpiment, As_2S_3	*N*	*Monoclinic*	$P2_1/n$	11.475(5)	9.577(4)	4.256(2)	90.68(5)	467.7(8)	4	Mullen and Nowacki 1972
Duranusite	Duranusite, As_4S	*N*	*Orthorhombic*	-	3.576	6.759	10.074	=α=γ=90 °C	243.5	2	Bonazzi and Bindi 2008
Duranusite	Duranusite, As_4S	*N*	*Orthorhombic*	*Pmna*	3.611(5)	6.755(8)	10.10(1)	=α=γ=90 °C	246.3(5)	2	Bonazzi et al. 2016
Anorpiment	Anorpiment	*N*	*Triclinic*	*P*1	5.7577(2)	8.7169(3)	10.2682(7)	α 78.152(7) β 75.817(7) γ 89.861(6)	488.38(4)	4	Kampf et al. 2011
Wakabayashilite	Wakabayashilite	*N*	*Monoclinic*	$P2_1$	25.17(4)	6.48(1)	25.24(8)	120.0	–	–	Kato et al. 1970
	Wakabayashilite	*N*	*Orthorhombic*	$Pna2_1$	25.262(1)	14.563(1)	6.492(1)	=α=γ=90 °C	2388.4(2)	4	Bonazzi et al. 2005
–	Orthorhombic (~As_4S_5)	*S*	*Orthorhombic*	*Pccn*	19.352(7)	10.166(3)	8.697(4)	=α=γ=90 °C	1711(1)	8	Bindi and Bonazzi 2007
Arsenolite	Arsenolite	*S*[l]	*Cubic*	*Fd3m*	11.07343(5)	–	–	–	1357.8	16	Ballirano and Maras 2002
Claudetite	Claudetite	*N*	*Monoclinic*	$P2_1/n - C_{2h}^5$	5.25(1)	12.99(1)	4.53(1)	93.88	–	4	Pertlik 1978a, b

N/S = natural or synthetic, *r.* = realgar, *s#* = sample, *Nonst.* = non-stoichiometric, *poly.* = polymorph, *light-exp.* = light exposed]

[a]Indexed byBonazzi et al. (1996)

[b]After 24-h exposure to polychromatic light (550-nm-long wavelength pass filter)

[c]In non-stoichiometric compounds the volume was found to linearly increase from β-As_4S_4 to alacranite *ss*. as a function of the S content

[d]In non-stoichiometric compounds the volume was found to linearly increase from β-As_4S_4 to alacranite *ss*. as a function of the S content

[e]Indexed by Bonazzi et al. (1996)

[f]Bonazzi et al. 2003b suggested to identify the compound analysed by Burns and Percival (2001) as the β-As_4S_4 unnamed phase and not as alacranite

[g]Indexed by Bonazzi et al. (1996)

[h]Obtained from natural realgar crystals, after 24-h exposure to polychromatic light (550-nm-long wavelength pass filter)

[i]Obtained by heating a realgar sample from Shimen (China) at 295 °C for 24 h

[j]Calculated from unit cell

[k]Synthetized using As:S = 1:1, 500–600 °C

[l]Obtained by oxydation of realgar

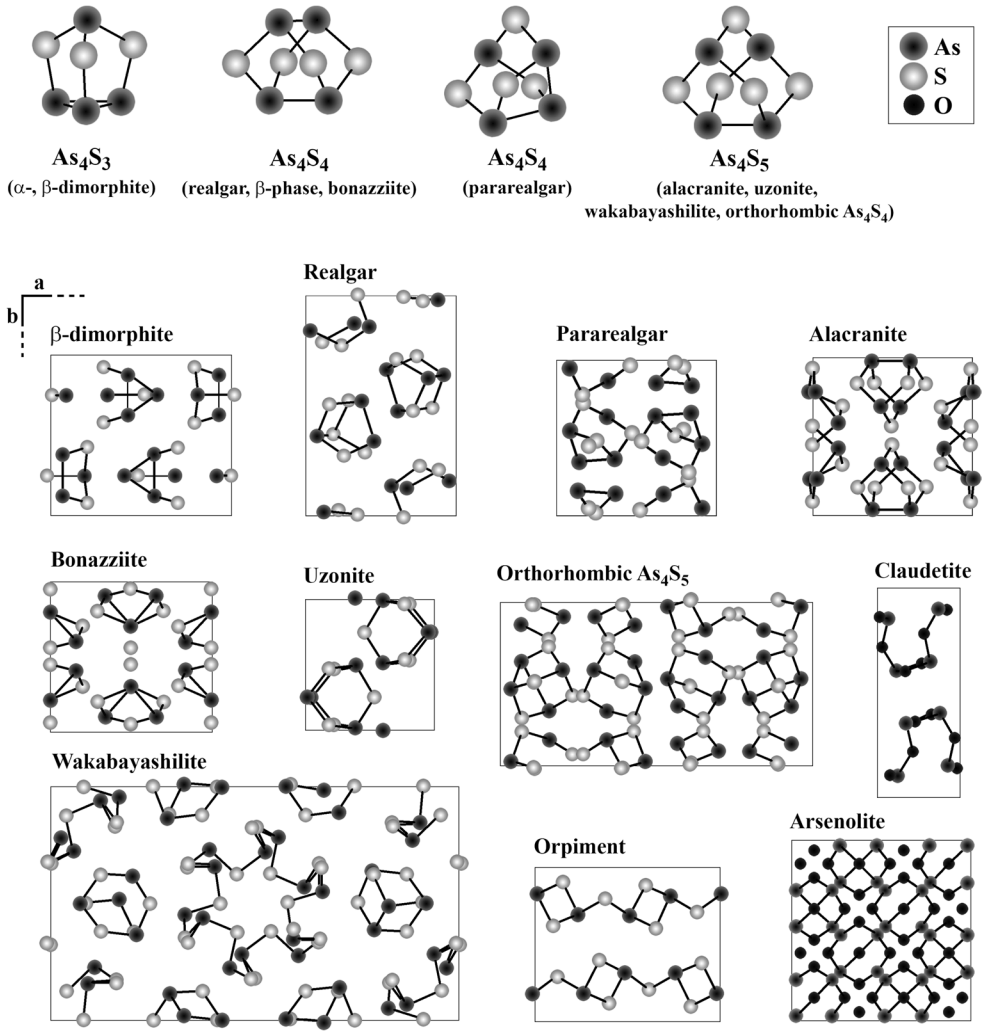

Fig. 2 The cage-like molecules and the corresponding mineralogical phases for which the crystal structure is shown along *c* axis (base drawings from Ruff database and Bonazzi and Bindi 2008)

realgar (70–95 °C), realgar + orpiment + uzonite + alacranite (50–75 °C) and orpiment + amorphous As sulfides (30–50 °C) assemblages and showed that the orpiment-uzonite (Fig. 3, Eq. 1) and the uzonite-alacranite (Fig. 3, Eq. 2) replacements were both reversible transformations.

During the same period, Žáček and Ondruš (1997) identified two similar arsenic sulfides in a burning waste pile of the Kateřina colliery in Radvanice (Bohemia). The first one corresponded to "true" alacranite (*sensu* Popova et al. 1986) while the second one, named monoclinic As_4S_4, was found to be isostructural with alacranite but with a lower parameter b (Table 1).

The studies proceeded in the following years with the identification of alacranite in the seafloor around Lihir Island (Papua New Guinea) by Burns and Percival (2001). Their study provided structural information on alacranite—defined as "the third polymorph of this composition, after realgar and pararealgar"—and led them to state that (a) the formula was As_4S_4 rather than As_8S_9; (b) it was "identical to that of synthetic α–As_4S_4"; and (c) it should have formed at relatively low temperatures, according to previous studies performed by Heinrich and Eadington (1986) and Migdisov and Bychkov (1998).

In 2002, Wilkin and Ford (2002) discovered that alacranite can also precipitate from solution through acid extraction and the following years marked a decisive step towards the definition of alacranite, β-phase and χ-phase (for the latter, see below the dedicated section).

The studies performed by Bonazzi et al. (2003a-b) took stock of the previous knowledge and definitively clarified the formulas and structure of these phases. Firstly, the As_8S_9 formula was restored for alacranite *s.s.* and the distinction between the natural compounds As_8S_9 (alacranite *s.s.*) and the unnamed β-As_4S_4 phase was highlighted and clarified

$$2As_2S_3\ \text{(orpiment)} = As_4S_5\ \text{(uzonite)} + S\ \text{(aq)} \quad \text{Eq. 1}$$

$$2As_4S_5\ \text{(uzonite)} = As_8S_9\ \text{(alacranite)} + S\ \text{(aq)} \quad \text{Eq. 2}$$

$$4FeAs_2 + 12O \rightarrow 2Fe_2O_3 + 2As_2O_3 \quad \text{Eq. 3}$$

$$As_2O_{3(aq)} + 3H_2S_{(g)} \rightarrow As_2S_{3(g)} + 3H_2O_{(l)} \quad \text{Eq. 4}$$

$$FeS_{(s)} + 2HCl_{(aq)} \xrightarrow{\Delta} H_2S_{(g)} \quad \text{Eq. 5}$$

$$CH_3CSNH_{2(g)} + H_2O_{(l)} \rightarrow CH_3CONH_{2(aq)} + H_2S_{(g)} \quad \text{Eq. 6}$$

$$\alpha\text{-phase (realgar)} \overset{\text{sunlight}}{\longleftrightarrow} \chi\text{-phase} \overset{\text{sunlight}}{\longleftrightarrow} \text{pararealgar} \quad \text{Eq. 7}$$

$$\text{Pararealgar} \rightarrow \chi\text{-phase} \rightarrow \beta\text{-phase} \rightarrow \alpha\text{-phase (realgar)} \quad \text{Eq. 8}$$

$$5As_4S_4 + 3O_2 \rightarrow 4As_4S_5 + 2As_2O_3 \quad \text{Eq. 9}$$

$$5As_4S_4\ \text{(realgar)} + 3O_2 + hv \rightarrow 4As_4S_5 + 2As_2O_3 \quad \text{Eq. 10}$$

$$As_4S_5 \rightarrow As_4S_4\ \text{(pararealgar)} + S \quad \text{Eq. 11}$$

$$As_4S_4\ \text{(realgar)} + S \rightarrow As_4S_5 \quad \text{Eq. 12}$$

$$As_4S_5 \rightarrow As_4S_4\ \text{(pararealgar)} + S \quad \text{Eq. 13}$$

$$9\beta As_4S_4 + 3O_2 \rightarrow 7As_4S_4 + 4AsS_2 + 2As_2O_3 \quad \text{Eq. 14}$$

$$7As_4S_4(r) + 3O_2 + \boldsymbol{hv} \rightarrow (4 - x/2)As_4S_4(p) + (4 - x)As_2S_3 + xAs_4S_5 + 2As_2O_3 \quad \text{Eq. 15}$$

$$\boldsymbol{a}As_4S_4(p) \rightarrow \boldsymbol{b}As_4S_4 + \boldsymbol{c}As_4S_4(r) + \boldsymbol{d}As_2S_3 + \boldsymbol{e}As_xS_y \quad \text{Eq. 16}$$

Fig. 3 Notable equations mentioned in text

(Table 1). Secondly, the existence of a continuous series between these two groups (realgar-type As_4S_4 and uzonite-type As_4S_5) was suggested (Bonazzi et al. 2003a; Bonazzi and Bindi 2008) and the gradual changes of the translation lattice simmetry from β-As_4S_4 (*C2/c*; V = 803(2) Å^3) to alacranite *s.s.* (*P2/c*; V = 860(3) Å^3) were explained by the "simultaneous presence of As_4S_4 (*C2/c*) and As_8S_9 (*P2/c*) microdomains". The current terminology sometimes uses the plural term alacranites to describe this β-As_4S_4-As_8S_9 series but the traces of the various passages (now outdated) which led to recognize alacranite as an ordered sequence of As_4S_4 and As_4S_5 molecules are still traceable, for example, in Strunz and Nickel (2001) and in the AMCSD (Downs and Hall-Wallace 2003).

In the past 10 years, the structural and vibrational properties and growth mechanisms of alacranite were further investigated (Gibbs et al. 2011; Pagliai et al. 2011) and new occurrences were reported by Mladenova (2000) and Bonazzi and Bindi (2008), in the Madzavoro deposit (eastern Rhodopes, Bulgaria) and the Sb—Hg deposit of Khaidarkan (Kyrgyzstan), respectively. Moreover, Mumford et al. (2013) demonstrated that alacranite (As_8S_9) can be precipitated by a novel As(V)-respiring anaerobe strain MPA-C3.

More information on the high-temperature (HT) unnamed β-As_4S_4 phase was instead acquired as part of the studies concerning the so-called χ-phase and the continuous involvement of Bonazzi and coworkers in the study of arsenic sulfides. These authors finally found a truly natural

specimen of this phase within the collection of the Museo di Storia Naturale, Firenze, coming from the Khaidarkan deposit mentioned above. This orange mineral—which was then named bonazziite—was approved by the IMA (no. 2013–141) in the year 2013 and therefore constitutes the natural analog to the previously identified synthetic β-As_4S_4 phase (Bindi et al. 2015a). Lastly, it is worth quoting Ledbetter et al. 2007 who discovered an arsenic-metabolizing organism able to produce β-realgar (*sensu* Muniz-Miranda et al. 1996).

Uzonite (As_4S_5)

H.J. Whitfield synthesized tetra-arsenic pentasulfide and solved its crystal structure in 1973 (Whitfield 1973b). In the year 1984, the IMA Commission approved uzonite as a new mineral (no. 1984–027) based on Popova and Polyakov (1985) who found this phase at the Uzon caldera (Russia). Twenty years later, Bindi et al. (2003) took up the studies previously carried out on Russian materials and provided the crystal structure of uzonite from the type locality. Uzonite is a soft (1.5 on the Mohs scale), yellow mineral which is not affected by light exposure (Bindi et al. 2003) and it is also found in Chinese and Indian medicinal remedies (Furuta and Sato 2016; Sharma et al. 2017).

Wakabayashilite [$(As,Sb)_6S_9$][As_4S_5]

This is a rare mineral characterized by As_4S_5 molecules similar to those of alacranite and uzonite. It was first identified by Kato et al. (1970) at the Nishinomaki mine (30 km west of Takasaki, Gunma). After Kato's work, the crystal structure was investigated by Scott and Nowacki (1975), using a realgar specimen from the White Caps mine (Manhattan, Nevada-W.W. Pinch of Rochester collection, New York) and then solved by Bonazzi et al. (2005), similarly using acicular crystals from the White Caps mine (Museo di Storia Naturale collection, Firenze). The chemical formula was modified to [$(As,Sb)_6S_9$][As_4S_6] by the former authors and then to [$(As,Sb)_6S_9$][As_4S_5] by the latter authors. Bonazzi et al. (2005) went into detail and described this phase as constituted by two structural units: (1) [M_6S_9] bundle-like unit (M = As, Sb) and (2) As_4S_5 cage-like molecules. The investigation later performed by Bindi et al. (2014a) confirmed the chemical formula provided by Bonazzi et al. (2005) and highlighted some analytical problems of the previous literature. Minor amounts of Cu, Zn and Tl were found to be common in several specimens and, for these cases, the new formula $M_x[(As,Sb)_6S_9][As_4S_5]$ (with M = Cu, Zn, Tl and $0.00 < x < 0.13$ a.p.f.u.) was provided (Bindi et al. 2014a). Lastly, light-exposure experiments were found to be irrelevant since they did not affect the crystal structure of wakabayashilite (Bonazzi et al. 2005).

Orpiment and anorpiment (As_2S_3)

Orpiment, from the Latin word *auripigmentum*, is a yellow phase which is currently exploited for semiconducting and optical applications. The first description of this mineral is lost in the history of mineralogy while the structural determinations were reported by Morimoto (1949, 1954) and Mullen and Nowacki (1972).

The greenish yellow anorpiment was approved by IMA in 2011. This phase is the triclinic dimorph of orpiment and was discovered at the Palomo mine in Peru (Castrovirreyna Province, Huancavelica Department) by Kampf et al. (2011). The mine is located in a volcanic area (andesitic lavas, pyroclastic rocks, tuffs and breccias) and the main ore minerals include pyrite, galena, sphalerite and chalcopyrite. Anorpiment was characterized as "a low-temperature hydrothermal mineral associated with dufrénoysite, muscovite, orpiment, pyrite, and realgar" and its structure was solved by its discoverers.

Duranusite (As_4S)

Johan et al. (1973) discovered this orthorhombic phase in the Duranus deposit (close to Mt. Séréna, Alpes-Maritimes, France) in association with native arsenic and realgar. The structure has been studied in detail by Kyono (2013) and Bonazzi et al. (2016). The former hypothesized As_4S molecular geometry while the latter demonstrated a layered structure that "consists of an alternated stacking along the [010] axis of two kinds of corrugated layers which match the As_2 and As_2S composition, respectively" (Bonazzi et al. 2016). Duranusite has also been found as a biogenic product by dissimilatory metal-reducing bacterium Shewanella sp. HN-41 (Lee et al. 2007).

Arsenolite and claudetite (As_2O_3)

These two secondary polymorph phases range in color from white to bluish and pale yellow, depending on the levels of impurities. Arsenolite's crystal structure was investigated by Bozorth (1923), Pertlik (1978a), Treacy and Taylor (1981) and Ballirano and Maras (2002) while that of claudetite was studied by Becker et al. (1951, 1954), Frueh (1951), Pertlik (1975 and 1978b) and Treacy and Taylor (1981).

Artificial As-based pigments

The use of arsenic-based artificial pigments is attested in numerous documents ranging from ancient treatises to encyclopedias and pharmaceutical prontuary (Grundmann and Rötter 2007). However, a problem that in many cases remains open concerns the natural or artificial origin of the pigments cited by the authors. For example, Pliny (*Naturalis*

Historia, 35, 12, 30[1]) listed the *auripigmentum* among natural pigments, clearly distinguishing it from those that "*finguntur*" (*i.e.* the artificial ones), among which realgar (*sandaraca*) is included. However, the problem is not limited to ancient times and, in fact, it is possible to find orpiment mentioned as an artificial pigment by Cennino Cennini (*Il libro dell'arte*, chapter 47[2]) as well as quasi-modern texts in which orpiment is erroneously identified (on the basis of the yellow color) instead of pararealgar or other yellow As-sulfides.

The production of artificial orpiment is documented in various literature sources (*e.g.*, Dossie 1764, Rose 1916, Merrifield 1967, reporting on the 1431 manuscript of Jehan Le Begue) and it has been reconstructed as a 4-steps process: (1) roasting of arsenic ores such as löllingite ($FeAs_2$) in iron boilers to produce arsenolite (Fig. 3, Eq. 3); (2) collection and selection of the formed arsenic crusts and elimination of impurities through sublimation; (3) heating of the resulting compound to obtain a light yellow arsenolite glass; and (4) addition of sulfur (3 wt%) to convert the former glass into a yellow glass (with ~ 97 wt% arsenolite) called '*gelber arsenik*' (Grundmann and Rötter 2007).

The production of these pigments for artistic purposes has long been investigated, starting from Wallert (1984) and West FitzHugh (1997); however, the first systematic work on this topic is due to Grundmann and Rötter (2007) who experimentally tested the production cycle and provided the necessary information to distinguish natural from artificial pigments. They prepared five series of tests, using two different wet-process precipitations (using thioacetamide for series I and hydrogen sulfide for series II) and three different dry-process cakes and/or sublimates (using natural orpiment for series III, natural orpiment + synthetic arsenolite for series IV and synthetic arsenolite + sulfur for series V). The first series of experiments (wet process I and II) produced two golden yellow amorphous powders, partially different from each other in color distribution, shape and state of aggregation but indistinguishable under the microscope if mixed. The second series of experiments (dry process III–V) showed that orpiment is formed only if orpiment itself is used as a raw material either by roasting (series III) or by roasting and sublimating (series IV). In these cases, the product also includes colourless arsenolite and, occasionally, alacranite members. In the absence of orpiment (series V), a mixture of colorless aggregates of arsenolite and yellow glassy drops and spherules (amorphous) are produced. The same authors claimed that the production of artificial As-based pigments may have been born in conjunction with the production of vermilion through the roasting of sulfur and arsenic ores and that the arsenolite smelters made it popular during the sixteenth century.

It has to be added, however, that this mining activity was initially aimed at gold extraction, along with silver and other precious metals, and it may have been this very activity that triggered the production of a by-product such as a pigment. The frequent natural association of arsenic with gold-bearing deposits (see the section on the As-sulfides occurrence below) suggests a close link between the beginning of the two processes. Moreover, arsenic is still nowadays a by-product of pyrometallurgical processes for copper and gold.

Proceeding further, Grundmann and Richter (2008), added a terminological note, specifying that "orpiment glass (g-As_2S_3)" should be used for arsenic sulfide particles molten and solidified from natural orpiment" while "arsenic sulfide glass (g-As_xS_x)" should be used for all other types of compounds of these series.

Additional experiments have been performed by Vermeulen et al. (2019) who synthetized (a) four compounds with different As:S ratio (40:60, 34:66, 30:70 and 25:75) and final colors (from orange to light yellow), using the melt-quenching method (800 °C for 48-h cold water; dry process) and (b) two yellow amorphous arsenic sulfide compounds (suitable for painting), using the wet-process (hydrochloric solution of arsenic trioxide treated with a stream of hydrogen sulfide-pyrite and thioacetamide). For all these compounds, the reaction series (Eqs. 4–6) and are provided in Fig. 3.

On a similar topic, a year earlier, Vermeulen et al. (2018a) had identified both orpiment and amorphous arsenic sulfide on two works of art (seventeenth to eighteenth centuries) and hypothesized that pararealgar was the starting material from which the amorphous arsenic sulfide was produced.

To conclude on the production of orpiment, it is also worth remembering the pigment King's yellow, which would have been produced through the sublimation of either "common orpiment" or a mixture of sulfur and arsenic, according toDossie (1764).[3] In this regard, West FitzHugh (1997) reported a note from a Boston store that in the 1970s listed

[1] "*Sunt autem colores austeri aut floridi.utrumque natura aut mixtura evenit.floridi sunt—quos dominus pingenti praestat—minium, Armenium, cinnabaris, chrysocolla, Indicum, purpurissum; ceteri austeri.ex omnibus alii nascuntur, alii fiunt. nascuntur Sinopis, rubrica, Paraetonium, Melinum, Eretria, auripigmentum; ceteri finguntur, primumque quos in metallis diximus, praeterea e vilioribus ochra, cerussa usta, sandaraca, sandyx, Syricum, atramentum*.".

[2] "*Questo tal colore è artificiato, e fatto d'archimia, ed è proprio tosco*." (https://archive.org/details/dicenninocennini00cenn/page/40/mode/2up?q=giallo).

[3] [On furnaces] "The furnace for subliming king's yellow must have a sand-pot; as the heat of the naked fire would be too great" (Dossie 1764, p. 20). [On 'Common orpiment'] "When purified by subliming, it becomes the king's yellow" (Dossie 1764, p. 98). [On sublimation] "Sublimation is the saising solid bodies in fumes, by means of heat: which fumes are afterwards collected by condensation, either in the upper part of the same vessel where they are raised, or in others properly adapted to it for that purpose" (Dossie 1764, p. 30. [On King's yellow] "This pigment must be prepared by mixing sulphur and arsenic by sublimation, which may be done in the following man-

King's yellow among the products imported from London and proposed a connection between the name of this pigment and the Arabic nomenclature where orpiment and realgar are referred to as "the two kings."

Less is known about realgar production. Pliny probably confuses realgar with minium since he includes the production of *sandaraca* with that of *cerussa* (*Naturalis Historia* 34, 54, 175–176[4]) but immediately after he adds a detail that could instead be true when he states that "it is found both in gold-mines and in silver-mines. The redder it is, the more pure and friable, and the more powerful its odour, the better it is in quality" (*Naturalis Historia* 34, 177, 55[5]). Undoubtedly, this description takes us back to the gold deposits and seems to contradict the artificial nature of the pigment (which probably referred to minium). To support this hypothesis, we can quote the words in Pliny's following book (*Naturalis Historia* 35, 22, 39[6]) in which he returns to the subject and specifies that there is also another type of *sandaraca* "prepared by calcining ceruse in the furnace."

The contemporary Dioscorides also seems to refer to both a natural and an artificial origin in his *De Materia Medica* (5, 121–122):

"*Arsenicum* is found in the same mines as *sandaraca*. The best is crusty, gold in colour and with crusts like fish scales (as it were) lying one over another, and it is not mixed with any other material. That which is found in Mysia (which is in Hellespont) is like this. There are two kinds: one as mentioned, and the other in clumps and like *sandaraca* in colour. It is brought from Pontus and Cappadocia. It is roasted as follows: place it in a new ceramic jar, set it over burning coals and stir it continuously; and when it is red-hot and has changed colour, cool it, beat it finely, and put it in jars. It is antiseptic, astringent, and scab forming with a burning, strong, biting strength, and it is one of those medicines that repress abnormal growths and make the hair fall out.

Sandaraca is most highly valued which is fully red, brittle, easily pounded into small pieces, and pure — looking like cinnabar in colour, and also having a sulphurous smell. It has the same properties and method of roasting as arsenicum. Used with rosin it heals loss of hair [alopecia], and with pitch it removes leprous nails. It is good with oil for lice infestations, and with grease it dissolves small swellings. It is also good with rosaceum for ulcers in the nostrils and mouth, and for other pustules, as well as for venereal warts. It is given with mead [honey wine] to those who spit up rotten matter, and it is made into an inhalant with rosin for old coughs, the smoke drawn through a funnel into the mouth. Licked in with honey it clears the voice, and it is given with rosin in a catapotion [pill] to the asthmatic." (Translation from Osbaldeston and Wood 2000).

Undoubtedly, the interest of Dioscorides is exclusively medical and pharmaceutical but the information about the production of arsenic and realgar can still be considered reliable.

Still browsing among ancient authors, Cennino Cennini (*Il libro dell'arte*, chapter 48[7]) informs about the highly toxic nature of the "*risalgallo*" but does not dwell on its nature or preparation. Conversely, Merrifield (1967), reporting on a seventeenth century manuscript, includes "red orpiment" as a product of the melting, cooling and grinding of orpiment.

West FitzHugh (1997) listed a few examples of modern production techniques such as heating a mixture of pyrite and arsenopyrite to obtain a mixture of realgar and orpiment, the fusion of sulfur and arsenic in the presence of carbon or the heating of orpiment with arsenic.

Lastly, Grundmann and Rötter (2007) inform us of the production run by the Güttler arsenolite smeltery, where a mixture of löllingite and sulfur was heated to obtain a red sublimation product.

The χ-phase and the light-induced variations in arsenic sulfides

Despite the fact that other studies on light-induced transformations of arsenic sulfides had already been published (*e.g.*, Bhatnagar and Rao 1923; Cahoon 1965; Keneman

Footnote 3 (continued)

ner: Take of arsenic powdered and flowers of sulphur in the proportion of twenty of the first to one of the second: and having put them into a sublimer, sublime them in a sand-heat, with such a furnace as is described p. 20, according to the general direction given p. 30. The operation being over, the king's yellow will be found in the upper part of the glass; which must be carefully separated from any caput mortuum or foul parts that maybe found in the glass with it. It must be afterwards reduced to an equal powder by levigation." (Dossie 1764, p. 90–91).

[4] "*Psimithium quoque, hoc est cerussam, plumbariae dant officinae, laudatissimam in Thodo.fit autem ramentis plumbi tenuissimis super vas aceti asperrimi inpositis atque ita destillantibus. quod ex eo cecidit in ipsum acetum, arefactum molitur et cribratur iterumque aceto admixto in pastillos dividitur et in sole siccatur aestate. fit et alio modo, addito in urceos aceti plumbo opturatos per dies X derasoque ceu situ ac rursus reiecto, donec deficiat materia. quod derasum est, teritur et cribratur et coquitur in patinis misceturque rudiculis, donec rufescat et simile sandaracae fiat. dein lavatur dulci aqua, donec nubeculae omnes eluantur. siccatur postea similiter et in pastillos dividitur. vis eius eadem quae supra dictis, lenissima tantum ex omnibus, praeterque ad candorem feminarum. est autem letalis potu sicut spuma argenti. postea cerussa ipsa, si coquatur, rufescit*.".

[5] "*Sandaracae quoque propemodum dicta natura est. invenitur autem et in aurariis et in argentariis metallis, melior quo magis rufa quoque magis virus sulpuris redolens ac pura friabilisque*.".

[6] "*Sandaracam et ochram Iubra tradidit in insula Rubri maris Topazo nasci, sed inde non pervehuntur ad nos. sandaraca quomodo fieret diximus. fit et adulterina ex cerussa in fornace cocta. color esse debet flammeus. pretium in libras asses quini*.".

[7] "*Questo colore è tossico proprio*".

et al. 1978; Stodulski et al. 1984); Douglass et al. (1992) first proved that the radiation wavelength is crucial for the transformation of realgar into pararealgar. In detail, the authors demonstrated that if realgar is exposed to UV and IR radiation or wavelengths shorter than 500 nm, no transformations occur. On the other hand, wavelengths greater than 560 nm (esp. above 610 nm) slow down the reaction rate, as they pass through the crystals without being absorbed "and little energy is being transferred to break bonds".

The research performed by Douglass (Table 2) and co-workers also led to the identification of an intermediate phase precursor to the formation of pararealgar, named χ-phase (Table 1), which formed after the LT α-phase (realgar, Fig. 3, Eq. 7) with variable times depending on which radiation wavelength was used. Moreover, the χ-phase was also detected in the reverse reaction as a precursor of the HT β-phase (Fig. 3, Eq. 8), performed at temperatures of 175 and 190 °C. Considering that "normal" β-phase (*i.e.*, not involved in the reverse reaction) took several weeks (at 240 °C) to transform into α-phase (realgar), the ~ 2 days it took for the reaction (Fig. 3, Eq. 8) to complete suggested that χ-phase played a role in accelerating the reaction.

Douglass' studies were immediately received in an archaeometric environment by Trentelman et al. 1996 who warned about the veracity of the current association red = realgar, yellow = orpiment and presented for the first time the identification of the χ-phase in the sixteenth-century (ca. 1547) painting '*The Dreams of Men*' by Tintoretto.

In the same year, Bonazzi and coworkers added an important piece of information as they clarified some aspects of the crystal structure of the χ-phase obtained from light-induced alteration of both realgar and the HT phase β-As_4S_4 (Tables 1 and 2) (Bonazzi et al. 1996). The authors observed that, increasing light-exposure, the formation of the χ-phase was "preceded by a strong anisotropic increase of the unit-cell volume" and determined that while in realgar it is *a* and *c* sin β which linearly increase (with *b* remaining unchanged), in the β-As_4S_4 phase it is instead *b* and *c* sin β that increase (with a decreasing) and the χ-phase so occurs after 1560 min. Last but not least, the authors first suggested to consider the χ-phase as an "expanded, less-ordered β phase" (Bonazzi et al. 1996, 2006), probably characterized by a lower molecular symmetry, as demonstrated also by the results provided by Muniz-Miranda et al. (1996) (Table 2, Fig. 4A).

A few years later, Bindi et al. (2003) tested uzonite and the negative evidence they obtained (*i.e.*, no transformation) suggested to the authors that only As_4S_4 molecules are affected by light exposure while the As_4S_5 molecules of uzonite are not. This new data led them to speculate that (a) light induces an increase of sulfur in the structure; (b) the increase of sulfur induces an increase of As_4S_5 molecules that, in turn, explains the increase of the unit-cell volume; and (c) likely, As_4S_5 molecules were not able to incorporate additional sulfur as the As_4S_4 were instead. The Eq. 9 (Fig. 3) was then proposed.

Kyono et al. (2005) followed a similar path and found comparable results as to the variation of the *a* and *c* sin β parameters and the unit-cell volume expansion, thus substantiating previous results. However, the authors further claimed that Eq. 9 does not necessary need light exposure to happen since small amount of oxygen are sufficient to trigger the reaction and, contrary to Bonazzi et al. (1996), suggested that the volume expansion of the unit-cell was only due to variable intermolecular distances. Moreover, although lacking experimental evidence (especially on S migration), they described the realgar transformation into pararealgar as the cycle illustrated in Fig. 4B: (a) free S atom combines with realgar (As_4S_4) and produces the As_4S_5 molecule; (b) the As_4S_5 molecule releases an S atom and becomes pararealgar (As_4S_4). The cycle can be further by the series of equations Eqs. 10–13 in Fig. 3 (from Naumov et al. 2007).

Following these results, Ballirano and Maras (2006) deepened the kinetics of the process and suggested that (a) the formation of the χ-phase and the expansion of realgar occur contemporaneously (not one before the other); and (b) the production of an intermediate As_4S_{4+x} phase occurs "because it represents the only sulfide phase that is able to sustain the presence of As_4S_5-type cages" (Table 2).

In the same year, Bonazzi et al. (2006) published a new paper on light-induced changes in As-sulfides where they investigated the reaction that led to the transformation of the β-As_4S_4-As_8S_9 series and the synthetic β-As_4S_3 phase into pararealgar (Table 2). Experimental data demonstrated that light-induced changes in these phases consist in a marked increase of the unit-cell volume in all crystals of the β-As_4S_4-As_8S_9 series but not in alacranite *s.s.* (stoichiometric As_8S_9) and synthetic β-As_4S_3. To explain the reasons for these diversified or imperceptible increases, the authors considered both the different types of molecules and their different packings, *i.e.* the two factors that determine the ability of the molecules to incorporate the sulfur necessary for the conversion from As_4S_4 to As_4S_5. Their conclusions, sometimes confirmatory or hypothetical, can be summarized as follows: (1) the increase of the exposure time provokes the increase of As_4S_5 molecules in the structure, due to the incorporation of sulfur by As_4S_4 that transforms into As_4S_5 (according to Eq. 12); (2) the negligible expansion of the stoichiometric alacranite unit-cell is tentatively explained by excluding alacranite microdomains (*P2/c*) from the reaction and thus implying that only β-As_4S_4 microdomains (*C2/c*) are involved in this light-induced alteration process; (3) only the As_4S_4 molecule is able of incorporating sulfur while the As_4S_3 and As_4S_5 molecules are not; (4) the complete transformation from β-As_4S_4 (*C2/c*) to pararealgar (As_4S_4; $P2_1/c$) does not imply a complete rearrangement since the packing

Table 2 Experimental condition of the irradiation experiments performed on arsenic compounds (chronological order)

Tested starting material	Sources and filters	Time	Experimental end product	Analytical technique	Reference
Realgar	UV-IR filter	2 weeks	No transformation	SEM + XRD	Douglass et al. 1992
	Fluorescent lighting	1 month	No transformation		
	Sunlight	1.25 h	χ-phase		
		0.9 h	First appearance of pararealgar		
		6–12 h	Complete alteration to pararealgar		
Realgar	Polychromatic light (550-nm-long wavelength pass filter)	–	χ-phase → pararealgar	XRD	Bonazzi et al. 1996
β-As_4S_4[1]	Polychromatic filtered light (550-nm-long wavelength pass filter) and laser light	(1st step in 1560 min)	χ-phase → pararealgar	XRD	Bonazzi et al. 1996, 2006
Realgar (acetone disp.)	Dichroic halogen lamp (550-nm-long wavelength pass filter)	–	Pararealgar (Fig. 3)	Raman, FTIR	Muniz-Miranda et al. 1996
β-As_4S_4[2]	Dichroic halogen lamp (550-nm-long wavelength pass filter)	–	Pararealgar (Fig. 3)	Raman, FTIR	Muniz-Miranda et al. 1996
Realgar	568 K (~295 °C)	1 week	Arsenolite	XRD	Ballirano and Maras 2002 (see also Ballirano 2012)
Uzonite	Dichroic halogen lamp polychromatic light (550-nm-long wavelength pass filter)	240 min steps (Tot = 1440 min)	No significant change	XRD	Bindi et al. 2003
Realgar	Quartz-tungsten-halogen lamp (full-spectrum radiation from the lamp)	–	As_4S_5 → pararealgar	XRD + XPS	Kyono et al. 2005
β-As_4S_4-As_8S_9 series	Polychromatic light (550-nm-long-wavelength pass filter)	24 h	Only partial conversion	XRD	Bonazzi et al. 2006
synthetic β-As_4S_3	Polychromatic light (550-nm-long-wavelength pass filter)	24 h	No significant change	XRD	Bonazzi et al. 2006
Realgar	15 V and 150 W quartz–tungsten–halogen lamp, set at 3–12 cm from the crystal (emission spectrum: 350–850 nm)	–	Pararealgar	XRD	Kyono 2007
Realgar	Natural sunlight	30, 60, 90,120,150,180, 1000 days	As_4S_5 → pararealgar	FTIR, XRPD	Naumov et al. 2007
Realgar	Continuous wave laser light at 1.96 eV, 2.33 eV	0 → disintegration (~100 h)	Uzonite → pararealgar	Raman, XRD	Naumov et al. 2010
β-As_4S_4[3]	Sample A = exposed to ambient air-dichroic halogen lamp	300 h light alteration	Pararealgar + arsenolite	XRD	Zoppi and Pratesi 2012
	Sample B = with pure isopropyl alcohol-dichroic halogen lamp	300 h light alteration	Pararealgar		
	Sample C = altered sample A + 12 wt% of yttrium-III oxide	220 °C for 1, 24, 72, 264 h	Alacranite + arsenolite		
	Sample D = altered sample B + 12 wt% of yttrium-III oxide	220 °C for 1, 24, 72, 264 h	χ-phase (exp.β-As_4S_4) + β-As_4S_4		

Table 2 (continued)

Tested starting material	Sources and filters	Time	Experimental end product	Analytical technique	Reference
Realgar (alcohol)	Eco Classic Philips (100 W; lux 5700 ± 53))	6, 9, 72 h, 1 week	χ-phase (As_4S_5) → parareal-gar + arsenolite	FTIR, Raman	Macchia et al. 2013
	Halogen Osram Halostar (50 W; lux 1980 ± 87) and Duluxstar (11 ≈ 51 W; lux 2023 ± 53) Mas-terline (45 W; lux 26,200 ± 45), Decostar (35 W; lux 22,040 ± 87); Osram Sylvania LED (13≈75 W; lux 16,946 ± 64)	Max. 1 week	~Same as above but slower		
Realgar[4]	Series AL = with pure isopropyl alcohol, unfiltered sun/lamp light	300 h	Pararealgar (99.7 wt%) + amorphous (0.3 wt%)	XRD, Raman	Pratesi and Zoppi 2015[5]
	Series AR = in air, unfiltered sun/ lamp light	300 h	Pararealgar (51 wt%) + arse-nolite (13 wt%) + uzonite (2 wt%) + amorphous (34 wt%)		
Realgar	Sunlight	30, 60, 90, 120, 180 days (+ 1000)	Pararealgar	FTIR, Raman, XRPD	Jovanovski and Makreski 2020
	Laser excitation of 632.8 nm (500–670 nm region)	3 h		Raman	

FTIR = Fourier transform infrared spectroscopy, *SEM* = scanning electron microscopy, *XRD* = X-ray diffraction, *XRPD* = X-ray photodiffraction, *XPS* = X-ray photoelectron spectroscopy, *disp.* = dispersed, *exp.* = expanded

[1]Obtained from a realgar sample from Shimen (China), through grounding and heating "at 295 °C in an evacuated silica tube in a horizontal furnace for 24 h" (Bonazzi et al. 1996).

[2]Obtained from a realgar sample from Shimen (China), through grounding and heating "at 295 °C for 24 h in an evacuated silica tube" (Muniz-Miranda et al. 1996).

[3]Obtained from a realgar sample from Shimen (China) kept in evacuated silica vial at 290 °C (horizontal furnace) for 4 h and then quenched in water to 0 °C.

[4]Specimen no. 46768 (Museo di Mineralogia dell'Università degli Studi di Firenze) from Shimen (China).

[5]Altered samples were further heated at 220 °C for a total of 1, 24, 72, 240, 504 and 672 h and the phase transformations were determined at each temperature range.

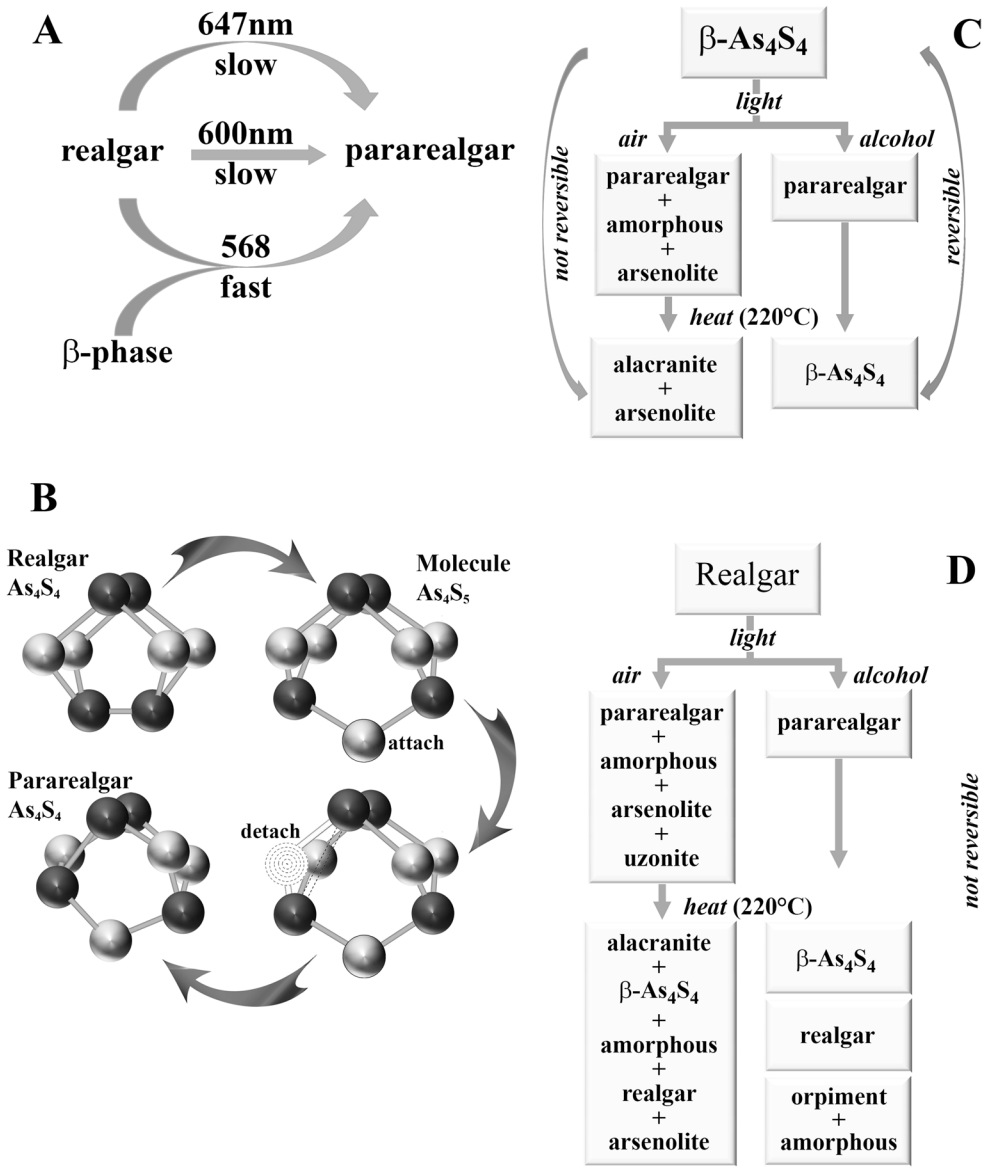

Fig. 4 The realgar→pararealgar transformation. **A** The transformation under monochromatic laser irradiation described by Muniz-Miranda et al. 1996 (modified from reference Fig. 1). **B** The cyclic transformation described by Kyono et al. 2005 (modified from reference Fig. 6). As specified by the authors, the fact that the As-As bonds are weaker than the As-S bonds, causes the free S atom to be inserted between the atoms of As. **C** The alteration of β-As_4S_4 when non/exposed to air and the following heat treatment investigated by Zoppi and Pratesi 2012 (modified from reference Fig. 5). **D** The alteration of realgar when non/exposed to air and the following heat treatment investigated by Pratesi and Zoppi 2015 (modified from reference Fig. 4)

of As_4S_4 molecules is nearly identical in their structures; (5) realgar has the same As_4S_4 molecule of β-As_4S_4; however, the increase in unit-cell volume of β-As_4S_4 is much higher than that in realgar. The limited increase in the volume of realgar can be due to an equally limited conversion of As_4S_4 to As_4S_5 or to pararealgar-type As_4S_4 molecules; (6) β-As_4S_4 (*C*2/*c*) microdomains in the alacranite series seem unable to incorporate sulfur since the conversion to pararealgar was partial (and none for As_8S_9 (*P*2/*c*) microdomains); (7) the χ-phase consists of a "β-As_4S_4 structure (*C*2/*c*) with As_4S_5 molecules randomly substituting for As_4S_4" (Bonazzi et al. 2006).

These works marked a milestone in the history of studies on this subject and, after them, the overall picture has remained essentially unchanged despite further details being gradually added. The newest achievements can be summarized as follows.

– A new orthorhombic phase (~ As_4S_5), produced by the light-induced alteration of a natural $As_4S_{4.35}$ crystal, was

discovered by Bindi and Bonazzi (2007) (Tables 1 and 2).
- Kyono 2007 verified that "the exposure time required for the phase transformation increases gradually as the light intensity decreases" (Table 2).
- The evidence of additional sulphur atoms was finally observed, thus substantiating and detailing the mechanism described by Kyono et al. (2005). The series of experiments performed by single-crystal X-ray photodiffraction (Naumov et al. 2007), Fourier transform infrared (FTIR) and Raman spectroscopies (Bujňáková et al. 2015) and steady-state single-crystal XRD (Naumov et al. 2010) contributed to directly observe the light-induced realgar → pararealgar transformation at the atomic scale and to visualize "the migration" of the sulphur atom (see also Jovanovski and Makreski 2020) (Table 2).
- The importance of the presence of oxygen in the transformation of both the β-As_4S_4 phase and realgar was highlighted by Zoppi and Pratesi (2012) and Pratesi and Zoppi (2015), respectively (Table 2, Fig. 4C, D). In Fig. 3, the reaction formulas provided by Pratesi and Zoppi (2015) for the alteration of β-As_4S_4 in air (Eq. 14), the light-induced alteration of realgar in air (Eq. 15 where $0 < x < 1$) and the heat-induced transformations of pararealgar obtained in the absence of air (Eq. 16, reporting the phases in the order b-e of appearance) are provided.
- The natural analog of the HT synthetic β-phase (*i.e.* bonazziite) was discovered by Bindi et al. (2015a, b, c).

The occurrence of AS-sulfides and some notes on their trade

Among the hundreds of sulfides known nowadays (see Vaughan and Corkhill 2017 for a detailed overview on sulfides), only pyrite (FeS_2), pyrrhotite ($Fe_{1-x}S$), galena (PbS), sphalerite [(Zn, Fe)S] and chalcopyrite ($CuFeS_2$) were classified as rock-forming minerals, based on their abundance (Bowles et al. 2011). As-sulfides are less abundant but the concentration of minable ore metals makes them important georesources but harbingers of potential air, water and soil pollution as the other metal sulfides.

Primary As-sulfides prevail over the other groups of As-bearing minerals and mainly occur in magmatic and hydrothermal environments (Eary 1992; Drewniak and Sklodowska 2013). However, the conditions for their formation are different. For example, high temperatures are commonly required for the formation of arsenopyrite, which is thus typically found in pegmatites, contact metamorphic rocks or, more rarely, in basalts (Drewniak and Sklodowska 2013). Microbial activity can even influence the formation of realgar, pararealgar and alacranite at ambient temperatures in sulfate-reducing environments (O'Day et al. 2004). In this regard, the studies performed by Newman et al. (1997) demonstrated that the bacterium *Desulfotomaculum auripigmentum* precipitates As_2S_3 both intra- and extracellularly, due to its ability to reduce As^{5+} to As^{3+} and S^{6+} to S^{-2}. A few years later, Huber et al. (2000) provided evidence of a new specie—the *pyrobaculum arsenaticum*—that "can precipitate realgar over its temperature range of growth" (*i.e.* 68–100 °C) and Demergasso et al. (2007) discussed the microbial involvement in the (abiotic) precipitation of arsenic minerals in borate deposits.

This topic is beyond the scope of this review but it should be pointed out that the literature is vast because it concerns important environmental remediation studies. The articles cited above are only examples and can be used for a first approach to the subject. To return instead to the geographical occurrence of these phases, it immediately becomes evident that, despite literature reports that the deposits exploited in historical times are located in the Carpathians, Caucasus, Gerogia, Armenia and Azerbaijan (Grundmann and Rötter 2007), the geological literature pays little attention to these occurrences while privileging deposits in which arsenic ores are associated with gold deposits. The frequent occurrence of arsenic and realgar in geothermal fluids and Carlin-type gold deposits (see, *e.g.*, Rytuba 1986, Ballantyne and Moore 1988, Boyle 1987, Arehart 1996) triggered, in fact, a large production of literature that we have tried to summarize in Table 3.

Data included in Table 3 are certainly partial because the selected literature includes only particularly large deposits that have been the subject of systematic studies while it excludes minor deposits that may have been exploited in antiquity. Mindat.org, for example, lists 796 occurrences (in 57 countries) only for realgar and these too are to be considered incomplete since not all countries have been studied with the same level of detail: Afghanistan (1), Albania (6), Argentina (8), Armenia (1), Australia (10), Austria (42), Belgium (1), Bolivia (6), Bosnia and Herzegovina (2), Bulgaria (3), Canada (21), Chile (15), China (120), Costa Rica (1), Czech Republic (9), Fiji (1), France (17), Georgia (3), Germany (43), Greece (4), Hungary (6), Indonesia (3), Iran (8), Ireland (1), Italy (54), Japan (14), Kazakhstan (2), Kyrgyzstan (3), Laos (1), Malaysia (8), Mexico (11), Morocco (2), Namibia (1), New Zealand (11), North Macedonia (4), Norway (1), Pacific Ocean (1), Papua New Guinea (1), Peru (19), Poland (2), Portugal (1), Romania (17), Russia (21), Serbia (3), Slovakia (19), Slovenia (2), South Africa (10), Sudan (1), Sweden (2), Switzerland (7), Taiwan (2), Tajikistan (1), Turkey (17), UK (2), Ukraine (2), USA (221), Uzbekistan (1), Vanuatu (1). However, while a review of all occurrences was beyond the scope of this review, we instead found it useful to show the most common mineralogical associations.

Other sources such as those mentioned by Dioscorides in Mysia, Pontus and Cappadocia (see above) or by Schafer (1955) in Hungary, western Georgia, Kurdistan, Shiraz, Takht-i-Sulaiman and Mt. Demawand in Persia are more difficult to localize and/or describe.

Despite these limitations, however, the data collected are sufficient to demonstrate three different aspects: (a) the wide availability of these As-sulfides, (b) the minerals with which they are generally associated; and c) the prevalence of realgar, orpiment and arsenopyrite compared to the other As-sulfides and As-oxides. Another consideration that can be made is that, apart from native elements, realgar is primarily associated with orpiment, arsenopyrite, chalcopyrite, cinnabar, galena, marcasite, pyrite, sphalerite, stibnite and gangue minerals such as barite, calcite, chalcedony, quartz and dolomite. The absence of pararealgar and sometimes also of orpiment in the literature sources should not be considered representative as it is legitimate to imagine that where realgar is, these two phases can also be present.

As for ancient trades, information is scarce. Pliny not only mentioned the island of Topazos in the Red Sea as a source of both *sandaraca* and *ochra Iubra* but also specified that neither of them were imported to Rome from that place (*Naturalis Historia* 35, 39, 22). Therefore, it is not well understood whether this news can be considered reliable since Topazos—*i.e.* the Zabargad Island (St. John's in English)—is well known for being the likely source of Egyptian peridot[8] and may therefore have exercised a certain suggestion. However, it is a quaternary volcanic island where realgar can therefore be present.

Also with reference to the trades mentioned by Dioscorides, we have no archaeological evidence to prove it or any useful arguments to discredit his information. On the other hand, most of the territories he mentioned have actually proved to be distribution areas of realgar (Table 3).

Lastly, Schafer (1955) claimed that Egyptian orpiment was thought to be of likely Persian origin while a Syrian, Cappadocian, Mysian, Pontic and Carmanian provenance was reconstructed for orpiment traded in Mediterranean Europe. The same Author stated that medieval painters imported their pigments chiefly from Asia Minor, while several sources at Burma, Khotan, Kucha, Aqsu, Malayse, Champa and Japan could have supplied the Chinese and, overall, Far-Eastern painters.

[8] The peridot corresponds to the green, gem quality Mg-rich olivine [$(Mg, Fe)_2SiO_4$]. The Egyptians attributed to this gem magical powers such as that of protection from the night (hence, "gem of the sun").

The use of arsenic-based pigments

A good review of the recorded occurrence of orpiment and realgar as pigments was published by West FitzHugh in (1997) as part of the third volume of the Artists' Pigments series. The review spans publications, analyses and personal communications from the 1960s until the mid-1990s and lists the occurrence of orpiment and realgar in objects and collections around the world, from the 1st Dynasty in Ancient Egypt (31st century B.C.) to 19th century Europe. Other, more partial reviews were published by Orna in 2015 and Scott in 2016, on mineral and Egyptian pigments (including arsenic pigments), respectively.

As expected, most of the historical records of arsenic-containing pigments refer to orpiment and realgar. West FitzHugh does mention other arsenic sulfide minerals such as pararealgar, alacranite, duranusite and dimorphite in her Artists' Pigments chapter, but does not document any occurrence of them as pigments, with the exception of samples taken from Tintoretto paintings. However, she rightly suggests that there may well be art objects where pararealgar may have formed over time as a result of light-induced degradation of an original realgar-containing pigment. Since then, pararealgar has been detected on many objects, both as a degradation product but also as a yellow pigment in its own right—assuming artists in the past would not have been able to tell the difference between mineral orpiment and mineral pararealgar (Corbeil and Helwig 1995; Trentelman et al. 1996; Burgio and Clark 2000, Mazzeo et al. 2004; Casadio et al. 2005 and references therein, Burgio et al. 2007; Burgio et al. 2008).

An intermediate phase between realgar and pararealgar (the so-called χ-phase) has also been detected on various types of artefacts, from Venetian paintings (Trentelman et al 1996), to 15th century Greek icons (Burgio et al. 2003), to ancient Egyptian papyri (Daniels and Leach 2004), to 9th century stuccoes from Samarra, Iraq (Burgio et al. 2007).

Orpiment, used alone or in admixture with other pigments, was recently identified on Egyptian sarcophagi (Vandenabeele et al 2007) and cartonnage (Gard et al. 2020), early Irish manuscripts (Burgio et al. 2013), Italian medieval and Renaissance manuscripts (Burgio et al 2010), English manuscripts (Panayotova et al 2017), Islamic manuscripts (Chaplin et al. 2006, Burgio et al. 2008), Persian manuscripts (Muralha et al. 2012a), Byzantine manuscripts (Daniilia and Andrikopoulos 2007), Cistercian manuscripts (Muralha et al. 2012b), Asian manuscripts (Nöller et al. 2015), Visigothic manuscripts (Carter et al. 2016), near-eastern icons (Lahlil and Martin 2012), Indian palm-leaf manuscripts (Singh and Sharma 2020), Tudor portrait miniatures (Burgio et al 2012), Tibetan wall paintings (Li et al. 2014b), Chilean archaeological sediments (Ogalde et al

Table 3 Typical occurrences of realgar: a literature search [search words: realgar, all fields; search engine: Scopus; excluded subject areas: Medicine, Pharmacology, Toxicology and Pharmaceutics, Biochemistry, Genetics and Molecular Biology, Immunology and Microbiology, Neuroscience, Health professions, Nursing, Veterinary, Psychology and Dentistry]. Some areas have been merged due to the difficulty of arriving at a synthesis on a single outcrop or mine (*e.g.*, publications in foreign languages or concerning water contamination). Gangue minerals are listed along with ore minerals to provide as complete a picture of the associations as possible. Further occurrences are listed in the main mineralogical databases such as mindat.org and mineralienatlas.de

Country	Deposits types	Mineralogical assemblage (alphabetical order)	Reference
Albania	Dawsonite and realgar-orpiment deposit, Koman area	Aragonite, barite, calcite, dawsonite, dolomite, gibbsite, greigite, gypsum, marcasite, orpiment, stibnite	Ferrini et al. 2003
Argentina	Spring deposit, Loma Blanca borate deposit	Aragonite, calcite, inyoite, teruggite, ulexite	Aristarain and Hurlbut 1968
	Mina Capillitas epithermal deposit, Catamarca	Duranusite, rhodochrosite, sphalerite	Mańquez-Zavalía et al. 1999
	*Gualcamayo Mining District	Chalcopyrite, cinnabar, galena, orpiment, marcasite, (As)pyrite, pyrrhotite, sphalerite	Bruno and Thompson 2019
Austria	Brecciated marbles, Carinthia	Orpiment, quartz	Göd and Zemann 2000
Bosnia	Čemernica Sb-Zn-Hg-W deposit	Arsenopyrite, barite, berthierite, boulangerite, chalcedony, chalcopyrite, cinnabar, enargite, ferberite, galena, jamcsonite, marcasite, plagionite, pyrite, pyrrhotite, quartz, siderite, sphalerite, stibnite, tetrahedrite	Jurković et al. 1999
Bulgaria	Mareshnitsa ore deposit	Alacranite, duranusite, pararealgar, marcasite, pyrite	Mladenova 2000
Canada	*Mindamar mine, Richmond, Nova Scotia	Chalcopyrite, chlorite, dolomite, galena, magnesite, pyrite, quartz, sericite, sphalerite, tennantite	Watson 1954
	*Archean Hemlo deposit, Ontario	Aktashite, arsenopyrite, chalcopyrite, cinnabar, kyanite, molybdenite, orpiment, quartz, pyrite, pyrrhotite, sillimanite, Hg-sphalerite, stibnite	Powell and Pattison 1997; Powell et al. 1999; Tomkins et al. 2004
	Mount Washington Cu deposit, British Columbia	Duranusite, quartz	Roberts et al. 1979
Czechia	Katerina colliery in Radvanice, Bohemia	Alacranite, anglesite, antimonite, arsenolite, bararite, cryptohalite, galena, greenockite, letovicite, mascagnite, molybdite, orpiment	Žáček and Ondruš 1997
China	*Chinese deposits in the Shaanxi, Guizhou and Hunan provinces (*e.g.*, Shuiyindong[a])	Arsenopyrite, barite, calcite, chalcopyrite, cinnabar, dolomite, fluorite, fuchsite, galena, (hydromica, limonite), orpiment, pentlandite, (As) pyrite, pyrrhotite, quartz, sphalerite, stibnite, tennantite, Tl-minerals	Liu and Geng 1985; Wang et al. 1999; Peters et al. 2007; Su et al. 2009; Huang et al. 2012; Tan et al. 2015; Xie et al. 2018; Yue et al. 2018
	Shimen orpiment-realgar deposit, Hunan[b]	Calcite, dolomite, orpiment, quartz, pharmacolite, weilite	Jingrong et al. 1993; Wilson 2007; Zhu et al. 2015
	*Dongbeizhai, Qiuluo, Manaoke, Laerma, Gala and Lianhecun gold deposits and Nongduke, Sichuan	Arsenopyrite, barite, bismuth minerals, calcite, cinnabar, (limonite,) marcasite, orpiment, pyrite, quartz, scheelite, stibnite, tennantite, uranite, zinckenite, tennantite	Zheng et al. 1991; Wang and Zhang 2001; Fu et al. 2002; Xu et al. 2005
	*Youjiang Basin, Nali and Shuiluo deposits, Guangxi	Arsenopyrite, chalcedony, cinnabar, pyrite, stibarsen, stibnite, wakabayashilite	Zhang 1985; Liu et al. 2001; Li et al. 2014a
	* Qinling belt (Jian Cha Ling, Yangshan, Mian-Lue-Ning and Manaoke)	Arsenopyrite, chalcopyrite, cinnabar, dolomite, galena, orpiment, pyrite, pyrrhotite, quartz, scheelite, sphalerite, stibnite	Mao et al. 2002; Vielreicher et al. 2003; Li et al. 2018
	*Youjiang Rift Basin, Yangtze Craton	Arsenopyrite, carbonate, chalcedony, cinnabar, marcasite, pyrite, stibnite	Liu et al. 2002

Table 3 (continued)

Country	Deposits types	Mineralogical assemblage (alphabetical order)	Reference
China	*Changkeng deposit, Guangdong	Arsenopyrite, barite, fluorite, marcasite, orpiment, pyrite, stibnite	Mao et al. 2007
	Baiyangping Pb–Zn-Cu-Ag deposit, Lanping, Yunnan	Argentite, (Co-)arsenopyrite, bournonite, chalcocite, chalcopyrite, cobaltine, galena, gratonite, jordanite, kongsbergite, orpiment, siegenite, sphalerite, tetrahedrite	Wang et al. 2015
	Jilongshan Cu–Au skarn deposit, Fengshan, Anhui	Barite, carbonate, coloradoite, electrum, fluorite, galena, marcasite, orpiment, pyrite, quartz, rhodochrosite, sphalerite	Han et al. 2020
	*Nongruri deposit, Riduo, Maizhokunggar, Tibet	Carbonate, quartz, stibnite	Liu et al. 2011
	Jiama copper polymetallic deposit, Tibet	Cu-minerals, orpiment, quartz and pyrite	Zheng et al. 2012
	*Sb metallogenic belt, Himalayan orogen, Tibet	Arsenopyrite, cinnabar, (limonite,) pyrite, quartz, stibnite, valentinite	Zhai et al. 2014
France	Realgar mine, Corsica	–	Tian et al. 1995; Migon and Mori 1999
	Jas Roux deposit, Hautes-Alpes	Andorite, aktashite, barite, chabourneite, laffittite, parapierrotite, pierrotite, pyrite, routhierite, smithite, sphalerite, stibnite, twinnite, zinckenite, wakabayashilite	Johan and Mantienne 2000
Georgia	Lukhumi realgar-orpiment deposit	Marcasite, orpiment, pyrite, quartz	Zhabin et al. 1990
India	*Barhi and Jhal metavolcano-sedimentary belt	Pyrite, stibnite	Talusani 2001
Indonesia	*Ratatotok district, Minahasa, North Sulawesi	Cinnabar, orpiment, stibnite	Turner et al. 1994
Iran	Sb-As mineralisations, Dashkasan-Baharlu	Cinnabar, metacinnabarite, orpiment, pyrite, stibiconite, stibnite	Golestaneh 1983
	*Zarshuran deposit	Barite, cinnabar, getchellite, orpiment, (Au-As-)pyrite, sphalerite, stibnite, Tl-minerals	Asadi et al. 1999, 2000; Mehrabi et al. 1999
	*Muteh mining region, Isfahan	Actinolite, biotite, chalcopyrite, chlorite, feldspars, muscovite, orpiment, pyrite, tremolite	Keshavarzi et al. 2012
	*Sari Gunay epithermal deposit	Cinnabar, orpiment	Richards et al. 2006
	*Arabshah epithermal deposit	Chalcopyrite, galena, orpiment, (As)pyrite, sphalerite	Afzal et al. 2017
	*Barika sulphide deposit (Pb–Zn-Cu)	Andorite, barikaite, electrum, ferdowsiite, galena, geocronite, guettardite, miargyrite, pyrargyrite, pyrite, seligmanite, smithite, sphalerite, stephanite, stibnite, tetrahedrite-tennantite, trechmannite	Tajeddin et al. 2019
Italy	Metapelites of Permian age, Maritime Alps	Danburite, dravitic tourmaline, graphite, mica, quartz	Cabella et al. 1987
	Monte Arsiccio mine, Apuan Alps, Tuscany	Aktashite, arsiccioite, baryte, boscardinite, cinnabar, cymrite, laffittite, pyrite, protochabournéite, sphalerite, stibnite	Biagioni et al. 2014a-b, 2020
	Cetine Sb-mine, Chiusdino, Siena	Aluminocopiapite, alunogen, azurite, chalcostibite, copiapite, copiapite, epsomite, ferrinatrite, fibroferrite, gibbsite, halotrichite-pickeringite, hexahydrite, hexahydrite, jarosite, jurbanite, klebelsbergite, malachite, melanterite, metavoltine, mirabilite, onoratoite, peretaite, pharmacosiderite, K-alum, roemerite, rostite, rozenite, scorodite, senarmontite, sideronatrite, tamarugite, tschermigite, uklonskovite, valentinite	Sabelli and Brizzi 1984; Brizzi et al. 1986
	Monte Sughereto, Lazio	–	Ballirano and Maras 2006

Table 3 (continued)

Country	Deposits types	Mineralogical assemblage (alphabetical order)	Reference
Italy	Solfatara volcano, Pozzuoli, Napoli	Adranosite, alacranite, cinnabar, dimorphite, efremovite, godovikovite, huizingite-(Al), kaolin, mascagnite, russoite	Armiero et al. 2007; Campostrini et al. 2019
	Fumarolic encrustation, Vulcano, Aeolian Islands	Barberiite, bismuthinite, cannizzarite, galenobismutite, malladrite	Garavelli and Vurro 1994
Japan	Abandoned As mine in Nishinomaki, Gunma	Quartz, pyrite, sericite	Fukushi et al. 2003
	Wakamiko crater in Kagoshima bay, south Kyushu	Barite, carbonates, gypsum, orpiment, pyrite, stibnite	Ishibashi et al. 2008
Kyrgyzstan	Khaydarkan deposit	Cinnabar, galkhaite, guadalcazarite, orpiment, pyrite, stibnite, wakabayashilite	Gruzdev et al. 1975, Spiridonov 1989
	*Kadamzhai and Chauvai Sb-Hg deposits	Aktashite, arsenopyrite, chalcopyrite, cinnabar, enargite, galkhaite, hematite, (limonite,) magnetite, marcasite, orpiment, pyrite, quartz, stibnite, tetrahedrite	Spiridonov et al. 1983; Nevolko et al. 2019
Laos	*Phapon deposit	(Au)calcite, orpiment	Guo et al. 2019
Mexico	Borate deposits, northern Sonora	Celestite, colemanite, gypsum, howlite, ulexite[c]	Miranda-Gasca et al. 1998
North Macedonia	*Allchar (or Alshar) hydrothermal As–Sb–Th deposit, Kavadarci	Calcite, Fe hydroxides, gypsite, jarosite, lorandite, marcasite, orpiment, pyrite, sericite, siderite, quartz, Tl-minerals	Ljubičić et al. 1988; Pavićević and El Goresy 1988; Alderton et al. 2014; Volkov et al. 2006
	Lojane As-Sb deposit	Albite, alunogen, annabergite, aragonite, arsenic, arsenolite, baryte, cattierite, chalcopyrite, chromite, coffinite, duranusite, epidote, eulytine, fluorapatite, galena, gersdorffite, gypsum, hercynite, hexahydrite, hörnesite, hydromagnesite, hydroxylapatite, kaňkite, kaolinite-group representatives, kermesite, laurite, (limonite,) magnesite, magnesiochromite, magnetite, marcasite, maucherite(?), millerite, molybdenite, monazite-(Ce), muscovite/illite, naldrettite(?), orpiment, pararealgar, parkerite(?), pentlandite, pickeringite, polydymite(?), pyrite, pyrrhotite, quartz, roméite-group, rozenite, rutile, scorodite, senarmontite, spinel, stibiconite, stibnite, tripuhyite(?), ullmannite, uraninite, uvarovite, vaesite, valentinite, violarite	Alderton et al. 2014; Tasev et al. 2018; Dordević et al. 2019
Peru	Ore veins of Casapalca	Calcite, stibnite	McKinstry and Noble 1932
	Atacocha Pb–Zn mine	Chalcopyrite, galena, jamesonite, pyrite, sphalerite	Johnson 1955
	Palomo mine Huancavelica Department	Barite, calcite, chalcopyrite, galena, orpiment, polybasite, proustite, pyrargite, pyrite, quartz, rhodochrosite, sphalerite, stibnite, tetrahedrite	Hyršl 2008
Poland	Baligród and Szczawnica	Cinnabar	Wojciechowski 2003
	Bystre, Polish Carpathians	Chalcopyrite, galena, malachite, marcasite, orpiment, pyrite, quartz, sphalerite, stibnite	Nieć et al. 2016
Romania	Suceava County, Western Moldavia	Calcite, kaolinite, pharmacolite	Fehér et al. 2016
Russia	Gal Khaya deposit in Sakha (former Yacutia)	Aktashite, greigite, orpiment, stibnite, wakabayashilite	Gruzdev et al. 1975
	Chagan-Uzun mercury deposit in the Altai Republic	Cinnabar, stibnite	Selin 1982
	Uzon caldera in Kamchatka	Orpiment, stibnite, uzonite	Popova and Polyakov 1985; Popova et al. 1986; Bychkov and Grichuk 1991; Migdisov and Bychkov, 1998

Table 3 (continued)

Country	Deposits types	Mineralogical assemblage (alphabetical order)	Reference
Russia	Cernicevo Sb deposits, southeast Rhodopes	Arsenopyrite, calcite, chalcopyrite, marcasite, pyrite, quartz, rhodochrosite, sphalerite, stibnite	Todorov and Mileva 1987
	*Vorontsovskoe deposit, north Urals	Arsenopyrite, chalcopyrite, dimorphite, löllingite, pyrite, quartz, orpiment, pyrite, routhierite, sericite, sphalerite, stibnite, gruzdevite-aktashite series	Sazonov et al. 1998; Murzin et al. 2017; Stepanov et al. 2017; Vikentyev et al. 2019
Serbia	Rujevac hydrothermal polymetallic Sb(As)-Pb–Zn vein-type ore deposit	Arsenopyrite, barite, calcite, chalcopyrite, dolomite, duranusite, fülöppite, galena, gratonite, greenockite, marcasite, orpiment, plagionite, pyrite, kermesite, plagionite, quartz, robinsonite, senarmontite, siderite, sphalerite, stibnite, sphalerite, tetrahedrite, twinnite, valentinite, zinkenite	Radosavljević et al. 2012, 2013, 2014
Slovakia	Malachov Hg-deposit	Arsenolite, arsenopyrite, calcite, chalcedony, cinnabar, dolomite, gypsum, marcasite, orpiment, pyrite, quartz	Dadová et al. 2016
Switzerland	Lengenbach quarry, Binntal	Adularia, aktashite, argentobaumhauerite, argentodufrénoysite, argentoliveingite, arsenic, baryte, baumhauerite, bernardite, canfieldite(te-rich), cerussite, coffinite, covellite, dolomite, dravite, dufrénoysite, eckerite, edenharterite, erniggliite, ferrostalderite, galena, gabrielite, hatchite, hutchinsonite, hydrocerussite, incomsartorite, imhofite, jentschite, jordanite, kaolinite, lengenbachite, liveingite, marrite, muscovite, nowackiite, orpiment, pararealgar, parapierrotite, philrothite, picotpaulite, proustite, pyrite, quadratite, quartz, ralphcannonite, rathite, realgar, richardsollyite, routhierite, rutile, sartorite, seligmannite, sicherite, silver, sinnerite, smithite, sphalerite, stalderite, tennantite, thalcusite, thorite, tochilinite, trechmannite, uraninite, wallisite, wurtzite, xanthoconite[d]	Graeser and Edenharter 1997; Graeser et al. 2001, 2006; Raber and Roth 2018; Bindi et al. 2014b, 2015b-c
Tajikistan	Hd-Sb deposit	Duranusite	Vershkovskaya et al. 1988
Tunisia	Oued Maden, Jebel Hallouf and Fedj Hassene Pb–Zn (Ba-Sr-F-Fe-Hg) hydrothermal ore deposits	Cerussite, chalcopyrite, galena, jordanite, orpiment, pyrite, smithsonite, sphalerite	Bejaoui et al. 2011; Jemmali et al. 2013
Turkey	Emet borate deposits (Igdeköy-Emet, Kütahya)	Cahnite, celestite, colemanite, hydroboracite, meyerhofferite, orpiment, teruggite, tunellite, ulexite, veatchite-A	Helvacı 1984; Çolak et al. 2003; Dogan and Dogan 2007; Dill et al. 2015
	Gözeçukuru As-Sb-Pb–Zn mine, Sahin, Kutahya	Arsenopyrite, galena, orpiment, pyrite, senarmontite, sphalerite, stibnite, valentinite	Arik 2012
	Evaporitic deposits of the Sivas (Ulaş) Basin	Celestite, chromite, (limonite,) marcasite, orpiment, psilomelane, pyrite, siderite-ankerite	Tekin et al. 2002
	*Kuscayiri copper deposit	Alunite, arsenopyrite, chalcopyrite, hematite, magnetite, pyrite, pyrophyllite, quartz, sericite	Yilmaz 2003
	*Sb-Hg deposits, Emirli and Halıköy, İzmir	Arsenopyrite, cinnabar, marcasite, orpiment, pyrite, stibnite	Akçay et al. 2006
	*Akoluk area, Ordu	Azurite, barite, chalcopyrite, cinnabar, galena, malachite, marcasite, orpiment, pyrite, quartz, sphalerite, stibnite, zinkenite	Celep et al. 2006; Yaylali-Abanuz and Tüysüz 2010, 2011
	*Porphyry-epithermal deposit, Çöpler, Erzincan	Arsenopyrite, chalcopyrite, galena, manganocalcite, marcasite, orpiment, arsenical pyrite, sphalerite, tennantite, tetrahedrite	Imer et al. 2016
USA	*Hg deposits of Utah	Calcite	Jewell and Parry 1988

Table 3 (continued)

Country	Deposits types	Mineralogical assemblage (alphabetical order)	Reference
USA	Royal Reward realgar mine, Washington	–	Dillhoff and Dillhoff 1991
	*Getchell and Twin Creeks deposits, Humboldt County, Nevada[e]	Adularia, ankerite-dolomite, arsenopyrite, calcite, chalcopyrite, cinnabar, diopside, fluorite, galena, galkhaite, garnet, illite, K-feldspar, kaolinite, marcasite, molybdenite, orpiment, pyrite, pyrrhotite, quartz, scheelite, sericite, siderite, sphalerite, stibnite, tellurides, wollastonite	Stolburg and Dunning 1985, Groff et al. 1997, Groff 2018; Groff 2019; Bowell et al. 1999; Cline and Hofstra 2000; Cline 2001; Tosdal et al. 2003
	*Gold Bar Mining Districts, Nevada	Calcite, barite, dolomite, orpiment, quartz, stibnite	Yigit et al. 2006
	*Cortez Hills deposit, Nevada	Aktashite, chalcopyrite, christite, pyrite, sphalerite	Maroun et al. 2017

Realgar is always present although never listed while native elements have been omitted. In the second column, localities marked with * correspond to deposits where also Au was found but not necessarily mined

[a]"One of the largest and highest grade stratabound Carlin-type gold deposits in China" (Tan et al. 2015)

[b]"The largest realgar deposit in Asia (…) mined for more than 1500 years" (Zhu et al. 2015); "worked since at least the sixth century AD primarily for medicinal arsenic compounds (important in Chinese medicine)." (Wilson 2007)

[c] "A realgar specimen has a $\delta^{34}S$ value of − 32.9, consistent with formation of sulfide by bacterial reduction of sulfate" (Miranda-Gasca et al. 1998)

[d]Thallium mineral are marked in bold

[e]"One of the world's leading producers of realgar crystals" (Stolburg and Dunning 1985)

2014), Tibetan artifacts from Dunhuang (Van Schaik et al 2015), Japanese interior decoration (Vermeulen et al 2015) and woodblock prints (Korenberg et al. 2019), paintings in Ethiopian churches (Gebremariam et al. 2016), Chinese reverse glass (Steger et al 2019) and chiaroscuro woodcuts (Laclavetine et al. 2019).

Realgar has also been detected on multiple types of objects of varied provenance. In addition to the occurrences documented by West Fitzugh, some of the more recent conclusive findings include Egyptian artifacts (Vandenabeele et al. 2000, Burgio and Clark 2000, Daniels and Leach 2004, Casadio et al 2005, Calza et al. 2008, Di Stefano and Fuchs 2011 and references therein, Castro et al. 2016, Scott 2018), manuscripts (Best et al. 1995, Clark and Gibbs 1997, Jurado-López et al. 2004, Burgio et al. 2010, Tanevska et al. 2014), wall paintings (Bianchin et al. 2007; Pagès-Camagna et al. 2010; Simonsen et al. 2015), tangkas (Ernst 2010) and paintings (Vermeulen et al. 2016).

Despite the rarity of alacranite, several authors identified it in different types of works of art: Gard et al. (2020) used Raman microscopy to document it on an Egyptian cartonnage from the Ptolemaic period (305–30 BC), together with orpiment, bonazziite, pararealgar and uzonite. Luo et al. (2016) detected it in Japanese woodblock prints (1864–1895) and suggest its presence is a consequence of the use of synthetic arsenic glass.

The artificial nature of alacranite has been frequently discussed and Grundmann et al. 2011 suggest that many of its occurrences in works of art may be of artificial origin.

It has long been suspected that many arsenic-containing pigments on works of art are of synthetic origin, since mentions of and recipes for them have been available since antiquity. However, it was not until very recently that their occurrence was proved and recognized. Japanese woodblock prints have been studied extensively and were shown to contain synthetic arsenic sulfides (Vermeulen and Leona 2019). Synthetic arsenic pigments were also detected in a French rococo oil painting and Japanese leather paper (Vermeulen et al. 2019), and arsenic sulfide glass was found in many early 18th-century designs for woven silk made by designer and weaver James Leman in London (Burgio et al. 2019).

Alteration and degradation

As mentioned in "Arsenic-based minerals and pigments" and "The use of arsenic-based pigments" sections of this chapter, arsenic-containing minerals are intrinsically unstable especially when exposed to light. It is not uncommon to see realgar mineral specimens develop a yellow 'dusting'—historically believed to be orpiment, but now known to be pararealgar or one of the intermediate phases—and orpiment specimens lose their vivid yellow character and become duller and greyer, due to the formation of arsenolite.

This awareness is reflected in a recent increase in studies concerning the alteration of As-bearing phases in works of art. The fact that some arsenic sulfides are altered by simple exposure to light makes artworks particularly sensitive when displayed, especially considering that other factors such as temperature, humidity and pollutants can contribute to the damage/alteration process.

The development of suitable lighting systems has been the focus of the experimental tests performed by Macchia et al. (2013); Blades et al. (2017) and Jo et al. (2019). Starting from the base concept that several pigments are semiconductors, Anaf et al. (2015) applied a thermodynamic approach to investigate their degradation phenomena and flagged up the pH of the environment as a crucial factor for the preservation of paintings. Keune et al. (2015, 2016) and Vermeulen et al. (2016) investigated the migration of several degraded arsenic sulfides in painting. In particular, Keune and coworkers provided the first evidence of water transport in the paint system and clearly visualized how the arsenic-based products of light-induced alteration (arsenites and arsenates) are mobilized and dispersed through the depth of the paint, along with being absorbed by chalk, gypsum, and other pigments such as lead white and iron-based earths. Their studies—chiefly performed by means of synchrotron radiation X-ray micro-analyses (As-K edge micro-X-ray absorption near edge structure)—also helped hypothesizing a 5-step process for arsenic trioxide: (1) formation; (2) dissolution in water, (3) oxidation to arsenic pentaoxide, (4) the reaction with other ions (*e.g.*, Pb and Ca) and, finally, (5) deposition as insoluble arsenate. Vanmeert et al. (2019) found mimetite and schulténite as decay products of realgar and orpiment (for lead-based pigments see Gliozzo and Ionescu 2021). Similarly, Hradil et al. (2014) found mimetite as the alteration product of orpiment and minium.

The review compiled by Coccato et al. 2017 summarize the state of the art on pigments' stability and conservation treatments.

On a similar subject, the importance of binders as stabilizers or otherwise was evaluated in the 1-year-long irradiation experiments performed by Feneis and Steinbach (2018) using hydroxypropylcellulose; and in the experiments performed by Vermeulen et al. (2018b) using gum arabic (suitable stabilizer), animal glue, egg white, linseed oil (intermediate impact) and egg yolk (worst binder in terms of pigment degradation).

Finally, the alteration of realgar must also be appropriately evaluated in an experimental setting due to its potential sensitivity to irradiation (see the "Analytical methods" section).

Analytical methods

The presence of an arsenic-containing yellow, orange, or red pigment can be easily confirmed in principle with any simple elemental technique—any scientific method that can reveal which elements are present on an object or in a sample. The most commonly used methods of this sort include X-ray fluorescence (XRF, see Bezur et al. 2020), scanning electron microscopy with energy-dispersive X-ray analysis (SEM–EDX, see Vermeulen et al. 2016) and laser-induced breakdown spectroscopy (LIBS, see Analytical Methods Committee, AMCTB No 91 2019; Westlake et al. 2012; Burgio et al. 2001). XRF can be used non-destructively and *in situ*, and usually provides qualitative or semi-quantitative information, making it clear if the arsenic-containing pigment is one of the main constituents or a minor or trace component in the object or sample. Data accuracy, however, decreases from laboratory to portable instrumentation. SEM–EDX usually involves sampling (although small objects can also be analyzed whole, and there are cases where samples can be reused for other investigations) and can provide semi-quantitative information. It is worth mentioning that there are two types of SEM equipment, field emission SEM (FE-SEM) and variable pressure or environmental SEM (ESEM), which allow the analysis of fragments small enough to enter the chamber and, net of calibration, provide a much more accurate analysis the flatter the sample surface is. LIBS entails the vaporization of a microscopic portion of an object or sample but can be done *in situ*. More detailed information about XRF and SEM–EDX can be found in Burgio (2021) in this TC.

However, if the exact arsenic species has to be identified, a molecular or mineralogical technique needs to be used. These can be invasive, minimally invasive or non-invasive, destructive or non-destructive, and can be used *in situ* or may require sampling. The ones most commonly used in cultural heritage since the late 1990s are Raman microscopy (Smith and Clark 2001; Analytical Methods Committee AMCTB No. 67 2015, Casadio et al 2016); Fourier-transform infrared spectroscopy (Vermeulen et al 2016), diffuse reflectance spectrophotometry (Analytical Methods Committee, AMCTB No 75 2016), optical microscopy (OM) and X-ray diffraction (XRD, see Cloutis et al. 2016; Lutterotti et al. 2016). Synchrotron radiation sources have allowed access to high-energy X-rays (with tunable depth capabilities, higher than those provided by conventional instrumentations) and have boosted the potential of many scientific techniques (Keune et al. 2015; Vermeulen et al. 2016; Janssens et al. 2016; Cotte et al. 2018).

Among the molecular techniques, the past two decades have asserted the preeminence of Raman microscopy: it is non-destructive, can be used *in situ* and on individual particles as small as 1 μm across, and provides the unambiguous molecular identification of the species under investigation (Clark 1995, 2007; Smith and Clark 2004; Bersani and Lottici 2016; Casadio et al 2016). It was Raman microscopy that proved that often the yellow arsenic-containing

pigment on works of art, manuscripts and museum objects was not orpiment but pararealgar or one of its polymorphs (Trentelman et al. 1996; Clark and Gibbs 1997). Pararealgar and other polymorphs were also found as light-induced degradation products on the surface of realgar mineral specimens (Burgio 2000, unpublished doctoral thesis data, see Fig. 5). And it was still Raman microscopy which helped identifying and characterizing arsenic glass used as a pigment (Vermeulen et al. 2015; Vermeulen and Leona 2019; Burgio et al. 2019).

Among mineralogical techniques, polarized optical microscopy on thin sections or dispersions has been long used for the identification of the phases. However, the destructiveness of the technique and the parallel development of other, more effective techniques, has limited its use in recent years. On the other hand, X-ray diffraction remains the main techniques for the identification of minerals and pigments. Moreover, while the structural study of new minerals necessarily requires sample preparation and laboratory instrumentation, the identification of known minerals and pigments can be carried out both in a destructive and non-destructive way. In the latter case, some recently developed portable XRD (sometimes combined with fluorescence; Gómez-Morón et al. 2016; de Viguerie et al. 2018), the scanners (MA-XRD; see Vanmeert et al. 2018; 2019; De Keyser et al. 2017; Uhlir et al. 2019; De Meyer et al. 2019a, b), and the XRD beamlines present at the synchrotrons (Vanmeert et al. 2015; Van Der Snickt et al. 2012; Van Der Snickt et al. 2012; Salvant et al. 2018; De Meyer et al. 2019a, b) have been used for the investigation of artworks. Moreover, X-ray diffraction allows both the incontrovertible identification of the pigment (qualitative analysis) and the quantitative determination of the various phases (QPA) by means of Rietveld analysis (Bish and Post 1993).

The XRD patterns of the main mineralogical phases/pigments are provided in Fig. 6.

Good practice guide—analysis protocol

In choosing the operating procedure, various factors must be taken into account: (1) operator safety; (2) preservation of the artwork; (3) type and accuracy of the data to be obtained.

Operator safety

It is more likely than not that arsenic pigments may be present in historical art objects; it is therefore advisable to adopt all the relevant health and safety precautions to avoid any risks for anyone who can come in contact with a potentially hazardous material.

Artwork preservation

Many of the studies discussed earlier in this chapter demonstrate that most naturally occurring arsenic-containing species are sensitive to light—even exposure to natural sunlight can trigger their molecular transformation and often cause a change in colour. With this in mind, analytical techniques should be chosen and employed with care and a specific protocol in mind, so as to avoid any experimental conditions which may affect any arsenic-containing pigment present.

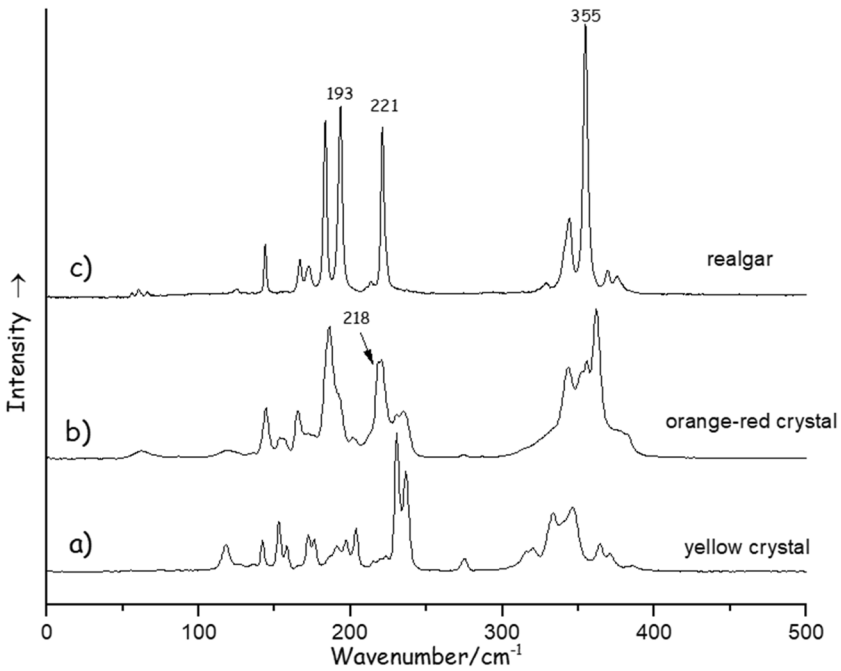

Fig. 5 FT-Raman spectra of a mineral sample of naturally degraded realgar. **a** Raman spectrum of a yellow crystal, identical to that of pure pararealgar. **b** Raman spectrum of an orange-red crystal, corresponding to the χ-phase, possibly mixed with small amounts of other polymorphs. **c** Raman spectrum of realgar. All spectra with 1064 nm excitation, 8 mW, resolution 1 cm^{-1} for **a** and **b** 0.5 cm^{-1} for **c**

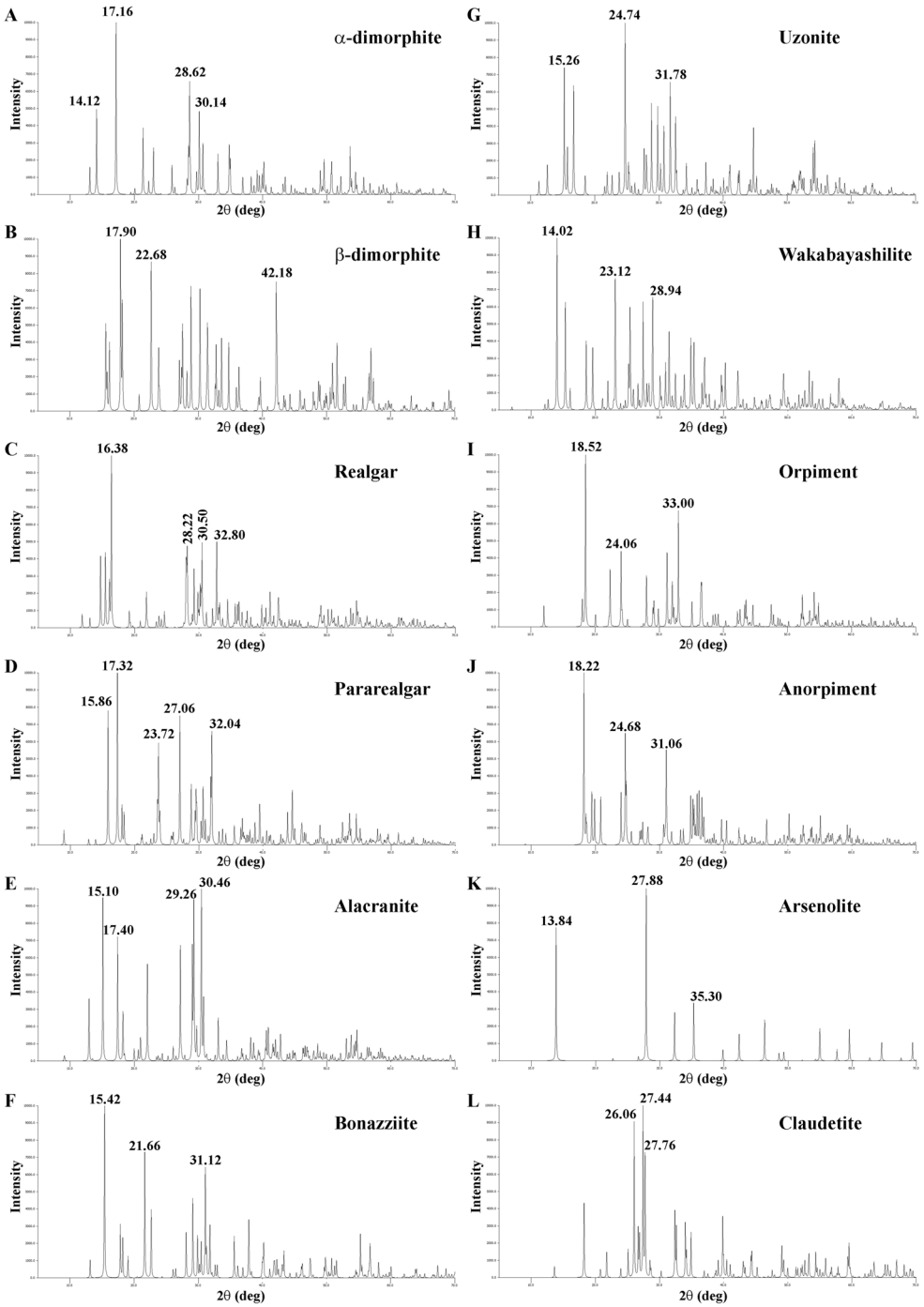

Fig. 6 XRD patterns (Cu-Kα). **A** α-dimorphite. **B** β-dimorphite. **C** Realgar. **D** Pararealgar. **E** Alacranite. **F** Bonazziite. **G** Uzonite. **H** Wakabayashilite. **I** Orpiment. **J** Anorpiment. **K** Arsenolite. **L** Claudetite. Structural data from **A** Whitfield (1970), **B** Whitfield (1973a, b), **C** and **I** Mullen and Nowacki (1972), **D** Bonazzi et al. (1995), **E** Bonazzi et al. (2003a, b), **F** Bindi et al. (2015a, b, c), **G** Bindi et al. (2003), **H** Bonazzi et al. (2005), **J** Kampf et al. (2011), **K** Ballirano and Maras (2002), **L** Pertlik (1978a). Graphics by Mercury software

For example, Raman microscopy is often the technique of choice when looking at the fast, non-destructive, non-intrusive characterization of arsenic-containing pigments in cultural heritage, but as a rule of thumb it is best to use the lowest available power density at the sample, and the longest available excitation wavelength. For example, studies performed in the late 1990s (Burgio 2000, unpublished PhD thesis data) showed that the irradiation of realgar with a low-power 514.5 nm laser (green) almost instantly produces a material the spectrum of which can be consistently interpreted as a 1:4 mixture of realgar and pararealgar. Another degradation product in these conditions is orpiment, As_2S_3, indicating that partial oxidation can occur at this wavelength.

A red laser (such as a He:Ne laser at 632.8 nm or a 647.1 Ar + laser) is safer, but only at low power. If the power density is too high, realgar easily converts into pararealgar and its polymorphs. Even safer are far red (785 nm) or near infrared (1064 nm) lasers.

Type of data and their accuracy

As mentioned earlier in this chapter, the analytical approach is different depending on whether the purpose of the analysis is to verify the presence of arsenic in general or the specific composition of any arsenic-containing pigments.

For the former, any of the elemental techniques described in "Analytical methods" section can be used. For the latter, a molecular technique will be needed. At this point, however, it seems useless to add that a mere identification of the chemical element can affect the quality of the overall research which, consequently, is incomplete and in no way definitive.

For this reason, Raman spectroscopy and/or X-ray diffraction should be preferred (if not considered mandatory) for research that aims to be considered accurate and complete. The complementary use of imaging techniques should be also desirable to obtain an overall picture of pigment distribution. For research, where there is both the need to operate non-destructively and the necessity to operate with a high-energy and high-penetrating beam, synchrotron techniques (SR-XRD, SR-XRF, XAS) can provide the necessary help.

Concluding summary of key concepts

- Contrary to what has often happened historically, it is not possible to deduce the identity of the arsenic-containing species simply from the color of the pigment or pigment mixture
- Arsenic-based minerals and compounds are numerous and can be found to be associated with realgar and orpiment in the ore sources. Therefore, it is necessary not only to pay due attention to "new" phases that are discovered but also to test the possible presence of other phases already known. It is not unheard of, in fact, that rare phases in nature are found in cultural materials.
- The choice of the analytical methodology must take into account the three criteria developed previously, namely the safety of the operator, that of the artwork, and the overall quality of the resulting data.
- As a first corollary to the previous point, care should be taken not to employ experimental conditions that can alter the composition of the pigments analyzed and convert one arsenic-containing pigment into another.
- As a second corollary, in the wide range of instruments available, precedence must be given to those that are able to incontrovertibly identify the pigment.

Authors' contributions Chapters "Arsenic-based minerals and pigments", "The occurrence of As-sulfides and some notes on their trade" by EG. Chapters "The use of arsenic-based pigments", "Alteration and degradation", "Analytical methods", "Good practice guide – analysis protocol", "Concluding summary of key concepts" by LB. Chapter "Introduction" by EG-LB. Language revision by LB.

Funding Open access funding provided by Università degli Studi di Bari Aldo Moro within the CRUI-CARE Agreement.

Availability of data and materials Data sharing is not applicable to this review article as no new data were created or analyzed in this study.

Declarations

Conflicts of interest The authors declare that they have no conflicts of interest.

Code availability Not applicable.

Open Access This article is licensed under a Creative Commons Attribution 4.0 International License, which permits use, sharing, adaptation, distribution and reproduction in any medium or format, as long as you give appropriate credit to the original author(s) and the source, provide a link to the Creative Commons licence, and indicate if changes were made. The images or other third party material in this article are included in the article's Creative Commons licence, unless indicated otherwise in a credit line to the material. If material is not included in the article's Creative Commons licence and your intended use is not permitted by statutory regulation or exceeds the permitted use, you will need to obtain permission directly from the copyright holder. To view a copy of this licence, visit http://creativecommons.org/licenses/by/4.0/.

References

Aceto M (2021) The palette of organic colourants in wall paintings. Archaeological and Anthropological Sciences. https://doi.org/10.1007/s12520-021-01392-3

Afzal P, Heidari SM, Ghaderi M, Yasrebi AB (2017) Determination of mineralization stages using correlation between geochemical fractal modeling and geological data in Arabshah sedimentary rock-hosted epithermal gold deposit, NW Iran. Ore Geol Rev 91:278–295. https://doi.org/10.1016/j.oregeorev.2017.09.021

Akçay M, Özkan HM, Moon CJ, Spiro B (2006) Geology, mineralogy and geochemistry of the gold-bearing stibnite and cinnabar deposits in the Emirli and Halıköy areas (Ödemiş, İzmir, West Turkey). Ore Geol Rev 29(1):19–51. https://doi.org/10.1016/j.oregeorev.2004.12.006

Alderton D, Serafimovski T, Burns L, Tasev G (2014) Distribution and mobility of arsenic and antimony at miner sites in Fyr Macedonia. Carpathian Journal of Earth and Environmental Sciences 9(1):43–56

Anaf W, Schalm O, Janssens K, De Wael K (2015) Understanding the (in)stability of semiconductor pigments by a thermodynamic approach. Dyes Pigm 113:409–415. https://doi.org/10.1016/j.dyepig.2014.09.015

Analytical Methods Committee, AMCTB No 67 (2015) Raman spectroscopy in cultural heritage: background paper. Analytical Methods 7(12):4844-4847.https://doi.org/10.1039/C5AY90036K

Analytical Methods Committee, AMCTB No 75 (2016) UV-visible-NIR reflectance spectrophotometry in cultural heritage: Background paper. Analytical Methods 8(30):5894-5896.https://doi.org/10.1039/C6AY90112C

Analytical Methods Committee, AMCTB No 91 (2019) Laser-induced breakdown spectroscopy (LIBS) in cultural heritage. Analytical Methods 11(45):5833-5836.https://doi.org/10.1039/c9ay90147g

Arehart GB (1996) Characteristics and origin of sediment-hosted disseminated gold deposits: a review. Ore Geol Rev 11(6):383–403. https://doi.org/10.1016/S0169-1368(96)00010-8

Arik F (2012) Genetic characteristics of the Gozecukuru As-Sb deposits near Kutahya, Turkey. J Geol Soc India 80(6):855–868. https://doi.org/10.1007/s12594-012-0214-9

Aristarain LF, Hurlbut Jr. CS (1968) Teruggite, 4CaO.MgO.6B_2O_3.As_2O_5.18H_2O. A new mineral from Jujuy, Argentina.American Mineralogist 53(11–12): 1815–1827

Arizzi A, Cultrone G (2021) Mortars and plasters – How to characterise hydraulic mortars. Archaeological and Anthropological Sciences. https://doi.org/10.1007/s12520-021-01404-2

Armiero V, Lirer L, Petrosino P (2007) The Solfatara: Volcanological survey and proposal of institution of a Geosite in Campi Flegrei. Rendiconti Della Societa Geologica Italiana 5(2):3–30

Asadi HH, Voncken JHL, Hale M (1999) Invisible gold at Zarshuran. Iran Economic Geology 94(8):1367–1374. https://doi.org/10.2113/gsecongeo.94.8.1367

Asadi HH, Voncken JHL, Kühnel RA, Hale M (2000) Petrography, mineralogy and geochemistry of the Zarshuran Carlin-like gold deposit, northwest Iran. Miner Deposita 35(7):656–671. https://doi.org/10.1007/s001260050269

Ballantyne JM, Moore JN (1988) Arsenic geochemistry in geothermal systems. Geochim Cosmochim Acta 52(2):475–483. https://doi.org/10.1016/0016-7037(88)90102-0

Ballirano P (2012) Thermal behavior of realgar As_4S_4, and of arsenolite As_2O_3 and non-stoichiometric As_8S_{8+x} crystals produced from As_4S_4 melt recrystallization. Am Miner 97(8–9):1320–1329. https://doi.org/10.2138/am.2012.4114

Ballirano P, Maras A (2002) Refinement of the crystal structure of arsenolite, As_2O_3. Zeitschrift Fur Kristallographie 217(1):177–178. https://doi.org/10.1524/ncrs.2002.217.1.177

Ballirano P, Maras A (2006) In-situ X-ray transmission powder diffraction study of the kinetics of the light induced alteration of realgar (α-As_4S_4). Eur J Mineral 18(5): 589–599. https://doi.org/10.1127/0935-1221/2006/0018-0589

Becker KA, Plieth K, Stranski IN (1951) Strukturuntersuchung der monoklinen arsenikmodifikation claudetit. Zeitschrift fur Anorganische und Allgemeine Chemie 266(6): 293–301 (German). https://doi.org/10.1002/zaac.19512660604

Becker KA, Plieth K, Stranski IN (1954) Strukturuntersuchung der monoklinen arsenikmodifikation claudetit II. Zeitschrift fur Anorganische und Allgemeine Chemie 275(6): 297–300 (German). https://doi.org/10.1002/zaac.19542750603

Becker H (2021) Pigment nomenclature in the ancient Near East, Greece, and Rome. Archaeological and Anthropological Sciences. https://doi.org/10.1007/s12520-021-01394-1

Bejaoui J, Bouhlel S, Barca D, Braham A (2011) The Vein-type Zn-(Pb, Cu, As, Hg) mineralization at Fedj Hassène orefield, North-Western Tunisia: Mineralogy, Trace Elements, Sulfur Isotopes and Fluid Inclusions. Estudios Geologicos 67(1):5–20. https://doi.org/10.3989/egeol.40214.118

Bersani D, Lottici PP (2016) Raman spectroscopy of minerals and mineral pigments in archaeometry. J Raman Spectrosc 47(5):499–530. https://doi.org/10.1002/jrs.4914

Best SP, Clark RJ, Daniels MA, Porter CA, Withnall R (1995) Identification by Raman microscopy and visible reflectance spectroscopy of pigments on an Icelandic manuscript. Stud Conserv 40(1):31–40. https://doi.org/10.0079/sic.1995.40.1.31

Bezur, A., Lee, L., Loubser, M., Trentelman, K. (2020) Handheld XRF in cultural heritage: a practical workbook for conservators, The Getty Conservation Institute, https://www.getty.edu/conservation/publications_resources/pdf_publications/pdf/handheld-xrf-cultural-heritage.pdf

Bhatnagar SS, Rao BL (1923) Die Umwandlung von Realgar in Auripigment und das analoge Verhalten von Arsensulfidhydrosol. Kolloid-Zeitschrift 33(3):159–164. https://doi.org/10.1007/BF01423366

Biagioni C, Bonaccorsi E, Moëlo Y, Orlandi P, Bindi L, D'Orazio M, Vezzoni S (2014a) Mercury-arsenic sulfosalts from the Apuan Alps (Tuscany, Italy). II. Arsiccioite, $AgHg_2TlAs_2S_6$, a new mineral from the Monte Arsiccio mine: Occurrence, crystal structure and crystal chemistry of the routhierite isotypic series. Mineralogical Magazine 78(1): 101–117. https://doi.org/10.1180/minmag.2014.078.1.08

Biagioni C, Bonaccorsi E, Moëlo Y, Orlandi P (2014b) Mercury-arsenic sulfosalts from the Apuan Alps (Tuscany, Italy). III. Aktashite, $Cu_6Hg_3As_4S_{12}$, and laffittite, $AgHgAsS_3$, from the Monte Arsiccio mine: Occurrence and crystal structure. Periodico di Mineralogia 83(1): 1–18. https://doi.org/10.2451/2014PM0001

Biagioni C, D'Orazio M, Fulignati P, George LL, Mauro D, Zaccarini F (2020) Sulfide melts in ore deposits from low-grade metamorphic settings: Insights from fluid and Tl-rich sulfosalt microinclusions from the Monte Arsiccio mine (Apuan Alps, Tuscany, Italy). Ore Geol Rev 123:103589. https://doi.org/10.1016/j.oregeorev.2020.103589

Bianchin S, Casellato U, Favaro M, Vigato PA (2007) Painting technique and state of conservation of wall paintings at Qusayr Amra. Amman-Jordan Journal of Cultural Heritage 8(3):289–293. https://doi.org/10.1016/j.culher.2007.05.002

Bin H, Gui-bin J, Meng Z, Xiao-bai X (2000) Determination of as species in extracts of the Chinese medicines realgar and orpiment by ion chromatography and hydride generation GFAAS.Atomic Spectroscopy 21(4): 143–148

Bindi L, Bonazzi P (2007) Light-induced alteration of arsenic sulfides: a new product with an orthorhombic crystal structure. Am Miner 92(4):617–620. https://doi.org/10.2138/am.2007.2332

Bindi L, Popova V, Bonazzi P (2003) Uzonite, AsS, from the type locality: single-crystal X-ray study and effects of exposure to light. Can Mineral 41:1463–1468. https://doi.org/10.2113/gscanmin.41.6.1463

Bindi L, Pratesi G, Muniz-Miranda M, Zoppi M, Chelazzi L, Lepore GO, Menchetti S (2015a) From ancient pigments to modern optoelectronic applications of arsenic sulfides: Bonazziite, the natural analogue of β-As4S4 from Khaidarkan deposit. Kyrgyzstan Mineralogical Magazine 79(1):121–131. https://doi.org/10.1180/minmag.2015.079.1.10

Bindi L, Biagioni C, Raber T, Roth P, Nestola F (2015c) Ralphcannonite, $AgZn_2TlAs_2S_6$, a new mineral of the routhierite isotypic series from Lengenbach, Binn Valley. Switzerland Mineralogical Magazine 79(5):1089–1098. https://doi.org/10.1180/minmag.2015.079.5.05

Bindi L, Bonazzi P, Zoppi M, Spry PG (2014a) Chemical variability in wakabayashilite: a real feature or an analytical artifact?.Mineralogical Magazine 78(3): 693–702. https://doi.org/10.1180/minmag.2014.078.3.16

Bindi L, Nestola F, Makovicky E, Guastoni A, De Battisti L (2014b) Tl-bearing sulfosalt from the Lengenbach quarry, Binn Valley, Switzerland: Philrothite, TlAs3S5.Mineralogical Magazine 78(1): 1–9. https://doi.org/10.1180/minmag.2014.078.1.01

Bindi L, Nestola F, Graeser S, Tropper P, Raber T (2015b) Eckerite, Ag_2CuAsS_3, a new Cu-bearing sulfosalt from Lengenbach quarry, Binn valley, Switzerland: Description and crystal structure.Mineralogical Magazine 79(3): 687–694. https://doi.org/10.1180/minmag.2015.079.3.13

Bish DL, Post JE (1993) Quantitative mineralogical analysis using the Rietveld full-pattern fitting method. Am Miner 78(9–10):932–940

Blades N, Lithgow K, Cannon-Brookes S, Mardaljevic J (2017) New tools for managing daylight exposure of works of art: case study of Hambletonian, Mount Stewart, Northern Ireland. J Inst Conserv 40(1):15–33. https://doi.org/10.1080/19455224.2016.1214610

Bonazzi P, Bindi L (2008) A crystallographic review of arsenic sulfides: Effects of chemical variations and changes induced by exposure to light. Zeitschrift Fur Kristallographie 223(1–2):132–147. https://doi.org/10.1524/zkri.2008.0011

Bonazzi P, Menchetti S, Pratesi G (1995) The crystal structure of pararealgar, As_4S_4. Am Miner 80:400–403
Bonazzi P, Menchetti S, Pratesi G, Muniz-Miranda M, Sbrana G (1996) Light-induced variations in realgar and β-As_4S_4: X-ray diffraction and Raman studies. Am Miner 81(7–8):874–880. https://doi.org/10.2138/am-1996-7-810
Bonazzi P, Bindi L, Popova V, Pratesi G, Menchetti S (2003b) Alacranite, As_8S_9: structural study of the holotype and re-assignment of the original chemical formula. Am Miner 88:1796–1800. https://doi.org/10.2138/am-2003-11-1220
Bonazzi P, Lampronti GI, Bindi L, Zanardi S (2005) Wakabayashilite, [(As, $Sb_)6_S9$] [A_s4_S5]: Crystal structure, pseudosymmetry, twinning, and revised chemical formula. Am Miner 90(7):1108–1114. https://doi.org/10.2138/am.2005.1809
Bonazzi P, Bindi L, Pratesi G, Menchetti S (2006) Light-induced changes in molecular arsenic sulfides: State of the art and new evidence by single-crystal X-ray diffraction. Am Miner 91(8–9):1323–1330. https://doi.org/10.2138/am.2006.2165
Bonazzi P, Lepore GO, Bindi L (2016) Molecular versus layered structure in arsenic sulfide minerals: The case of duranusite, As_4S. Eur J Mineral 28(1):147–151. https://doi.org/10.1127/ejm/2015/0027-2474
Bonazzi P, Bindi L, Olmi F, Menchetti S (2003a) How many alacranites do exist? A structural study of non-stoichiometric As_8S_{9-x} crystals.European Journal of Mineralogy 15: 283–288. https://doi.org/10.1127/0935-1221/2003/0015-0283
Bowell RJ, Baumann M, Gingrich M, Tretbar D, Perkins WF, Fisher PC (1999) The occurrence of gold at the Getchell mine. Nevada Journal of Geochemical Exploration 67(1–3):127–143. https://doi.org/10.1016/S0375-6742(99)00062-X
Bowles JFW, Howie RA, Vaughan DJ, Zussman J (2011) Non-silicates: oxides, hydroxides and sulfides. Rock-Forming Minerals, 5A. London: Geological Society, pp. 920
Boyle RW (1987) Gold deposits in turbidite sequences: their geology, geochemistry and history of the theories of their origin. Geol Assoc Can Spec Pap 32:1–13
Bozorth RM (1923) The crystal structures of the cubic forms of arsenious and antimonous oxides. J Am Chem Soc 45(7):1621–1627. https://doi.org/10.1021/ja01660a006
Brecoulaki H (2014) "Precious colours" in ancient greek polychromy and painting: Material aspects and symbolic values. Revue Archeologique 57(1):3–35. https://doi.org/10.3917/arch.141.0003
Brizzi G, Ciselli I, Santucci A (1986) Ultime novita da le Cetine di Cotorniano (SI). Rivista Mineralogica Italiana 9(4):145–155
Bruno NE, Thompson TB (2019) Gualcamayo mining District, Argentina: an example of Carlin-like Au deposits. Ore Geology Reviews 111:102953. https://doi.org/10.1016/j.oregeorev.2019.102953
Bryndzya LT, Kleppa OJ (1988) Standard molar enthalpies of formation of realgar (α-AsS) and orpiment (As_2S_3) by high-temperature direct-synthesis calorimetry. J Chem Thermodyn 20(6):755–764. https://doi.org/10.1016/0021-9614(88)90028-6
Bujňáková Z, Baláž P, Makreski P, Jovanovski G, Čaplovičová M, Čaplovič Ľ, Shpotyuk O, Ingram A, Lee T-C, Cheng J-J, Sedlák J, Turianicová E, Zorkovská A (2015) Arsenic sulfide nanoparticles prepared by milling: properties, free-volume characterization, and anti-cancer effects. J Mater Sci 50(4):1973–1985. https://doi.org/10.1007/s10853-014-8763-5
Burgio L, Clark RJ (2000) Comparative pigment analysis of six modern Egyptian papyri and an authentic one of the 13th century BC by Raman microscopy and other techniques. J Raman Spectrosc 31(5):395–401. https://doi.org/10.1016/j.saa.2012.02.020
Burgio L, Melessanaki K, Doulgeridis M, Clark RJH, Anglos D (2001) Pigment identification in paintings employing laser induced breakdown spectroscopy and Raman microscopy. Spectrochim Acta, Part B 56(6):905–913. https://doi.org/10.1016/S0584-8547(01)00215-4
Burgio L, Clark RJ, Theodoraki K (2003) Raman microscopy of Greek icons: identification of unusual pigments. Spectrochim Acta Part A Mol Biomol Spectrosc 59(10):2371–2389. https://doi.org/10.1016/S1386-1425(03)00079-9
Burgio L, Clark RJ, Rosser-Owen M (2007) Raman analysis of ninth-century Iraqi stuccoes from Samarra. J Archaeol Sci 34(5):756–762. https://doi.org/10.1016/j.jas.2006.08.002
Burgio L, Clark RJ, Muralha VS, Stanley T (2008) Pigment analysis by Raman microscopy of the non-figurative illumination in 16th-to 18th-century Islamic manuscripts. J Raman Spectrosc 39(10):1482–1493. https://doi.org/10.1002/jrs.2027
Burgio L, Clark RJ, Hark RR (2010) Raman microscopy and x-ray fluorescence analysis of pigments on medieval and Renaissance Italian manuscript cuttings. Proc Natl Acad Sci 107(13):5726–5731. https://doi.org/10.1073/pnas.0914797107
Burgio L, Cesaratto A, Derbyshire A (2012) Comparison of English portrait miniatures using Raman microscopy and other techniques. J Raman Spectrosc 43(11):1713–1721
Burgio L, Manca R, Browne C, Button V, Horsfall Turner O, Rutherston J (2019) Orange for gold?Arsenic sulfide glass on the V&A Leman Album. J Raman Spectrosc 50(8):1169–1176. https://doi.org/10.1002/jrs.5612
Burgio L, Bioletti S, Mehan B (2013) Non-destructive, in situ analysis of three early medieval manuscripts from Trinity College Library Dublin (Codex Usserianus Primus, Book of Durrow, Book of Armagh), in Making Histories: Proceedings of the Sixth International Conference on Insular Art, York 2011
Burgio L (2000) Analysis of pigments on art objects by Raman microscopy and other techniques. Doctoral dissertation, University of London.
Burgio L (2021) Pigments, dyes and inks – their analysis on manuscripts, scrolls and papyri. Archaeological and Anthropological Sciences. https://doi.org/10.1007/s12520-021-01403-3
Burns PC, Percival JB (2001) Alacranite, A_s4_S4: a new occurrence, new formula, and determination of the crystal structure. Can Mineral 39(3):809–818. https://doi.org/10.2113/gscanmin.39.3.809
Buzgar N, Buzatu A, Apopei A-I, Cotiugă V (2014) In situ Raman spectroscopy at the Voroneţ Monastery (16th century, Romania): New results for green and blue pigments. Vib Spectrosc 72:142–148. https://doi.org/10.1016/j.vibspec.2014.03.008
Bychkov AY, Grichuk DV (1991) A thermodynamic model for the Sb-As mineralization in the Uzon caldera.Geochemistry International 28(11): 68–78
Cabella R, Cortesogno L, Lucchetti G (1987) Danburite-bearing mineralizations in metapelites of Permian age (Ligurian Brianconnais, Maritime Alps, Italy). Neues Jahrb Mineral Monatsh 7:289–294
Cahoon BG (1965) Polymorphism of arsenic sulfide (AsS). In: Hurlbut, C.S. (Ed.) Research on chemistry and physics of inorganic systems under extreme high pressure and temperature. U.S. National Technical Information Service, Document AD 633148, pp. 42–52
Calza C, Anjos MJ, Mendonça De Souza SMF, Brancaglion A Jr, Lopes RT (2008) X-ray microfluorescence with synchrotron radiation applied in the analysis of pigments from ancient Egypt. Appl Phys A Mater Sci Process 90(1):75–79. https://doi.org/10.1007/s00339-007-4234-z
Campostrini I, Demartin F, Scavini M (2019) Russoite, NH4ClAs23+O3(H2O)0.5, a new phylloarsenite mineral from Solfatara di Pozzuoli, Napoli, Italy. Mineralogical Magazine 83(1): 89–94. https://doi.org/10.1180/minmag.2017.081.097
Caroselli M, Ruffolo SA, Piqué F (2021) Mortars and plasters – How to manage mortars and plasters conservation. Archaeological and Anthropological Sciences. https://doi.org/10.1007/s12520-021-01409-x

Carter EA, Perez FR, Garcia JM, Edwards HG (2016) Raman spectroscopic analysis of an important Visigothic historiated manuscript. Philosophical Transactions of the Royal Society a: Mathematical, Physical and Engineering Sciences 374(2082):20160041. https://doi.org/10.1098/rsta.2016.0041

Casadio F, Daher C, Bellot-Gurlet L (2016) Raman spectroscopy of cultural heritage materials: overview of applications and new frontiers in instrumentation, sampling modalities, and data processing. Top Curr Chem 374(5):62. https://doi.org/10.1007/s41061-016-0061-z

Casadio F, Heye E, Manchester K (2005) From the molecular to the spectacular: a statue of Osiris through the eyes of a scientist, a conservator, and a curator. Art Institute of Chicago Museum Studies, 8–105

Castro LNC, Calza C, Freitas RP, Brancaglion A Jr., Lopes RT (2016) Analysis of ancient Egypt artifacts using X-ray fluorescence. In: IMEKO International Conference on Metrology for Archaeology and Cultural Heritage, MetroArcheo 2016 (Torino, Italy, 19–21 October 2016), pp. 119–123

Catelani T, Perito B, Bellucci F, Lee SS, Fenter P, Newville M, Rimondi V, Pratesi G, Costagliola P (2018) Arsenic uptake in bacterial calcite. Geochim Cosmochim Acta 222:642–654. https://doi.org/10.1016/j.gca.2017.11.013

Cavallo G, Riccardi MP (2021) Glass-based pigments in painting. Archaeological and Anthropological Sciences https://doi.org/10.1007/s12520-021-01453-7

Celep O, Alp I, Deveci H, Vicil M, Yilmaz T (2006) The investigation of gold and silver recovery from Akoluk (Ordu -Turkey) ore. In: 6th International Scientific Conference on Modern Management of Mine Producing, Geology and Environmental protection, SGEM 2006 (Albena, Bulgaria 12 June 2006 - 16 June 2006), pp. 251–258

Chaplin TD, Clark RJ, McKay A, Pugh S (2006) Raman spectroscopic analysis of selected astronomical and cartographic folios from the early 13th century Islamic 'Book of Curiosities of the Sciences and Marvels for the Eyes'. Journal of Raman Spectroscopy: an International Journal for Original Work in All Aspects of Raman Spectroscopy, including Higher Order Processes, and Also Brillouin and Rayleigh Scattering 37(8):865–877

Clark AH (1970) Alpha-arsenic sulfide, from mina Alacrán, Pampa Larga, Chile. The American Mineralogist 55:1338–1344

Clark RJ (1995) Raman microscopy: application to the identification of pigments on medieval manuscripts. Chem Soc Rev 24(3):187–196. https://doi.org/10.1039/CS9952400187

Clark RJ (2007) Raman microscopy as a structural and analytical tool in the fields of art and archaeology. J Mol Struct 834:74–80. https://doi.org/10.1016/j.molstruc.2007.01.031

Clark RJH, Gibbs PJ (1997) Identification of lead(II) sulfide and pararealgar on a 13th century manuscript by Raman microscopy. Chem Commun 11:1003–1004. https://doi.org/10.1039/a701837a

Cline JS (2001) Timing of gold and arsenic sulfide mineral deposition at the Getchell carlin-type gold deposit. North-Central Nevada Economic Geology 96(1):75–89. https://doi.org/10.2113/gsecongeo.96.1.75

Cline JS, Hofstra AA (2000) Ore-fluid evolution at the Getchell Carlin-type gold deposit, Nevada, USA.European Journal of Mineralogy 12(1): 195–212. https://doi.org/10.1127/ejm/12/1/0195

Cloutis E, Norman L, Cuddy M, Mann P (2016) Spectral reflectance (350–2500 nm) properties of historic artists' pigments. II. Red–Orange–Yellow Chromates, Jarosites, Organics, Lead (–Tin) Oxides, Sulphides, Nitrites and Antimonates. Journal of Near Infrared Spectroscopy 24(2):119–140. https://doi.org/10.1255/jnirs.1207

Coccato A, Moens L, Vandenabeele P (2017) On the stability of mediaeval inorganic pigments: a literature review of the effect of climate, material selection, biological activity, analysis and conservation treatments. Heritage Science 5(1):12. https://doi.org/10.1186/s40494-017-0125-6

Çolak M, Gemici Ü, Tarcan G (2003) The effects of colemanite deposits on the arsenic concentrations of soil and ground water in Igdeköy-Emet, Kütahya, Turkey. Water Air Soil Pollut 149(1–4):127–143. https://doi.org/10.1023/A:1025642331692

Corbeil M-C, Helwig K (1995) An occurrence of pararealgar as an original or altered artists' pigment. Stud Conserv 40(2):133–138. https://doi.org/10.1179/sic.1995.40.2.133

Cotte M, Genty-Vincent A, Janssens K, Susini J (2018) Applications of synchrotron X-ray nano-probes in the field of cultural heritage. C R Phys 19(7):575–588. https://doi.org/10.1016/j.crhy.2018.07.002

Dadová J, Andráš P, Kupka J, Krnáč J, Andráš P Jr, Hroncová E, Midula P (2016) Mercury contamination from historical mining territory at Malachov Hg-deposit (Central Slovakia). Environ Sci Pollut Res 23(3):2914–2927. https://doi.org/10.1007/s11356-015-5527-y

Daniels V, Leach B (2004) The occurrence and alteration of realgar on Ancient Egyptian papyri. Stud Conserv 49(2):73–84. https://doi.org/10.1179/sic.2004.49.2.73

Daniilia S, Andrikopoulos KS (2007) Issues relating to the common origin of two Byzantine miniatures: In situ examination with Raman spectroscopy and optical microscopy. J Raman Spectrosc 38(3):332–343. https://doi.org/10.1002/jrs.1648

Darbandi MP, Taheri J (2018) Using sulfur-containing minerals in medicine: Iranian traditional documents and modern pharmaceutical terminology. Earth Sciences History 37(1):25–33. https://doi.org/10.17704/1944-6178-37.1.25

De Meyer S, Vanmeert F, Vertongen R, van Loon A, Gonzalez V, van der Snickt G, Vandivere A, Janssens K (2019b) Imaging secondary reaction products at the surface of Vermeer's Girl with the Pearl Earring by means of macroscopic X-ray powder diffraction scanning. Heritage Science 7(1):67. https://doi.org/10.1186/s40494-019-0309-3

De Meyer S, Vanmeert F, Vertongen R, Van Loon A, Gonzalez V, Delaney J, Dooley K, Dik J, Van der Snickt G, Vandivere A, Janssens K (2019a) Macroscopic x-ray powder diffraction imaging reveals Vermeer's discriminating use of lead white pigments in Girl with a Pearl Earring. Science Advances 5(8): eaax1975. https://doi.org/10.1126/sciadv.aax1975

de Viguerie L, Glanville H, Ducouret G, Jacquemot P, Dang PA, Walter P (2018) Re-interpretation of the Old Masters' practices through optical and rheological investigation: The presence of calcite. C R Phys 19(7):543–552. https://doi.org/10.1016/j.crhy.2018.11.003

DeLaine J (2021) Production, transport and on-site organisation of Roman mortars and plasters. Archaeological and Anthropological Sciences. https://doi.org/10.1007/s12520-021-01401-5

Demergasso CS, Guillermo CD, Lorena EG, Mur JJP, Pedrós-Alió C (2007) Microbial precipitation of arsenic sulfides in andean salt flats. Geomicrobiol J 24(2):111–123. https://doi.org/10.1080/01490450701266605

Di Stefano LM, Fuchs R (2011) Characterisation of the pigments in a Ptolemaic Egyptian Book of the Dead papyrus. Archaeol Anthropol Sci 3(3):29–244. https://doi.org/10.1007/s12520-011-0054-3

Dill HG (2010) The "chessboard" classification scheme of mineral deposits: Mineralogy and geology from aluminum to zirconium. Earth Sci Rev 100(1–4):1–420. https://doi.org/10.1016/j.earscirev.2009.10.011

Dill HG, Kaufhold S, Helvaci C (2015) The physical-chemical regime of argillaceous interseam sediments in the Emet borate district, Turkey: a transition from non-metallic volcano-sedimentary to metallic epithermal deposits. J Geochem Explor 156:44–60. https://doi.org/10.1016/j.gexplo.2015.05.001

Dillhoff RM, Dillhoff TA (1991) Realgar from the Royal Reward mine, King County. Washington Rocks & Minerals 66(4):310–314. https://doi.org/10.1080/00357529.1991.11761635

Dogan M, Dogan AU (2007) Arsenic mineralization, source, distribution, and abundance in the Kutahya region of the western Anatolia. Turkey Environmental Geochemistry and Health 29(2):119–129. https://doi.org/10.1007/s10653-006-9071-z

Domingo Sanz I, Chieli A (2021) Characterising the pigments and paints of prehistoric artists. Archaeological and Anthropological Sciences. https://doi.org/10.1007/s12520-021-01397-y

Dordević T, Kolitsch U, Serafimovski T, Tasev G, Tepe N, Stoger-Pollach M, Hofmann T, Boev B (2019) Mineralogy and weathering of realgar-rich tailings at a former As-Sb-Cr mine at Lojane. North Macedonia Canadian Mineralogist 57(3):403–423. https://doi.org/10.3749/canmin.1800074

Dossie R (1764) The Handmaid to the Arts, Vol. I, Second Edition. London: Jean Nourse

Douglass DL, Shing C, Wang G (1992) The light-induced alteration of realgar to pararealgar. Am Miner 77:1266–1274

Downs RT, Hall-Wallace M (2003) The American Mineralogist Crystal Structure Database. Am Miner 88:247–250

Drahota P, Filippi M (2009) Secondary arsenic minerals in the environment: a review. Environ Int 35(8):1243–1255. https://doi.org/10.1016/j.envint.2009.07.004

Drewniak L, Sklodowska A (2013) Arsenic-transforming microbes and their role in biomining processes.Environmental Science and Pollution Research International 20(11): 7728–7739. https://doi.org/10.1007/s11356-012-1449-0

Eary LE (1992) The solubility of amorphous As_2S_3 from 25 to 90° C. Geochim Cosmochim Acta 56(6):2267–2280. https://doi.org/10.1016/0016-7037(92)90188-O

Ergenç D, Fort R, Varas−Muriel MJ, Alvarez de Buergo M (2021) Mortars and plasters – how to characterise aerial mortars and plasters. Archaeological and Anthropological Sciences. https://doi.org/10.1007/s12520-021-01398-x

Ernst RR (2010) In situ Raman microscopy applied to large Central Asian paintings. J Raman Spectrosc 41(3):275–284. https://doi.org/10.1002/jrs.2443

Fehér B, Szakáll S, Kristály F, Zajzon N (2016) Mineralogical mosaics from the Carpathian-Pannonian region 3. Foldtani Kozlony 146(1):47–60

Feneis C, Steinbach S (2018) Investigations on the light damage to mineral pigments - Colors in time [Untersuchungen zur Lichtschädigung an mineralischen Pigmenten – Farben im Laufe der Zeit].Bauphysik 40(4): 214–219 (German). https://doi.org/10.1002/bapi.201810022

Ferrini V, Martarelli L, De Vito C, Çina A, Deda T (2003) The Koman dawsonite and realgar-orpiment deposit, Northern Albania: Inferences on processes of formation. Can Mineral 41(2):413–427. https://doi.org/10.2113/gscanmin.41.2.413

Frankel LH, Zoltai T (1973) Crystallography of dimorphites. Zeitschrift für Kristallographie 138: 161–166. https://doi.org/10.1524/zkri.1973.138.jg.161

Frueh AJ (1951) The crystal structure of claudetite (monoclinic As_2O_3). Am Miner 36:833–850

Fu S-H, Gu X-X, Wang P (2002) Characteristics of the gold-bearing minerals and their significance to the ore genesis of the Manaoke gold deposit, northwestern Sichuan. Journal of the Chengdu Institute of Technology 29(4):422–427

Fukushi K, Sasaki M, Sato T, Yanase N, Amano H, Ikeda H (2003) A natural attenuation of arsenic in drainage from an abandoned arsenic mine dump. Appl Geochem 18(8):1267–1278. https://doi.org/10.1016/S0883-2927(03)00011-8

Furuta E, Sato N (2016) Quantitative and structural analyses of hazardous elements in Chinese medicines and herbs.Toxicological and Environmental Chemistry 98(7): 814–827. DOI: https://doi.org/10.1080/02772248.2015.1135927

Garavelli A, Vurro F (1994) Barberiite, NH_4BF_4, a new mineral from Vulcano, Aeolian Islands. Italy American Mineralogist 79(3–4):381–384

Gard FS, Santos DM, Daizo MB, Freire E, Reinoso M, Halac EB (2020) Pigments analysis of an Egyptian cartonnage by means of XPS and Raman spectroscopy.Applied Physics A: Materials Science and Processing 126(3): 218. https://doi.org/10.1007/s00339-020-3386-y

Gavezzotti A, Demartin F, Castellano C, Campostrini I (2013) Polymorphism of As_4S_3 (tris-(μ_2-sulfido)-tetra-arsenic): Accurate structure refinement on natural α- and β-dimorphites and inferred room temperature thermodynamic properties.Physics and Chemistry of Minerals 40(2): 175–182. https://doi.org/10.1007/s00269-012-0559-z

Gebremariam KF, Kvittingen L, Nicholson DG (2016) Multi-analytical investigation into painting materials and techniques: The wall paintings of Abuna Yemata Guh church. Heritage Science 4(1):32. https://doi.org/10.1186/s40494-016-0101-6

Gibbs GV, Wallace AF, Downs RT, Ross NL, Cox DF, Rosso KM (2011) Thioarsenides: a case for long-range Lewis acid-base-directed van der Waals interactions. Phys Chem Miner 38(4):267–291. https://doi.org/10.1007/s00269-010-0402-3

Gliozzo E, Ionescu C (2021) Pigments – Lead-based whites, reds, yellows and oranges and their alteration phases. Archaeological and Anthropological Sciences. https://doi.org/10.1007/s12520-021-01407-z

Gliozzo E, Pizzo A, La Russa MF (2021) Mortars, plasters and pigments − Research questions and sampling criteria. Archaeological and Anthropological Sciences. https://doi.org/10.1007/s12520-021-01393-2

Gliozzo E (2021) Pigments – Mercury-based red (cinnabar-vermilion) and white (calomel) and their degradation products. Archaeological and Anthropological Sciences. https://doi.org/10.1007/s12520-021-01402-4

Göd R, Zemann J (2000) Native arsenic - realgar mineralization in marbles from Saualpe, Carinthia. Austria Mineralogy and Petrology 70(1–2):37–53. https://doi.org/10.1007/s007100070012

Golestaneh F (1983) Antimony-arsenic mineralisation of Dashkasan-Baharlu, West-Iran.Monograph Series on Mineral Deposits 22: 165–178.

Gómez-Morón MA, Ortiz P, Martín-Ramírez JM, Ortiz R, Castaing J (2016) A new insight into the vaults of the kings in the Alhambra (Granada, Spain) by combination of portable XRD and XRF. Microchemical Journal 125: 260–265. https://doi.org/10.1016/j.microc.2015.11.023

Graeser S, Edenharter A (1997) Jentschite (TlPbAs2SbS6) - A new sulphosalt mineral from Lengenbach, Binntal (Switzerland). Mineral Mag 61(1):131–137. https://doi.org/10.1180/minmag.1997.061.404.13

Graeser S, Berlepsch P, Makovicky E, Balić-Žǔnić T (2001) Sicherite, $TlAg_2(As, Sb_)3_S6$, a new sulfosalt mineral from Lengenbach (Binntal, Switzerland): Description and structure determination. Am Miner 86(9):1087–1093. https://doi.org/10.2138/am-2001-8-916

Graeser S, Topa D, Balić-Žunić T, Makovicky E (2006) Gabrielite, Tl_2AgCu_2 As_3S_7, a new species of thallium sulfosalt from Lengenbach, Binntal. Switzerland Canadian Mineralogist 44(1):135–140. https://doi.org/10.2113/gscanmin.44.1.135

Groff JA (2018) Fluid mixing during late-stage Carlin-type mineralization in the Getchell and Twin Creeks deposits, Nevada. Ore Geol Rev 101:960–965. https://doi.org/10.1016/j.oregeorev.2018.08.009

Groff JA (2019) Evidence of boiling and epithermal vein mineralization in Carlin-type deposits on the Getchell trend, Nevada. Ore Geol Rev 106:340–350. https://doi.org/10.1016/j.oregeorev.2019.02.013

Groff JA, Heizler MT, Mcintosh WC, Norman DI (1997) $^{40}Ar/^{39}Ar$ dating and mineral paragenesis for Carlin-type gold deposits along the Getchell trend, Nevada: Evidence for cretaceous and tertiary gold mineralization. Econ Geol 92(5):601–622. https://doi.org/10.2113/gsecongeo.92.5.601

Grundmann G, Rötter C (2007) 'Artificial orpiment': microscopic, diffractometric and chemical characteristics of synthesis products in comparison to natural orpiment. In: Rötter, C., Grundmann, G., Richter, M., Van Loon, A., Keune, K., Boersma, A., Rapp, K. (Eds.) Auripigment / Orpiment. Studien zu dem Mineral und den künstlichen Produkten / Studies on the mineral and the artificial products.Materialien aus dem Institut für Baugeschichte, Kunstgeschichte, Restaurierung mit Architekturmuseum, Technischer Universität MünchenMünchen: Siegl, pp. 105–136.

Grundmann G, Ivleva N, Richter M, Stege H, Haisch C (2011) The rediscovery of sublimed arsenic sulfide pigments in painting and polychromy: applications of Raman microspectroscopy. In: Studying old master paintings: technology and practice. The National Gallery Technical Bulletin 30th Anniversary Conference Postprints, pp. 269–76.

Grundmann G, Richter M (2008) Current research on artificial arsenic sulfide pigments in artworks: a short review. Chimia 62(11):903–907. https://doi.org/10.2533/chimia.2008.903

Gruzdev VS, Volgin VY, Shumkova NG, Chernitsova NM, Ivanov VS (1975) Wakabayashilite, (As, $Sb_1 2_S 3$ from arsenic-antimony-mercury deposits of the U.S.S.R. Doklady, Academy of Sciences of the USSR, Earth Science Sections 224:103–106

Guo L, Hou L, Liu S, Zhang Q, Xu S, Shi M, Zeng X (2019) Ore-fluid sources and genesis of Phapon gold deposit, Laos: Constraint from REE and C, O, S isotopic characteristics.Mineral Deposits 38(2): 233–250 (Chinese). https://doi.org/10.16111/j.0258-7106.2019.02.001

Hall HT (1966) The systems Ag-Sb-S, Ag-As-S, and Ag-Bi-S: phase relations and mineralogical significance. Thesis (PhD)-Brown University, pp. 172.

Han Y, Mao J, Xie G, Lehmann B (2020) Linkage of distal vein–type Au mineralization in carbonate rocks with Cu–Au skarn mineralization in the Fengshan area, Eastern China: Mineralogy and stable isotope geochemistry. Ore Geol Rev 119:103306. https://doi.org/10.1016/j.oregeorev.2019.103306

Hawthorne FC, Burke EAJ, Ercit TS, Grew ES, Grice JD, Jambor JL, Puziewicz J, Roberts AC, Vanko DA (1988) New mineral names. Am Miner 73:189–199

Heinrich CA, Eadington PJ (1986) Thermodynamic predictions of the hydrothermal chemistry of arsenic, and their significance for the paragenetic sequence of some cassiterite – arsenopyrite – base metal sulfide deposits.Economic Geology 81(3): 511–529. https://doi.org/10.2113/gsecongeo.81.3.511

Helvacı C (1984) Occurrence of rare borate minerals: Veatchite-A, tunellite, teruggite and cahnite in the Emet borate deposits. Turkey Mineralium Deposita 19(3):217–226. https://doi.org/10.1007/BF00199788

Henke K (2009) Arsenic: Environmental Chemistry. Wiley, Health Threats and Waste Treatment, p 569

Hradil D, Hradilová J, Bezdička P, Švarcová S, Čermáková Z, Košařová V, Němec I (2014) Crocoite $PbCrO_4$and mimetite $Pb_5(AsO_4)_3Cl$: Rare minerals in highly degraded mediaeval murals in Northern Bohemia. J Raman Spectrosc 45(9):848–858. https://doi.org/10.1002/jrs.4556

Huang J-G, Li H-J, Li W-J, Dong L (2012) Element geochemistry of ore-bearing rock series in the Getang gold deposit. Guizhou Province Geology in China 39(5):1318–1326 **(Chinese)**

Huber R, Sacher M, Vollmann A, Huber H, Rose D (2000) Respiration of arsenate and selenate by hyperthermophilic Archaea. Syst Appl Microbiol 23(3):305–314. https://doi.org/10.1016/S0723-2020(00)80058-2

Hyršl J (2008) The Palomo mine Huancavelica Department. Peru Mineralogical Record 39(2):95–99

Imer A, Richards JP, Muehlenbachs K (2016) Hydrothermal evolution of the Çöpler porphyry-epithermal Au deposit, Erzincan Province. Central Eastern Turkey Economic Geology 111(7):1619–1658. https://doi.org/10.2113/econgeo.111.7.1619

Ishibashi J-I, Nakaseama M, Seguchi M, Yamashita T, Doi S, Sakamoto T, Shimada K, Shimada N, Noguchi T, Oomori T, Kusakabe M, Yamanaka T (2008) Marine shallow-water hydrothermal activity and mineralization at the Wakamiko crater in Kagoshima bay, south Kyushu, Japan. J Volcanol Geoth Res 173(1–2):84–98. https://doi.org/10.1016/j.jvolgeores.2007.12.041

Ito T, Morimoto N, Sadanaga R (1952) The crystal structure of realgar. Acta Crystallogr A 5:775–782. https://doi.org/10.1107/S0365110X52002112

Janssens K, Van der Snickt G, Vanmeert F, Legrand S, Nuyts G, Alfeld M, Monico L, Anaf W, De Nolf W, Vermeulen M, Verbeeck J, De Wael K (2016) Non-invasive and non-destructive examination of artistic pigments, paints, and paintings by means of X-ray methods. Top Curr Chem 374(6):81. https://doi.org/10.1007/s41061-016-0079-2

Jemmali N, Souissi F, Carranza EJM, Bouabdellah M (2013) Lead and sulfur isotope constraints on the genesis of the polymetallic mineralization at Oued Maden, Jebel Hallouf and Fedj Hassene carbonate-hosted Pb-Zn (As-Cu-Hg-Sb) deposits, Northern Tunisia. J Geochem Explor 132:6–14. https://doi.org/10.1016/j.gexplo.2013.03.004

Jewell PW, Parry WT (1988) Geochemistry of the Mercur gold deposit (Utah, U.S.A.). Chemical Geology 69(3–4): 245–265. https://doi.org/10.1016/0009-2541(88)90038-1

Jingrong Z, Wei W, Fan Y, Tong C (1993) The hot-spring genesis of the Shimen realgar deposit, northwest Hunan. Chin J Geochem 12(2):137–147. https://doi.org/10.1007/BF02842195

Jo S, Ryu SR, Jang W, Kwon O-S, Rhee B, Lee YE, Kim D, Kim J, Shin K (2019) LED illumination-induced fading of traditional Korean pigments. J Cult Herit 37:129–136. https://doi.org/10.1016/j.culher.2018.11.005

Johan Z, Mantienne J (2000) Thallium-rich mineralization at Jas Roux, Hautes-Alpes, France: A complex epithermal, sediment-hosted, ore-forming system. Journal of the Czech Geological Society 45(1–2):63–77

Johan Z, Laforêt C, Picot P, Feraud J (1973) La duranusite, As_4S, un nouveau minéral. Bulletin De La Société Française De Minéralogie Et De Cristallographie 96(2):131–134

Johnson RF (1955) Geology of the Atacocha mine. Econ Geol 50(3):249–270. https://doi.org/10.2113/gsecongeo.50.3.249

Jovanovski G, Makreski P (2020) Intriguing minerals: photoinduced solid-state transition of realgar to pararealgar—direct atomic scale observation and visualization. Chem Texts 6(1):5. https://doi.org/10.1007/s40828-019-0100-9

Jurado-López A, Demko O, Clark RJ, Jacobs D (2004) Analysis of the palette of a precious 16th century illuminated Turkish manuscript by Raman microscopy. J Raman Spectrosc 35(2):119–124

Jurković I, Ramović M, Zec F (1999) Chemical and geochemical characteristics of the Cemernica antimonite deposit in the Mid-Bosnian Schist Mountains. Rudarsko Geolosko Naftni Zbornik 11:1–16

Kampf AR, Downs RT, Housley RM, Jenkins RA, Hyrsl J (2011) Anorpiment, As_2S_3, the triclinic dimorph of orpiment. Mineral Mag 75(6):2857–2867. https://doi.org/10.1180/minmag.2011.075.6.2857

Kato A, Sakurai KI, Oshumi K (1970) Introduction to Japanese minerals. Geological Survey of Japan, pp. 92–93

Keneman SA, Bordogna J, Zemel JN (1978) Evaporated films of arsenic trisulfide: physical model of effects of light exposure and heat cycling. J Appl Phys 49:4663–4673. https://doi.org/10.1063/1.325555

Keshavarzi B, Moore F, Rastmanesh F, Kermani M (2012) Arsenic in the Muteh gold mining district, Isfahan. Iran Environmental Earth Sciences 67(4):959–970. https://doi.org/10.1007/s12665-012-1532-3

Keune K, Mass J, Meirer F, Pottasch C, Van Loon A, Hull A, Church J, Pouyet E, Cotte M, Mehta A (2015) Tracking the transformation and transport of arsenic sulfide pigments in paints: Synchrotron-based X-ray micro-analyses. J Anal at Spectrom 30(3):813–827. https://doi.org/10.1039/c4ja00424h

Keune K, Mass J, Mehta A, Church J, Meirer F (2016) Analytical imaging studies of the migration of degraded orpiment, realgar, and emerald green pigments in historic paintings and related conservation issues. Heritage Science 4(1):10. https://doi.org/10.1186/s40494-016-0078-1

De Keyser N, Van der Snickt G, Van Loon A, Legrand S, Wallert A, Janssens K (2017) Jan Davidsz. de Heem (1606–1684): a technical examination of fruit and flower still lifes combining MA-XRF scanning, cross-section analysis and technical historical sources. Heritage Science 5: 38. https://doi.org/10.1186/s40494-017-0151-4

Knapp CW, Christidis GE, Venieri D, Gounaki I, Gibney-Vamvakari J, Stillings M, Photos-Jones E (2021) The ecology and bioactivity of some Greco-Roman medicinal minerals: the case of Melos earth pigments. Archaeological and Anthropological Sciences. https://doi.org/10.1007/s12520-021-01396-z

Korenberg CF, Pereira-Pardo L, McElhinney PJ, Dyer J (2019) Developing a systematic approach to determine the sequence of impressions of Japanese woodblock prints: the case of Hokusai's 'Red Fuji'. Heritage Science 7(1):1–11. https://doi.org/10.1186/s40494-019-0318-2

Krenner J (1907) Die Krystallform und optischen Eigenschaften des Schullerschen Arsensulfides.Über den Dimorphin der Solfatara in den phlegräischen Feldern (The crystal form and optical properties of the arsenic sulfide prepared by Schuller.Dimorphite from the Solfatara in the Phlegraean Fields). Z. Kristallogr. Mineral. Zeitschrift für Kristallographie43(1): 476–484. DOI: https://doi.org/10.1524/zkri.1907.43.1.476

Kutoglu A (1976) Darstellung und kristallstruktur einer neuen isomeren form von As_4S_4.Zeitschrift flir anorganische und allgemeine Chemie 419(2): 176–184. DOI: https://doi.org/10.1002/zaac.19764190211

Kyono A (2009) Molecular conformation and anion configuration variations for As_4S_4 and As_4Se_4 in an anion-substituted solid solution. Am Miner 94(4):451–460. https://doi.org/10.2138/am.2009.3075

Kyono A, Kimata M, Hatta T (2005) Light-induced degradation dynamics in realgar: in situ structural investigation using single-crystal X-ray diffraction study and X-ray photoelectron spectroscopy. Am Miner 90(10):1563–1570. https://doi.org/10.2138/am.2005.1785

Kyono A (2007) Experimental study of the effect of light intensity on arsenic sulfide (As_4S_4) alteration.Journal of Photochemistry and Photobiology A: Chemistry 189(1): 15–22. DOI: https://doi.org/10.1016/j.jphotochem.2006.12.043

Kyono A (2013) Ab initio quantum chemical investigation of arsenic sulfide molecular diversity from As_4S_6 and As_4.Physics and Chemistry of Minerals 40(9): 717–731. https://doi.org/10.1007/s00269-013-0607-3

La Russa MF, Ruffolo SA (2021) Mortars and plasters – How to characterise mortars and plasters degradation. Archaeological and Anthropological Sciences. https://doi.org/10.1007/s12520-021-01405-1

Laclavetine K, Boust C, Clivet L, Le Hô AS, Laval E, Mathis R, Menu M, Pagliano E, Salmon X, Selbach V, Vrand C, Lepape S (2019) Non-invasive study of 16th century Northern European chiaroscuro woodcuts: First insights. Microchem J 144:419–430. https://doi.org/10.1016/j.microc.2018.10.003

Lahlil S, Martin E (2012) Characterisation of 18 Melkite icons dating from the 17th to the 19th c. AD.Journal of Cultural Heritage13(3): 332–338. https://doi.org/10.1016/j.culher.2011.11.004

Lancaster LC (2021) Mortars and plasters – How mortars were made. The Literary Sources. Archaeological and Anthropological Sciences. https://doi.org/10.1007/s12520-021-01395-0

Lausen C (1928) Hydrous sulphates formed under fumarolic conditions at the United Verde mine. Amrican Mineralogist 13(6):227–229

Ledbetter RN, Connon SA, Neal AL, Dohnalkova A, Magnuson TS (2007) Biogenic mineral production by a novel arsenic-metabolizing thermophilic bacterium from the Alvord Basin. Oregon Applied and Environmental Microbiology 73(18):5928–5936. https://doi.org/10.1128/AEM.00371-07

Lee M-K, Saunders JA, Wilkin RT, Mohammad S (2006) Geochemical modeling of arsenic speciation and mobilization: Implications for bioremediation. In: O'Day P.A., Vlassopoulos D., Meng X., Benning L.G. (Eds.) Advances in Arsenic Research. ACS Symposium Series, 915. Oxford: University Press, pp. 398–413.

Lee J-H, Kim M-G, Yoo B, Myung NV, Maeng J, Lee T, Dohnalkova AC, Fredrickson JK, Sadowsky MJ, Hur H-G (2007) Biogenic formation of photoactive arsenic-sulfide nanotubes by Shewanella sp. strain HN-41. Proceedings of the National Academy of Sciences of the United States of America 104(51): 20410–20415. https://doi.org/10.1073/pnas.0707595104

Li ZW, Liu CD, Zhao XQ, Lu JH, Guo GL (2014a) The mineral characteristics and occurrence of gold in Nali gold deposit, Guangxi. Advanced Materials Research 936:2383–2388. https://doi.org/10.4028/www.scientific.net/AMR.936.2383

Li Z, Wang L, Ma Q, Mei J (2014b) A scientific study of the pigments in the wall paintings at Jokhang Monastery in Lhasa, Tibet. China Heritage Science 2(1):21. https://doi.org/10.1186/s40494-014-0021-2

Li N, Deng J, Yang L-Q, Groves DI, Liu X-W, Dai W-G (2018) Constraints on depositional conditions and ore-fluid source for orogenic gold districts in the West Qinling Orogen, China: Implications from sulfide assemblages and their trace-element geochemistry. Ore Geol Rev 102:204–219. https://doi.org/10.1016/j.oregeorev.2018.08.025

Liu D, Geng W (1985) On the mineral association and mineralization conditions of the Carlin-type gold deposits in China. Geochimica 3:277–282 (**Chinese**)

Liu J, Jie YE, Ying H, Liu J, Chen X (2001) A preliminary study on micro-disseminated sediment-hosted gold in the Youjiang basin, South China. J Mineral Petrol Sci 96(6):243–255. https://doi.org/10.2465/jmps.96.243

Liu J, Ye J, Ying H, Liu J, Zheng M, Gu X (2002) Sediment-hosted micro-disseminated gold mineralization constrained by basin paleo-topographic highs in the Youjiang basin, South China. J Asian Earth Sci 20(5):517–533. https://doi.org/10.1016/S1367-9120(01)00053-0

Liu J, Lu Y, Wu Q, Goyer RA, Waalkes MP (2008) Mineral arsenicals in traditional medicines: Orpiment, realgar, and arsenolite. J Pharmacol Exp Ther 326(2):363–368. https://doi.org/10.1124/jpet.108.139543

Liu Y, Hou Z, Yang Z, Xie Y, Li Y, Du D (2011) Study on fluid inclusion of Nongruri gold deposit, Tibet. China Acta Petrologica Sinica 27(2):2150–2158 (**Chinese**)

Ljubičić A, Krčmar M, Kaučić S, Logan BA (1988) Experimental determination of uranium and thorium in Allchar ore.Nuclear Instruments and Methods in Physics Research Section A 271(2): 262–263. https://doi.org/10.1016/0168-9002(88)90164-7

Luo Y, Basso E, Smith HD, Leona M (2016) Synthetic arsenic sulfides in Japanese prints of the Meiji period. Heritage Science 4(1):17. https://doi.org/10.1186/s40494-016-0087-0

Lutterotti L, Dell'Amore F, Angelucci DE, Carrer F, Gialanella S (2016) Combined X-ray diffraction and fluorescence analysis in

the cultural heritage field. Microchem J 126:423–430. https://doi.org/10.1016/j.microc.2015.12.031
Macchia A, Nunziante Cesaro S, Campanella L, Maras A, Rocchia M, Roscioli G (2013) Which light for cultural heritage: Comparison of light sources with respect to realgar photodegradation. J Appl Spectrosc 80(5):637–643. https://doi.org/10.1007/s10812-013-9820-6
Mao J, Qiu Y, Goldfarb RJ, Zhang Z, Garwin S, Fengshou R (2002) Geology, distribution, and classification of gold deposits in the western Qinling belt, central China. Miner Deposita 37(3–4):352–377. https://doi.org/10.1007/s00126-001-0249-0
Mao X-D, Wu W-H, Huang S-J (2007) Ore types and mineral assemblage of the Changkeng Au-Ag deposit, Guangdong, South China. Journal of Chengdu University of Technology 34(1):7–14
Maroun LRC, Cline JS, Simon A, Anderson P, Muntean J (2017) High-grade gold deposition and collapse breccia formation, Cortez Hills carlin-Type gold deposit, Nevada, USA. Econ Geol 112(4):707–740. https://doi.org/10.2113/econgeo.112.4.707
Mańquez-Zavalía F, Craig JR, Solberg TN (1999) Duranusite, product of realgar alteration, Mina Capillitas. Argentina Canadian Mineralogist 37(5):1255–1259
Mastrotheodoros GP, Beltsios KG, Bassiakos Y (2021) Pigments – Iron-based red, yellow and brown ochres. Archaeological and Anthropological Sciences (forthcoming)
Matin M, Pollard AM (2017) From ore to pigment: a description of the minerals and an experimental study of cobalt ore processing from the Kāshān mine. Iran Archaeometry 59(4):731–746. https://doi.org/10.1111/arcm.12272
Mazzeo R, Baraldi P, Lujan R, Fagnano C (2004) Characterization of mural painting pigments from the Thubchen Lakhang temple in Lo Manthang. Nepal Journal of Raman Spectroscopy 35(8–9):678–685. https://doi.org/10.1002/jrs.1203
McKinstry HE, Noble JA (1932) The veins of Casapalca. Peru Economic Geology 27(6):501–522. https://doi.org/10.2113/gsecongeo.27.6.501
Mehrabi B, Yardley BWD, Cann JR (1999) Sediment-hosted disseminated gold mineralisation at Zarshuran. NW Iran Mineralium Deposita 34(7):673–696. https://doi.org/10.1007/s001260050227
Merrifield MP (1967) Original treatises on the arts of painting. Dover Publications, New York
Migdisov Bychkov AAAY (1998) The behaviour of metals and sulphur during the formation of hydrothermal mercury-antimony-arsenic mineralization, Uzon caldera, Kamchatka, Russia. J Volcanol Geoth Res 84(1):153–171. https://doi.org/10.1016/S0377-0273(98)00038-9
Migon C, Mori C (1999) Arsenic and antimony release from sediments in a Mediterranean estuary. Hydrobiologia 392(1):81–88. https://doi.org/10.1023/A:1003561609548
Miller WH, Schipper HM, Lee JS, Singer J, Waxman S (2002) Mechanisms of action of arsenic trioxide. Cancer Research 62: 3893–3903. PubMed ID: 12124315
Mindat - https://www.mindat.org
Mineralienatlas - https://www.mineralienatlas.de
Miranda-Gasca MA, Gomez-Caballero JA, Eastoe, C.J.a, (1998) Borate deposits of northern Sonora, Mexico: stratigraphy, tectonics, stable isotopes, and fluid inclusions. Econ Geol 93(4):510–523. https://doi.org/10.2113/gsecongeo.93.4.510
Mladenova V (2000) Alacranite and duranusite from Mareshnitsa occurrence, Eastern Rhodopes – new minerals for Bulgaria. Comptes Rendus De L'academie Bulgare Des Sciences 53(4):67–70
Mödlinger M, Cziegler A, Macció D, Schnideritsch H, Sabatini B (2018) Archaeological Arsenical Bronzes and Equilibrium in the As-Cu System. Metall Mater Trans B 49(5):2505–2513. https://doi.org/10.1007/s11663-018-1322-8
Mödlinger M, de Oro Calderon R, Haubner R (2019) Arsenic loss during metallurgical processing of arsenical bronze.Archaeological and Anthropological Sciences 11(1): 133–140. https://doi.org/10.1007/s12520-017-0534-1
Morimoto N (1954) The crystal structure of orpiment (As_2S_3) refined. Mineral J 1(3):160–169
Morimoto N (1949) The crystal structure of orpiment. X-rays 5(3–4): 115–120 (Japanese). https://doi.org/10.5940/jcrsj1940.5.115
Mullen DJE, Nowacki W (1972) Refinement of the crystal structures of realgar, AsS and orpiment, As_2S_3. Z Kristallogr 136:48–65. https://doi.org/10.1524/zkri.1972.136.1-2.48
Mumford AC, Yee N, Young LY (2013) Precipitation of alacranite (As8S9) by a novel As(V)-respiring anaerobe strain MPA-C3. Environ Microbiol 15(10):2748–2760. https://doi.org/10.1111/1462-2920.12136
Muniz-Miranda M, Sbrana G, Bonazzi P, Menchetti S, Pratesi G (1996) Spectroscopic investigation and normal mode analysis of As_4S_4 polymorphs.Spectrochimica Acta A 52: 1391–1401. https://doi.org/10.1016/0584-8539(96)01698-4
Muralha VSF, Burgio L, Clark RJH (2012a) Raman spectroscopy analysis of pigments on 16–17th c. Persian manuscripts. Spectrochimica Acta - Part a: Molecular and Biomolecular Spectroscopy 92:21–28. https://doi.org/10.1016/j.saa.2012.02.020
Muralha VSF, Miguel C, Melo MJ (2012b) Micro-Raman study of Medieval Cistercian 12–13th century manuscripts: Santa Maria de Alcobaça. Portugal Journal of Raman Spectroscopy 43(11):1737–1746. https://doi.org/10.1002/jrs.4065
Murat Z (2021) Wall paintings through the ages. The medieval period (Italy, 12^{th}-15^{th} century). Archaeological and Anthropological Sciences. https://doi.org/10.1007/s12520-021-01410-4
Murzin VV, Naumov EA, Azovskova OB, Varlamov DA, Rovnushkin MY, Pirajno F (2017) The Vorontsovskoe Au-Hg-As ore deposit (Northern Urals, Russia): Geological setting, ore mineralogy, geochemistry, geochronology and genetic model.Ore Geology Reviews 85: 271–298. https://doi.org/10.1016/j.oregeorev.2016.10.037
Naumov P, Makreski P, Jovanovski G (2007) Direct atomic scale observation of linkage isomerization of As_4S_4 clusters during the photoinduced transition of realgar to pararealgar. Inorg Chem 46(25):10624–10631. https://doi.org/10.1021/ic701299w
Naumov P, Makreski P, Petruševski G, Runčevski T, Jovanovski G (2010) Visualization of a discrete solid-state process with steady-state X-ray diffraction: observation of hopping of sulfur atoms in single crystals of realgar.Journal of the American Chemical Society 132(33): 11398–11401. https://doi.org/10.1021/ja1030672
Nevolko PA, Hnylko OM, Mokrushnikov VP, Gibsher AS, Redin YO, Zhimulev FI, Drovzhak AE, Svetlitskaya TV, Fomynikh PA, Karavashkin MI (2019) Geology and geochemistry of the Kadamzhai and Chauvai gold-antimony-mercury deposits: Implications for new province of Carlin-type gold deposits at the Southern Tien Shan (Kyrgyzstan). Ore Geol Rev 105:551–571. https://doi.org/10.1016/j.oregeorev.2018.12.014
Newman DK, Beveridge TJ, Morel F (1997) Precipitation of arsenic trisulfide by Desulfotomaculum auripigmentum. Applied and Environmental Microbiology 63(5): 2022–2028
Nieć M, Radwanek-Bąk B, Lenik P (2016) Outline of metallogeny of the Polish Carpathians - Ore deposit models and the possibility of discovery hidden ore deposits. Biuletyn - Panstwowego Instytutu Geologicznego 467: 9–40 (Polish). https://doi.org/10.5604/01.3001.0009.4584
Nöller R, Hahn O, Hahn O (2015) Illuminated Manuscripts from Turfan Tracing Silk Road Glamour by Analyzing Pigments. Science and Technology of Archaeological Research 1(2):50–59. https://doi.org/10.1080/20548923.2015.1133120
Nriagu J (2002) Arsenic poisoning through the ages. In: Frankenberger WT (ed) Environmental Chemistry of Arsenic. Marcel Dekker, New York, pp 1–26

O'Day PA (2006) Chemistry and mineralogy of arsenic. Elements 2(2):77–83. https://doi.org/10.2113/gselements.2.2.77

O'Day PA, Vlassopoulos D, Root R, Rivera N (2004) The influence of sulfur and iron on dissolved arsenic concentrations in the shallow subsurface under changing redox conditions. PNAS 101(38):13703–13708. https://doi.org/10.1073/pnas.0402775101

Ogalde JP, Salas CO, Lara N, Leyton P, Paipa C, Campos-Vallette M, Arriaza B (2014) Multi-instrumental identification of orpiment in archaeological mortuary contexts.Journal of the Chilean Chemical Society 59(3): 2571–2573. https://doi.org/10.4067/S0717-97072014000300010

Orna MV (2015) Historic mineral pigments: Colorful benchmarks of ancient civilizations. In: Rasmussen S.C. (Ed.) Chemical Technology in Antiquity. ACS Symposium Series, 1211. Washington: American Chemical Society, pp. 17–69.

Osbaldeston TA, Wood RP (2000) De materia medica: Being an herbal with many other medicinal materials: written in Greek in the first century of the common era: a new indexed version in modern English. Johannesburg: IBIDIS, pp. 927

Pagès-Camagna S, Laval E, Vigears D, Duran A (2010) Non-destructive and in situ analysis of Egyptian wall paintings by X-ray diffraction and X-ray fluorescence portable systems. Appl Phys A Mater Sci Process 100(3):671–681. https://doi.org/10.1007/s00339-010-5667-3

Pagliai M, Bonazzi P, Bindi L, Muniz-Miranda M, Cardini G (2011) Structural and vibrational properties of arsenic sulfides: Alacranite (As_8S_9). J Phys Chem A 115(17):4558–4562. https://doi.org/10.1021/jp201097k

Panayotova S, Pereira-Pardo L, Ricciardi P (2017) Illuminators' materials and techniques in fourteenth-century English manuscripts. Manuscripts in the Making: Art and Science 1:47–64

Pavićević MK, El Goresy A (1988) Crven Dol Tl deposit in Allchar: Mineralogical investigation, chemical composition of Tl minerals and genetic implications. Nucl Instrum Methods Phys Res, Sect A 271(2):297–300. https://doi.org/10.1016/0168-9002(88)90172-6

Pérez-Arantegui J (2021) Not only wall paintings – Pigments for cosmetics. Archaeological and Anthropological Sciences. https://doi.org/10.1007/s12520-021-01399-w

Pertlik F (1975) The crystal structure of the monoclinic form of As_2O_3(claudetite II) [Die Kristallstruktur der monoklinen Form von As_2O_3 (Claudetit II)]. Monatshefte für Chemie 106(3): 755–762 (German). https://doi.org/10.1007/BF00902181

Pertlik F (1978a) Structure refinement of cubic As_2O_3 (arsenolite) with single crystal data.Czechoslovak Journal of Physics 28(2): 170–176

Pertlik F (1978b) Refinement of the crystal structure of the mineral claudetite, As_2O_3 ("Claudetite I") [Verfeinerung der Kristallstruktur des Minerals Claudetit, As_2O_3 ("Claudetit I")].Monatshefte für Chemie 109(2): 277–282 (German). https://doi.org/10.1007/BF00906344

Peters SG, Jiazhan H, Zhiping L, Chenggui J (2007) Sedimentary rock-hosted Au deposits of the Dian-Qian-Gui area, Guizhou, and Yunnan Provinces, and Guangxi District. China Ore Geology Reviews 31(1–4):170–204. https://doi.org/10.1016/j.oregeorev.2005.03.014

Plant JA, Bone J, Voulvoulis N, Kinniburgh DG, Smedley PL, Fordyce FM, Klinck B (2014) Arsenic and selenium. In: Holland, H.D., Turekain, K.K. (Eds.) Environmental geochemistry. Treatise on Geochemistry, 11. Oxford, UK: Elsevier, pp. 13–57

Popova VI, Popov VA, Clark A, Polyakov VO, Borisovski SE (1986) Alacranite As_8S_9; a new mineral.Zapiski Vsesoyuznogo Mineralogicheskogo Obshchestva (Zap.Vses.Mineral.Obshchest.)115: 360–368 (Russian)

Popova VI, Polyakov VO (1985) Uzonite As_4S_5 – a new arsenic sulfide from Kamchatka. Zap Vses Mineral O-Va 114:369–373 (**Russian)**

Porter EJ, Sheldrick GM (1972) Crystal structure of a new crystalline modification of tetra-arsenic tetrasulfide (2,4,6,8-tetrathia-1,3,5,7-tetra-arsatricyclo[3,3,0,$0^{3,7}$]-octane). J Chem Soc, Dalton Trans 13:1347–1349

Powell WG, Pattison DRM (1997) An exsolution origin for low-temperature sulfides at the Hemlo gold deposit, Ontario. Canada Economic Geology 92(5):569–577. https://doi.org/10.2113/gsecongeo.92.5.569

Powell WG, Pattison DRM, Johnston P (1999) Metamorphic history of the Hemlo gold deposit from Al_2SiO_5 mineral assemblages, with implications for the timing of mineralization. Can J Earth Sci 36(1):33–46. https://doi.org/10.1139/e98-078

Pratesi G, Zoppi M (2015) An insight into the inverse transformation of realgar altered by light. Am Miner 100(5–6):1222–1229. https://doi.org/10.2138/am-2015-5045

Raber T, Roth P (2018) The Lengenbach Quarry in Switzerland: classic locality for rare thallium sulfosalts.Minerals 8: 409. https://doi.org/10.3390/min8090409

Radosavljević SA, Stojanović JN, Pačevski AM (2012) Hg-bearing sphalerite from the Rujevac polymetallic ore deposit, Podrinje Metallogenic District, Serbia: Compositional variations and zoning. Chem Erde 72(3):237–244. https://doi.org/10.1016/j.chemer.2011.12.003

Radosavljević SA, Stojanović JN, Radosavljević-Mihajlović AS, Kašić VD (2013) Polymetallic mineralization of the Boranja orefield, Podrinje Metallogenic District, Serbia: zonality, mineral associations and genetic features. Periodico Di Mineralogia 82(1):61–87. https://doi.org/10.2451/2013PM0004

Radosavljević SA, Stojanović JN, Radosavljević-Mihajlović AS, Vuković NS (2014) Rujevac Sb-Pb-Zn-As polymetallic deposit, Boranja orefield, Western Serbia: Native arsenic and arsenic mineralization. Mineral Petrol 108(1):111–122. https://doi.org/10.1007/s00710-013-0291-5

Richards JP, Wilkinson D, Ullrich T (2006) Geology of the Sari Gunay epithermal gold deposit, northwest Iran. Econ Geol 101(8):1455–1496. https://doi.org/10.2113/gsecongeo.101.8.1455

Roberts AC, Ansell HG, Bonardi M (1980) Pararealgar, a new polymorph of AsS, from British Columbia. Can Mineral 18:525–527

Roberts AC, Plant AG, Bonardi M (1979) Duranusite from the Mount Washington copper deposit, Comox district, Vancouver Island, British Columbia [Canada]. Scientific and technical Notes in Current Research Part C. Geological Survey of Canada 79–1C: 97–98

Roland GW (1972) Concerning the α-AsS ↔ realgar inversion. Can Mineral 11(2):520–525

Roland GW (1966) Phase Relations and Geological Application of the System Ag-As-S.Unpublished doctoral thesis, Lehigh University, 191 pp

Rose F (1916) Die Mineralfarben und die durch Mineralstoffe Erzeugten Farbungen. Verlag von Otto Spamer, Leipzig

Rötter C, Grundmann G, Richter M (2007) Auripigment: Studien zu dem Mineral und den künstlichen Produkten= Orpiment: studies on the mineral and the artificial products

Ruff - https://rruff.info/index.htm

Rytuba JJ (1986) Arsenic minerals as indicators of conditions of gold deposition in Carlin-type gold deposits.Journal of Geochemical Exploration 25(1–2): 237–238. https://doi.org/10.1016/0375-6742(86)90024-5

Sabatini BJ, Cziegler A, Mödlinger M (2020) Casting simulations of arsenical copper: new insights into prehistoric metal production and materials.JOM 72(9): 3269–3278. https://doi.org/10.1007/s11837-020-04210-8

Sabelli C, Brizzi G (1984) Alteration minerals of the Cetine mine, Tuscany. Italy Mineralogical Record 15(1):27–36

Salvadori M, Sbrolli C (2021) Wall paintings through the ages. The Roman period: Republic and early Empire. Archaeological and Anthropological Sciences. https://doi.org/10.1007/s12520-021-01411-3

Salvant J, Williams J, Ganio M, Casadio F, Daher C, Sutherland K, Monico L, Vanmeert F, De Meyer S, Janssens K, Cartwright C, Walton M (2018) A Roman Egyptian painting workshop: technical investigation of the portraits from Tebtunis. Egypt Archaeometry 60(4):815–833. https://doi.org/10.1111/arcm.12351

Saunders JA, Lee M-K, Shamsudduha M, Dhakal P, Uddin A, Chowdury MT, Ahmed KM (2008) Geochemistry and mineralogy of arsenic in (natural) anaerobic groundwaters.Applied Geochemistry 23(11): 3205–3214. https://doi.org/10.1016/j.apgeochem.2008.07.002

Sazonov VN, Murzin VV, Grigor'ev NA (1998) Vorontsovsk gold deposit: an example of Carlin-type mineralization in the Urals. Russia Geology of Ore Deposits 40(2):139–151

Scacchi A (1850) Memorie geologiche sulla Campania e relazione dell'Incendio accaduto nel Vesuvio nel mese di Febbrajo del 1850. Reale Accademia della Scienze di Napoli, pp. 190

Schafer EH (1955) Orpiment and realgar in Chinese technology and tradition. J Am Orient Soc 75(2):73–89

Scott DA (2016) A review of ancient Egyptian pigments and cosmetics. Stud Conserv 61(4):185–202. https://doi.org/10.1179/2047058414Y.0000000162

Scott DA (2018) Egyptian Sarcophagi and Mummies in the San Diego Museum of Man: Some Technical Studies. Stud Conserv 63(4):215–235. https://doi.org/10.1080/00393630.2017.1331549

Scott DJ, Nowacki W (1975) New data on wakabayashilite. Can Mineral 13:418–419

Selin PF (1982) The geological features of the deep horizons and the mineral zonation of the Chagan-Uzun mercury deposit. Geologiya Rudnykh Mestorozhdenij 24(5):57–62

Sharma V, Samal AK, Chaudhary AK, Srivastava RK (2017) Characterization and comparative physico-chemical studies of Manahshila (traditionally used arsenic mineral) and the corresponding polymorphs of realgar (As_4S_4). Curr Sci 112(9):1936–1941. https://doi.org/10.18520/cs/v112/i09/1936-1941

Simonsen, KP, Bøllingtoft, P, Sanyova, J, Wangdu, P, Scharff, M, Redsted Rasmussen, A (2015) Tibetan wall painting: Investigation of materials and techniques and DNA analysis of proteinaceous binding medium. International Journal of Conservation Science 6(3): 323-334.

Singh MR, Sharma D (2020) Investigation of pigments on an Indian palm leaf manuscript (18th-19th century) by SEM-EDX and other techniques. Restaurator 41(1):46–95. https://doi.org/10.1515/res-2019-0006

Smith GD, Clark RJ (2001) Raman microscopy in art history and conservation science. Stud Conserv 46(sup1):92–106. https://doi.org/10.1179/sic.2001.46.Supplement-1.92

Smith GD, Clark RJ (2004) Raman microscopy in archaeological science. J Archaeol Sci 31(8):1137–1160. https://doi.org/10.1016/j.jas.2004.02.008

Spiridonov EM (1989) Wakabayashilite (As, $Sb_{)1}1_{S1}8$ of the Khaidarkan deposit. Novye Dannye Mineralakh 36:166–170

Spiridonov EM, Krapiva LY, Stepanov VI, Chvileva TN (1983) Antimony aktashite from the Chauvay mercury deposit, Soviet Central Asia. Doklady, Academy of Sciences of the USSR, Earth Science Section 261:171–175

Steger S, Oesterle D, Mayer R, Hahn O, Bretz S, Geiger G (2019) First insights into Chinese reverse glass paintings gained by non-invasive spectroscopic analysis—tracing a cultural dialogue. Archaeol Anthropol Sci 11(8):4025–4034. https://doi.org/10.1007/s12520-019-00799-3

Stepanov SYu, Sharpenok LN, Antonov AV (2017) Fluid-explosive breccias of the vorontsovskoe gold deposit (the North Urals). Zapiski Rossiiskogo Mineralogicheskogo Obshchestva 146(1):29–43 (**Russian**)

Stodulski, L.a, Farrell, E.b, Newman, R. (1984) Identification of ancient Persian pigments from Persepolis and Pasargadae. Stud Conserv 29(3):143–154. https://doi.org/10.1179/sic.1984.29.3.143

Stolburg CS, Dunning GE (1985) The Getchell mine, Humboldt County. Mineralogical Record 16(1):15–23

Strunz H, Nickel EH (2001) Strunz mineralogical tables. Chemical-Structural Mineral Classification System.9th Ed. Schweizerbart, Stuttgart, Germany

Su W, Heinrich CA, Pettke T, Zhang X, Hu R, Xia B (2009) Sediment-hosted gold deposits in Guizhou, China: Products of wall-rock sulfidation by deep crustal fluids.Economic Geology 104(1): 73–93. https://doi.org/10.2113/gsecongeo.104.1.73

Švarcová S, Hradil D, Hradilová J, Čermáková Z (2021) Pigments – copper-based greens and blues. Archaeological and Anthropological Sciences. https://doi.org/10.1007/s12520-021-01406-0

Tajeddin HA, Rastad E, Yaghoubpour A, Maghfouri S, Peter JM, Goldfarb R, Mohajjel M (2019) The Barika gold-bearing Kuroko-type volcanogenic massive sulfide (VMS) deposit, Sanandaj-Sirjan zone. Iran Ore Geology Reviews 113:103081. https://doi.org/10.1016/j.oregeorev.2019.103081

Talusani RVR (2001) Possible Carlin-type disseminated gold mineralization in the Mahakoshal fold belt. Central India Ore Geology Reviews 17(4):241–247. https://doi.org/10.1016/S0169-1368(00)00016-0

Tan Q-P, Xia Y, Xie Z-J, Yan J (2015) Migration paths and precipitation mechanisms of ore-forming fluids at the Shuiyindong Carlin-type gold deposit, Guizhou, China. Ore Geol Rev 69:140–156. https://doi.org/10.1016/j.oregeorev.2015.02.006

Tanevska V, Nastova I, Minčeva-Šukarova B, Grupče O, Ozcatal M, Kavčić M, Jakovlevska-Spirovska Z (2014) Spectroscopic analysis of pigments and inks in manuscripts: II. Islamic illuminated manuscripts (16th-18th century). Vib Spectrosc 73:127–137. https://doi.org/10.1016/j.vibspec.2014.05.008

Tasev G, Serafimovski T, Boev B, Gjorgjiev L (2018) Morphological types of mineralization in the Lojane as-sb deposit, Republic of Macedonia. In: International Multidisciplinary Scientific GeoConference Surveying Geology and Mining Ecology Management, SGEM (Albena, Bulgaria, 2–8 July 2018). 18 (1–3), pp. 601–608.

Tekin E, Varol B, Ayan Z, Satir M (2002) Epigenetic origin of celestite deposits in the Tertiary Sivas Basin: new mineralogical and geochemical evidence. Neues Jahrb Mineral Monatsh 7:289–318. https://doi.org/10.1127/0028-3649/2002/2002-0289

Tian R-C, Migon C, Mori C, Orsini A (1995) Arsenic and antimony contamination in a riverine environment affected by an abandoned realgar mine. Toxicol Environ Chem 52(1–4):221–230. https://doi.org/10.1080/02772249509358263

Todorov T, Mileva S (1987) Geology and mineralogy of the quartz-antimonite deposits Cernicevo, southeast Rhodopes. Godishnik - Komitet Po Geologii 27:105–115 **(Russian)**

Tomkins AG, Pattison DRM, Zaleski E (2004) The Hemlo Gold Deposit, Ontario: an example of melting and mobilization of a precious metal-sulfosalt assemblage during amphibolite facies metamorphism amd deformation. Econ Geol 99(6):1063–1084. https://doi.org/10.2113/gsecongeo.99.6.1063

Tosdal RM, Cline JS, Fanning CM, Wooden JL (2003) Lead in the Getchell-Turquoise ridge Carlin-type gold deposits from the perspective of potential igneous and sedimentary rock sources in Northern Nevada: implications for fluid and metal sources. Econ Geol 98(6):1198–1211. https://doi.org/10.2113/gsecongeo.98.6.1189

Treacy DJ, Taylor PC (1981) Nuclear quadrupole resonance in two crystalline forms of As_2O_3, arsenolite and claudetite I. Solid State Commun 40(2):135–138. https://doi.org/10.1016/0038-1098(81)90153-8

Trentelman K, Stodulski L, Pavlosky M (1996) Characterization of pararealgar and other light-induced transformation products from realgar by Raman microspectroscopy. Anal Chem 68(10):1755–1761. https://doi.org/10.1021/ac951097o

Turner SJ, Flindell PA, Hendri D, Hardjana I, Lauricella PF, Lindsay RP, Marpaung B, White GP (1994) Sediment-hosted gold mineralisation in the Ratatotok district, North Sulawesi. Indonesia Journal of Geochemical Exploration 50(1–3):317–336. https://doi.org/10.1016/0375-6742(94)90029-9

Uhlir K, Gironda M, Bombelli L, Eder M, Aresi N, Groschner G, Griesser M (2019) Rembrandt's Old Woman Praying, 1629/30: A look below the surface using X-ray fluorescence mapping.X-Ray Spectrometry 48(4): 293–302. https://doi.org/10.1002/xrs.2985

Van Der Snickt G, Janssens K, Dik J, De Nolf W, Vanmeert F, Jaroszewicz J, Cotte M, Falkenberg G, Van Der Loeff L (2012) Combined use of synchrotron radiation based micro-X-ray fluorescence, micro-X-ray diffraction, micro-X-ray absorption near-edge, and micro-fourier transform infrared spectroscopies for revealing an alternative degradation pathway of the pigment cadmium yellow in a painting by Van Gogh. Anal Chem 84(23):10221–10228. https://doi.org/10.1021/ac3015627

Van Schaik S, Helman-Wazny A, Nöller R (2015) Writing, painting and sketching at dunhuang: assessing the materiality and function of early Tibetan manuscripts and ritual items.Journal of Archaeological Science 53: 110–132. https://doi.org/10.1016/j.jas.2014.09.018

Vandenabeele P, Von Bohlen A, Moens L, Klockenkämper R, Joukes F, Dewispelaere G (2000) Spectroscopic examination of two Egyptian masks: A combined method approach. Anal Lett 33(15):3315–3332. https://doi.org/10.1080/00032719.2000.10399503

Vandenabeele P, Tate J, Moens L (2007) Non-destructive analysis of museum objects by fibre-optic Raman spectroscopy. Anal Bioanal Chem 387(3):813–819. https://doi.org/10.1007/s00216-006-0758-x

Vanmeert F, Vandersnickt G, Janssens K (2015) Plumbonacrite identified by X-ray powder diffraction tomography as a missing link during degradation of red lead in a Van Gogh painting. Angewandte Chemie - International Edition 54(12):3607–3610. https://doi.org/10.1002/anie.201411691

Vanmeert F, De Nolf W, Dik J, Janssens K (2018) Macroscopic X-ray powder diffraction scanning: possibilities for quantitative and depth-selective parchment analysis.Analytical Chemistry90(11): 6445–6452. https://doi.org/10.1021/acs.analchem.8b00241

Vanmeert F, De Keyser N, Van Loon A, Klaassen L, Noble P, Janssens K (2019) Transmission and reflection mode macroscopic X-ray powder diffraction imaging for the noninvasive visualization of paint degradation in still life paintings by Jan Davidsz. de Heem. Analytical Chemistry 91(11): 7153–7161. https://doi.org/10.1021/acs.analchem.9b00328

Vaughan DJ, Corkhill CL (2017) Mineralogy of sulfides. Elements 13:81–87. https://doi.org/10.2113/gselements.13.2.81

Vermeulen M, Leona M (2019) Evidence of early amorphous arsenic sulfide production and use in Edo period Japanese woodblock prints by Hokusai and Kunisada. Heritage Science 7(1):73. https://doi.org/10.1186/s40494-019-0318-2

Vermeulen M, Sanyova J, Janssens K (2015) Identification of artificial orpiment in the interior decorations of the Japanese tower in Laeken, Brussels. Belgium Heritage Science 3(9):3–9. https://doi.org/10.1186/s40494-015-0040-7

Vermeulen M, Nuyts G, Sanyova J, Vila A, Buti D, Suuronen J-P, Janssens K (2016) Visualization of As(III) and As(v) distributions in degraded paint micro-samples from Baroque- and Rococo-era paintings. J Anal at Spectrom 31(9):1913–1921. https://doi.org/10.1039/c6ja00134c

Vermeulen M, Saverwyns S, Coudray A, Janssens K, Sanyova J (2018a) Identification by Raman spectroscopy of pararealgar as a starting material in the synthesis of amorphous arsenic sulfide pigments. Dyes Pigm 149:290–297. https://doi.org/10.1016/j.dyepig.2017.10.009

Vermeulen M, Janssens K, Sanyova J, Rahemi V, McGlinchey C, De Wael K (2018b) Assessing the stability of arsenic sulfide pigments and influence of the binding media on their degradation by means of spectroscopic and electrochemical techniques. Microchem J 138:82–91. https://doi.org/10.1016/j.microc.2018.01.004

Vermeulen M, Palka K, Vlček M, Sanyova J (2019) Study of dry- and wet-process amorphous arsenic sulfides: Synthesis, Raman reference spectra, and identification in historical art materials. J Raman Spectrosc 50(3):396–406. https://doi.org/10.1002/jrs.5534

Vershkovskaya OV, Blinov VA, Kulikova IM, Chvileva TN, Gorshkov, Ye.N. (1988) Duranusite from a mercury-antimony deposit of central Tadzhikistan. Doklady Earth Science Sections 303(6):115–118

Vielreicher RM, Vielreicher NM, Hagemann SG, Jones G (2003) Fault zone evolution and its controls on ore-grade distribution at the Jian Cha Ling gold deposit, western Qinling region, central China. Miner Deposita 38(5):538–554. https://doi.org/10.1007/s00126-002-0333-0

Vikentyev IV, Tyukova EE, Vikent'eva OV, Chugaev AV, Dubinina EO, Prokofiev VY, Murzin VV (2019) Vorontsovka Carlin-style gold deposit in the North Urals: Mineralogy, fluid inclusion and isotope data for genetic model. Chem Geol 508:144–166. https://doi.org/10.1016/j.chemgeo.2018.07.020

Vitti, P. (2021) Mortars and masonry - Structural lime and gypsum mortars in Antiquity and Middle Ages. Archaeological and Anthropological Sciences. https://doi.org/10.1007/s12520-021-01408-y

Volkov AV, Serafimovski T, Kochneva NT, Tomson IN, Tasev G (2006) The Alshar epithermal Au-As-Sb-Tl deposit, southern Macedonia. Geol Ore Deposits 48(3):175–192. https://doi.org/10.1134/S1075701506030020

Wallert, A. (1984) Orpiment and realgar.Maltechnik-Restauro 90(4): 45–57

Wang X-C, Zhang Z-R (2001) Geology of sedimentary rock-hosted disseminated gold deposits in northwestern Sichuan. China International Geology Review 43(1):69–90. https://doi.org/10.2747/1938-2839.43.1.90

Wang X-H, Hou Z-Q, Song Y-C, Zhang H-R (2015) Geological, fluid inclusion and isotopic studies of the Baiyangping Pb-Zn-Cu-Ag polymetallic deposit, Lanping basin, Yunnan province, China. J Asian Earth Sci 111:853–871. https://doi.org/10.1016/j.jseaes.2015.08.009

Wang, L., Mu, Z., Lou, X. (1999) Gold-bearing minerals and gold-existing states at Zimudang gold deposit.Kuangwu Yanshi 19(3): 77–81 (Chinese).

Watson KD (1954) Paragenesis of the zinc-lead-copper deposits at the Mindamar mine. Nova Scotia Economic Geology 49(4):389–412. https://doi.org/10.2113/gsecongeo.49.4.389

Webmineral - http://www.webmineral.com

West FitzHugh E (1997) Orpiment and realgar. In: West FitzHugh, R.L. (Ed.) Artists' pigments. A handbook of their history and characteristics.Vol. 3. National Gallery of Art, Washington: Archetype Publications, London, pp. 370

Westlake P, Siozos P, Philippidis A, Apostolaki C, Derham B, Terlixi A, Perdikatsis V, Jones R, Anglos D (2012) Studying pigments on painted plaster in Minoan, Roman and Early Byzantine Crete.

A multi-analytical technique approach.Analytical and Bioanalytical Chemistry 402(4): 1413–1432. https://doi.org/10.1007/s00216-011-5281-z

Whitfield HJ (1973a) Crystal structure of the β-form of tetra-arsenic trisulfide.Journal of the Chemical Society. Dalton Trans 17:1737–1738. https://doi.org/10.1039/DT9730001737

Whitfield HJ (1973b) Crystal and molecular structure of tetra-arsenic pentasulfide.Journal of the Chemical Society. Dalton Trans 17:1740–1742. https://doi.org/10.1039/DT9730001740

Whitfield HJ (1970) The crystal structure of tetra-arsenic trisulfide. Journal of the Chemical Society A: Inorganic, Physical, and Theoretical Chemistry, pp. 1800–1803. https://doi.org/10.1039/J19700001800

Wilkin RT, Ford RG (2002) Use of hydrochloric acid for determining solid-phase arsenic partitioning in sulfidic sediments. Environ Sci Technol 36(22):4921–4927. https://doi.org/10.1021/es025862+

Wilson WE (2007) The Shimen mine: Jiepaiyu, Shimen County, Hunan Province. China Mineralogical Record 38(1):43–53

Wojciechowski A (2003) Mercury and gold occurrences in the Baligród and Szczawnica areas (Polish part of the Carpathian Mts) [Wystapienia rteci i złota w rejonie Baligrodu oraz Szczawnicy (polska cześć Karpat)].Przeglad Geologiczny 51(2): 131–138 (Polish)

Xie Z, Xia Y, Cline JS, Pribil MJ, Koenig A, Tan Q, Wei D, Wang Z, Yan J (2018) Magmatic origin for sediment-hosted au deposits, Guizhou Province, China: In situ chemistry and sulfur isotope composition of pyrites, shuiyindong and Jinfeng deposits. Econ Geol 113(7):1627–1652. https://doi.org/10.5382/econgeo.2018.4607

Xu Y-P, Yao L, Li J-J (2005) Geological characteristics and deposits prognostic of Nongduke Au-Ag ores in Changtai of Sichuan. Wutan Huatan Jisuan Jishu 27(3): 4–5+241–245 (Chinese)

Yaylali-Abanuz G, Tüysüz N (2010) Chemical, mineralogical, and mass-change examinations across a gold bearing vein zone in the Akoluk area, Ordu, NE Turkey. Neues Jahrb Mineral Abh 187(1):11–22. https://doi.org/10.1127/0077-7757/2010/0157

Yaylali-Abanuz G, Tüysüz N (2011) Statistical evaluation of the geochemical data from Akoluk epithermal gold area (Ulubey-Ordu). NE Turkey Geochemical Journal 45(3):209–219. https://doi.org/10.2343/geochemj.1.0116

Yigit O, Hofstra AH, Hitzman MW, Nelson EP (2006) Geology and geochemistry of jasperoids from the Gold Bar district. Nevada Mineralium Deposita 41(6):527–547. https://doi.org/10.1007/s00126-006-0080-8

Yilmaz H (2003) Exploration at the kuscayiri Au (Cu) prospect and its implications for porphyry-related mineralization in Western Turkey. J Geochem Explor 77(2–3):133–150. https://doi.org/10.1016/S0375-6742(02)00274-1

Yue S-W, Li D-F, Bagas L, Fang J, Lin Z-W (2018) Geology and isotope systematics of the Jianchaling Au deposit, Shaanxi province, China: Implications for mineral genesis. Geosciences 8(4):120. https://doi.org/10.3390/geosciences8040120

Žáček V, Ondruš P (1997) Mineralogyof recentlyformed sublimates from Kateřina colliery in Radvanice, Eastern Bohemia, Czech Republic. Bulletin of the Czech Geological Survey 72(3):289–302

Zhabin AG, Samsonova NS, Chuchua IB, Yaroshevich VZ, Arevadze DV, Shubitidze DS (1990) Ore-Bearing Metasomattcally Altered Limestones of the Black Shale Association. Int Geol Rev 32(11):1145–1155. https://doi.org/10.1080/00206819009465846

Zhai W, Sun X, Yi J, Zhang X, Mo R, Zhou F, Wei H, Zeng Q (2014) Geology, geochemistry, and genesis of orogenic gold-antimony mineralization in the Himalayan Orogen, South Tibet, China. Ore Geology Reviews 58(C): 68–90. https://doi.org/10.1016/j.oregeorev.2013.11.001

Zhang B (1985) The discovery of wakabayashilite in China. Acta Mineralogica Sinica 5:270–274 (**Chinese**)

Zheng M, Zhou Y, Gu X (1991) Isotopic compositions in the Dongbeizhai fine-disseminated gold deposit, Sichuan province, and their genetic implications. Sci Geol Sin 2:159–173 **(Chinese)**

Zheng W-B, Tang J-X, Wang X-W, Wang H, Ying L-J, Zhong Y-F, Zhong W-TA (2012) Analysis on gold metallization in Jiama copper polymetallic deposit, Tibet. Jilin Daxue Xuebao (Diqiu Kexue Ban)/Journal of Jilin University 42(Suppl. 1): 181–196 (Chinese)

Zhu X, Wang R, Lu X, Liu H, Li J, Ouyang B, Lu J (2015) Secondary minerals of weathered orpiment-realgar-bearing tailings in Shimen carbonate-type realgar mine, Changde. Central China Mineralogy and Petrology 109(1):15. https://doi.org/10.1007/s00710-014-0344-4

Zoppi M, Pratesi G (2012) The dual behavior of the β-As_4S_4 altered by light. Am Miner 97(5–6):890–896. https://doi.org/10.2138/am.2012.3968

Publisher's note Springer Nature remains neutral with regard to jurisdictional claims in published maps and institutional affiliations.